

Petrofacies and Detrital Geochronology of the Upper Pottsville Conglomerate
Magnafacies, Cahaba Synclinorium, Southern Appalachian Fold and Thrust Belt,
Alabama

by

Ziaul Haque

A thesis submitted to the Graduate Faculty of
Auburn University
in partial fulfillment of the
requirements for the Degree of
Master of Science

Auburn, Alabama
August 6, 2016

Keywords: Appalachian, Cahaba, Conglomerate, Pottsville, Petrofacies, Geochronology

Copyright 2016 by Ziaul Haque

Approved by

Ashraf Uddin, Chair, Professor of Geosciences
Willis E. Hames, Professor of Geosciences
David T. King, Jr., Professor of Geosciences
Charles E. Savrda, Professor of Geosciences

ABSTRACT

Measures of abundance of extraformational conglomerates and clast composition, taken together, can be used to unravel the unroofing history of an orogenic belt. An attempt has been made in this study to develop a new approach to assess sediment provenance based on coarse detritus. Known as the “conglomerate measures” in the Cahaba synclinorium, the uppermost Pottsville Formation consists of conglomerates and subordinate sandstone, shale, and coal. These siliciclastic sediments were deposited during the Alleghenian orogeny primarily in braidplain-anastomosis environments in Alabama and Mississippi.

Clasts in conglomerates of the upper Pottsville Formation consist mainly of sedimentary lithic fragments (chert, sandstone, and mudstone), metasedimentary lithic fragments (phyllite, schist, quartzite), and volcanic and plutonic rock fragments. Compositional similarities between clasts in the upper part of the Pottsville in the Cahaba basin and lithologies of Valley and Ridge, Piedmont, and Blue Ridge provinces suggest that the sediments were derived from proximal sources in the southern Appalachian provinces. Composite modal analysis and ternary plots of sandstone composition in conglomerate matrix in the Cahaba basin indicate mostly a ‘recycled orogenic’ provenance. Matrix compositions also indicate that the source of the upper Pottsville sediments was to the east and southeast in the evolving Appalachians.

Heavy mineral assemblages in sandstones suggest a medium- to high-grade metamorphic source terrane in the Piedmont. Chemical compositions of garnets (Sp-Alm-Py) indicate an amphibolitic facies provenance and the dominance of almandine garnets suggest that a medium- to high-grade metamorphic source supplied a large quantity of sediment to the Cahaba basin.

A whole rock $^{40}\text{Ar}/^{39}\text{Ar}$ age of an andesite clast (~323 Ma) suggests andesitic volcanism during Alleghenian orogeny. Minimum age of a metatonalite clast (~295 Ma) suggests minimum depositional age of the Pottsville Formation in the Cahaba synclinorium, which indicate that the Cahaba section continued to receive Alleghenian metamorphic detritus later than previously thought.

ACKNOWLEDGMENTS

This research is the product of contributions from many people, organizations and companies, and without their technical, financial and mental support it would not have been possible to finish the work. At the beginning I want to mention my advisor Dr. Ashraf Uddin, without whom I could not even think to start this work. From the beginning to the end, he has helped me in all possible ways to complete this research. I also want to thank my other committee members, Dr. Charles Savrda, Dr. Willis Hames and Dr. David King for their suggestions. I would like to mention Dr. Jack Pashin and Dr. Mark Steltenpohl for many in-depth discussions on sedimentation and tectonics of the Appalachian fold and thrust belt. I would like to thank Dr. Willis Hames for geochronologic analysis in his ANIMAL lab and many fruitful discussions. I am also grateful to Christopher Fleisher, coordinator of the microprobe laboratory at the University of Georgia, for helping with microprobe analysis. I also would like to thank the National Science Foundation (NSF 0911687), Geological Society of America, American Association of Petroleum Geologists, Gulf Coast Association of Geological Societies, and Auburn University for their financial support. I am grateful to the Geosciences department at Auburn University for assistance in completing this work. I also thank Safak Ozsarac for his help and support throughout the time at Auburn. Finally, I would like to thank my friends and family from here and back in Bangladesh whom supported and motivated me through all the great and hard times I have encountered during pursuit of my Master's degree.

TABLE OF CONTENTS

ABSTRACT	ii
ACKNOWLEDGMENTS	iv
LIST OF FIGURES	viii
LIST OF TABLES	xiii
CHAPTER 1: INTRODUCTION	1
1.1 Introduction	1
1.2 Provenance Study of Conglomerate	4
1.3 Study Area.....	5
1.4 Previous Studies	8
CHAPTER 2: REGIONAL TECTONIC SETTING AND FORMATION OF CAHABA BASIN.....	13
2.1 Introduction	13
2.1.1 Taconic Orogeny	17
2.1.2 Acadian Orogeny	18
2.1.3 Alleghenian Orogeny.....	19
2.3 Pottsville Formation	25
2.3.1 Introduction	25
2.3.2 Conglomerate Measures	27
2.3.3 Depositional Environment of Conglomerate Measures.....	29
2.3.4 Core Locations.....	30
CHAPTER 3: CONGLOMERATE PETROGRAPHY	34
3.1 Introduction	34
3.2 Methodology	35

3.3 Conglomerate Clast Petrography	39
3.3.1 Igneous Clast Lithology and Petrography	42
3.3.2 Metamorphic Clast Lithology and Petrography	44
3.3.3 Sedimentary Clast Lithology and Petrography.....	48
3.3.4 Sand Grain (matrix) Point Counting.....	53
3.4 Interpretation of Conglomerate Petrography Data.....	60
CHAPTER 4: HEAVY MINERAL ANALYSIS	63
4.1 Introduction	63
4.2 Methodology	63
4.3 Results	64
4.4 Discussion	71
CHAPTER 5: GARNET CHEMISTRY	72
5.1 Introduction	72
5.2 Electron Microprobe Methodology	75
5.3 Results	78
5.4 Interpretations.....	85
CHAPTER 6: $^{40}\text{Ar}/^{39}\text{Ar}$ GEOCHRONOLOGY	86
6.1 Introduction	86
6.2 $^{40}\text{Ar}/^{39}\text{Ar}$ Dating	86
6.3 Methodology	87
6.4 Results	94
6.5 Interpretation of $^{40}\text{Ar}/^{39}\text{Ar}$ Age Dates	97
CHAPTER 7: DISCUSSION AND CONCLUSIONS	98
7.1 General Paleozoic Lithology of the Provinces in the Cahaba Basin Vicinity.....	98
7.2 Comparison of Provenance of Upper Pottsville with the Lower Pottsville in Cahaba Basin.....	102

7.3 Discussions of the Provenance of Upper Pottsville Conglomerate.....	105
7.4 Conclusions	109
REFERENCES	111
APPENDICES	124

LIST OF FIGURES

Figure 1: Map of the southern Appalachian region showing the location of Appalachian lithotectonic units including Piedmont and Carolina superterrane. BWb, CS, and CoS show the locations of Black Warrior basin, Cahaba synclinorium and Coosa synclinorium, respectively (modified after Merschat, 2009).....	3
Figure 2: Map of Pennsylvanian paleogeography of Appalachian depocenters showing the thickness of Pottsville sediments in different Appalachian foreland basins (after Greb et al., 2008).	7
Figure 3: Location map of the Black Warrior basin, Cahaba synclinorium and Coosa synclinorium in central Alabama (not to scale).	8
Figure 4: Generalized stratigraphic column of the Pottsville Formation in the Cahaba basin showing stratigraphic intervals examined by previous researchers (modified from Pashin et al., 1995; Peavy, 2008).....	11
Figure 5: Structural cross sections of the Pottsville Formation in the Cahaba basin. The clastic wedge thickens to the southeast, indicating a source area located to the southeast (modified from Pashin and Carroll, 1999).....	12
Figure 6: The rotational transpressive collision of Gondwana with Laurentia to form the supercontinent Pangea at the end of the Paleozoic. Features in red were active at the time indicated (after Hatcher, 2002).	15
Figure 7: Tectonic models of Appalachian orogenies (from Lutgens and Tarbuck, 2015). (A) Pre-Taconic event when a volcanic arc, the microcontinent Avalonia, and Africa were converging towards North America. (B) Collision between a volcanic arc and North America (Taconic orogeny). (C) Collision between the microcontinent Avalonia and North Amercia (Acadian orogeny). (D) Final collision between Africa and North America (Alleghenian orogeny).	16
Figure 8: Generalized geologic map of Cahaba and adjacent basins and cross section along the Black Warrior basin (BWB) through the Coosa basin (CoS). The BWB and Cahaba synclinorium (CS) are separated by the Birmingham anticlinorium (BA), and the Cahaba and Coosa synclinoria are separated by the Helena thrust (HT). The inset map shows the location of Cahaba and Coosa synclinorium in central Alabama (modified from Thomas and Bayona, 2005; Pashin et al., 2010).	22
Figure 9: Generalized stratigraphic column of Cahaba basin.....	24
Figure 10: Composite stratigraphic section for the Cahaba synclinorium and adjacent basins. Three magnafacies of the Pottsville Formation—lower quartzarenite measures, middle mudstone measures, and upper conglomerate measures—were delineated in the Cahaba basin by Pashin et al. (1995).....	26
Figure 11: The right column shows the generalized stratigraphic column of the conglomerate measures of the Pottsville Fotmation in Cahaba synclinorium. The left column shows the cyclothemic sequences measured from Helena through	

Maylene coal zones in the Joy Manufacturing H.B (JMHB) core. Blue arrows show fining upward sequences that indicate long-term aggradation in fluvial systems (modified from Pashin et al., 1995)	28
Figure 12: Location of the two drill cores in the Cahaba basin (purple). Green diamond shows the location of SOMED core and red diamond shows the location of Joy Manufacturing H.B. core.	31
Figure 13: Cores of the Pottsville conglomerate measures, Joy Manufacturing H.B. core.	32
Figure 14: Representative core samples of the Pottsville conglomerate measures collected from SOMED core.	33
Figure 15: Grid technique used to quantify the volume percentage of various clast types versus the volume of matrix in the conglomerate thin sections. Each of the square grids represents five percent (5%) of the total thin-section area. Clast percentage was counted in each of the grids and then added to get the total percentage of each type of clast in the thin section.	37
Figure 16: Pie diagrams showing the average percentages of different clasts in conglomerate samples with stratigraphic position (core depth) in the conglomerate measures from both cores. (A) Percentages of clasts from depths less than 100 ft, (B) Percentages of clasts in the depth range of around 500 ft, and (C) Clast percentages at depths greater than 1000 ft. (Lm = metamorphic clasts, Ls = sedimentary clasts, Lv = volcanic clasts).....	40
Figure 17: Bar diagrams showing the percentages of different clast types in conglomerate samples with depth (in feet) in Joy Manufacturing H.B core.	41
Figure 18: Representative photomicrographs from conglomerate samples showing volcanic clasts and other clast types in the Pottsville conglomerate measures. Most of the feldspar lacks observable twinning, however, polysynthetic and simple twins are visible in a minority of crystals suggesting both plagioclase and sanidine are present. (A) Laths of plagioclase and sanidine crystals. (B) Volcanic clast (Lv) and chert. Volcanic clasts are mainly dacite and andesite.....	43
Figure 19: Representative photomicrographs of quartzite clasts in the Pottsville conglomerate measures. (A) Quartzite (Lm1) grain with metamorphic fabric from sample ZBH-11. Red circles show triple junctions at ~120°, green circles show subgrains, yellow circles show straight grain boundaries, pink circles show serrated and bulged grain boundaries. (B) Typical fabric of dynamically recrystallized quartz formed by SGR (sample ZBH-2).....	46
Figure 20: Representative photomicrographs of metamorphic clasts (Lm) in the Pottsville conglomerate measures, including low-grade phyllites with a parallel arrangement of quartz and muscovite crystals in sample ZBH-10 (A) and sample ZBH-2 (B).47	
Figure 21: Representative photomicrographs of chert clasts in the upper Pottsville conglomerates. (A) Dark black to light black chert clast with mosaic textures formed due to the interlocking microcrystalline quartz (crossed polarized light). (B)	

Chert clast with quartz veins. Quartz crystals are polygonal in shape and strain free. Qtz = Quartz.....	49
Figure 22: Representative photomicrographs of chert clasts in the upper Pottsville conglomerate. (A) Microcrystals of quartz with a chalcedony. (B) Chert with dolomite rhombs.	50
Figure 23: Representative photomicrographs of sedimentary lithic clasts. (A) Sandstone clast dominated by quartz (sample ZHS-1). (B) Sandy siltstone clasts dominated by monocristalline quartz (sample ZHS-3).....	51
Figure 24: Representative photomicrographs of fine-grained sedimentary lithic clasts in the Pottsville conglomerate measures. (A) Siltstone clast with fine sand-sized quartz. (B) Fine-grained mudstone clast (Ls). ..	52
Figure 25: Representative photomicrographs showing sedimentary lithic pebbles (siltsone and sandstone) and matrix in conglomerate. Sedimentary lithics are mature and consists of silt- and fine sand-sized grains of mostly monocristalline quartz. In contrast, grains in the matrix are medium to coarse sand and consist of a mixture of chert, Ls, Lm, Qp, Qm and less common plagioclase. (A) Sedimentary lithic pebble (left) and matrix (right). (B) Matrix in Pottsville conglomerate consists of the mixture of chert, Ls, Lm, Qp, Qm and rare plagioclase.	54
Figure 26: QtFL ternary diagram showing the provenance fields of sand-sized grains in upper Pottsville conglomerate samples. Standard deviation polygon is drawn around the mean (shown as red and pink diamond). Provenance fields are from Dickinson (1985). Qt = total quartz, F = total feldspar grains, L = lithic grains..	56
Figure 27: QmFLt ternary diagram showing the provenance fields of sand-sized grains in the upper Pottsville conglomerate samples. Standard deviation polygon is drawn around the mean (shown as red and pink diamond). Provenance fields are from Dickinson (1985). Qm = monocristalline quartz, F = total feldspar grains, Lt = lithic grains and chert.....	57
Figure 28: QpLvLs ternary diagram showing the provenance fields of sand-sized grains in upper Pottsville conglomerate samples. Standard deviation polygon is drawn around the mean (shown as red and pink diamond). Provenance fields are from Dickinson (1985). Qp = total quartz, Lv = volcanic lithic grains, Ls = sedimentary lithic grains.....	58
Figure 29: QmPK ternary diagram showing the provenance fields of sand-sized grains in upper Pottsville conglomerate samples. Standard deviation polygon is drawn around the mean (shown as red and pink diamond). Provenance fields are from Weltje (2006). Qm = monocristalline quartz, P = plagioclase feldspar grains, K = potassium feldspar.	59
Figure 30: Bar diagram shows the weight percentages of heavy minerals in samples from the upper Pottsville conglomerate measure.	66
Figure 31: Bar diagram showing the distribution of the most common heavy minerals in the upper Pottsville conglomerate measures, Cahaba synclinorium, Alabama. Blue	

horizontal dashed line shows the average trend line of ZTR (ZTR- Zircon-Tourmaline-Rutile).	68
Figure 32: Representative photomicrographs of heavy mineral assemblages from the upper Pottsville conglomerate measures. (A) Rt = rutile, Zr = Zircon, Gt = Garnet, and other opaque minerals from sample ZH-10. (B) Rt = rutile, Zr = zircon, and other opaque minerals from sample ZHS-16. Both photos taken in crossed polarized light.	69
Figure 33: Representative photomicrographs of heavy mineral assemblages from the upper Pottsville conglomerate measures. (A) Zircons (Zr) in sample ZH-10. (B) Backscattered image of heavy minerals on which elemental analyses were performed. Rt = Rutile, Py = Pyrite, Zr = Zircon, Apa = Apatite.....	70
Figure 34: Representative backscatter electron image of garnet grains (Gt) and a quartz grain. Due to the higher atomic number garnet grains are bright compare to the surrounding quartz grain. Garnet grains are surrounded and uniform brightness of the garnet grains suggest uniform atomic distribution.....	77
Figure 35: Chemical composition of garnets from upper Pottsville Formation in Cahaba basin plotted on (Py+Alm)-Sp-Gro ternary diagram (adapted from Nanayama, 1997). ..	80
Figure 36: Chemical composition of garnets from upper Pottsville Formation in Cahaba basin plotted on (Sp+Gro)-Py-Alm ternary diagram (adapted from Nanayama, 1997). ..	81
Figure 37: Chemical composition of garnets from upper Pottsville Formation in Cahaba basin plotted on (Alm+Sp)-Gr-Py ternary diagram (adapted from Nanayama, 1997). ..	82
Figure 38: Chemical composition of garnets from upper Pottsville Formation in Cahaba basin plotted on Sp-Alm-Py ternary diagram (adapted from Nanayama, 1997)..	83
Figure 39: Relationship between Pottsville garnet chemistry and metamorphic pressures and temperatures. Dashed black lines are isopleths of constant Fe/(Fe+Mg) calculated assuming garnet in equilibrium with biotite and a pelitic source rocks (from Spear and Cheney, 1989). ..	84
Figure 40: Lithologic column of Conglomerate measures in Joy Manufacturing H.B core with sample locations. ZH -4 is a metatonalite clast and ZH-21 is an andesite clast.	89
Figure 41: Examples of conglomerate slices used to identify and extract igneous clasts for $^{40}\text{Ar}/^{39}\text{Ar}$ analysis.....	90
Figure 42: A representative photomicrograph of fragments of metavolcanic clast after crushing from sample ZH-4. (A) Showing few fragments of the clast containing feldspar (Felds) and quartz (Qtz) which has relict igneous texture.	91
Figure 43: A representative photomicrograph of fragments of volcanic clast after crushing from sample ZH-21. (A) Showing an andesite clast fragments containing feldspar (Felds) and plagioclase laths (Plag micro).....	92

Figure 44: Characteristic X-ray diffraction pattern for metatonalite showing the bulk composition of sample ZH-4. The metatonalite sample is dominantly consists of labradorite, albite and quartz.....	93
Figure 45: $^{40}\text{Ar}/^{39}\text{Ar}$ age spectra from an andesite clast separated from upper Pottsville Formation. (A) Release pattern of Ar37/39 from andesite sample. (B) Duplicate $^{40}\text{Ar}/^{39}\text{Ar}$ age spectra for two aliquots of fresh andesite separated from a single pebble. $^{40}\text{Ar}/^{39}\text{Ar}$ release pattern shows evidence of radiogenic argon loss from low retentivity K-rich sites. Over the major part of the release, the constant ($^{40}\text{Ar}/^{39}\text{Ar}$) ratio indicates a crystallization age of 325.7 ± 2.2 Ma and 320.2 ± 4.2 Ma for this sample (see appendix-C for raw data). Pink line shows the age of a volcanic ash bed (308.5 ± 1.5 Ma) reported by Uddin et al., (2010) for an upper marine section of the Pottsville Formation in Mississippi.	95
Figure 46: $^{40}\text{Ar}/^{39}\text{Ar}$ age spectra from a metatonalite clast separated from upper Pottsville Formation. (A) Release pattern of Ar37/39 from metatonalite. (B) $^{40}\text{Ar}/^{39}\text{Ar}$ age spectrum from an aliquot of plagioclase separated from metatonalite. $^{40}\text{Ar}/^{39}\text{Ar}$ release pattern shows evidence of unsupported excess argon in K-rich phase during the first ~20% ^{39}ArK release and then the following ages reflect age of Ca rich phase with a minimum age of ~295 Ma (see appendix-C for raw data). Pink line shows the age of a volcanic ash bed (308.5 ± 1.5 Ma) reported by Uddin et al., (2010) for an upper marine section of the Pottsville Formation in Mississippi.	96
Figure 47: Geologic map showing the various lithotectonic units in the Alabama Piedmont province (modified after Osborne, 1988; Hatcher et al., 1990; Steltenpohl, 2005).	101
Figure 48: Compositional comparison of sands from the Pottsville Formation from the present work and previous studies, (A). Shows QtFL ternary plot. (B). Shows QmFLt ternary plot. Blue polygon shows the composition of sandstone from the lower Pottsville (quartzarenite and mudstone measures; from Peavy, 2008), black polygon shows the composition of sandstone from the Straven Conglomerate (from Osborne, 1988), and pink and red polygons show the composition of sands from the conglomerate measures in SOMED core and JMHB core, respectively (this study). The result of the present work in comparison with previous studies show that the lithic content increases up section.....	104
Figure 49: Profile plot of changes in percentage of clast types with stratigraphic position in the upper Pottsville conglomerate measures. Percentages of metamorphic lithics (Lm) increase and percentages of sedimentary lithics (Ls) and chert decrease upsection. Percentages of volcanic clasts (Lv) show no clear pattern throughout the section.	108

LIST OF TABLES

Table 1: Recalculated compositional parameters for sand-sized grains (matrix) used in this study. Primary parameters are after Graham et al. (1976), Dickinson and Suczek (1979), Dorsey (1988), and Uddin and Lundberg (1998).....	38
Table 2: Normalized modal analysis of sand-sized grains from SOMED and JHMB cores from the upper Pottsville Formation in Cahaba synclinorium.....	55
Table 3: Normalized abundances of heavy minerals of the upper Pottsville conglomerate measures, Cahaba Basin, Alabama. (ZTR- Zircon-Tourmaline – Rutile).	67
Table 4: End-member compositions and typical sources of the common rock-forming garnets (Mange and Maurer, 1992).....	73

CHAPTER 1: INTRODUCTION

1.1 Introduction

Sedimentary basins associated with mountain belts are important repositories that hold evidence of orogenic processes and interrelationships among tectonic events, climatic conditions, and erosional histories (Uddin and Lundberg, 1998, 2004). The Appalachian orogenic belt records three separate mountain-building events: the Middle Ordovician Taconic orogeny, the Devonian Acadian orogeny, and the Pennsylvanian-Permian Alleghenian orogeny. The Alleghenian orogeny is the youngest and most pervasive event that affected the central and southern Appalachians; its deformation stretched from Alabama to New England and extended inward as far as Tennessee (Secor et al., 1986; Hatcher et al., 1989). The Ouachita belt is an east-west trending extension of the Appalachians located in west-central Arkansas and southeastern Oklahoma, with roots extending as far south as central Texas. This belt also experienced uplift during the Alleghenian orogeny. The analysis of syn-orogenic sediments in the Appalachian foreland basins provides valuable information on the tectonic and erosional histories of the Paleozoic. The Paleozoic Appalachian-Cahaba clastic system serves as an analog to the Cenozoic Himalayan-Bengal system (Graham et al., 1975, 1976). The Pottsville Formation is a clastic wedge that was deposited in the Appalachian foreland basin during the Alleghenian orogeny. Previous workers have proposed conflicting interpretations regarding the clastic sediment sources for the Pottsville Formation (e.g., Schlee, 1963; Mack et al., 1983; Demirpolat, 1989; and Liu and Gastaldo, 1992). Some workers consider the Ouachita mountain belt as a source for the Pottsville clastics (Mack et al., 1983),

whereas several recent works suggest that the Pottsville Formation was derived from the deformed and uplifted southern Appalachians (Peavy, 2008; Gomes, 2012; Moore, 2012). Understanding the detrital history of the Pottsville Formation will help in unraveling the tectonic evolution of the Appalachian mountain belt and in understanding the deposition in the Cahaba foreland basin during Pennsylvanian time. Previous provenance studies of the Pottsville Formation have produced conflicting interpretations, and most have focused on strata below the conglomerate measures targeted in the current study. The hypothesis I test in this thesis is: Sediments in the upper part of the Pottsville Formation were derived from the eastern areas of the Appalachian, including the eastern Piedmont and Carolina terrane (Fig. 1).

The current research involves petrofacies evaluation of the upper Pottsville Formation in the Cahaba synclinorium in Alabama in order to determine the provenance of these siliciclastic sediments. This investigation focuses on conglomerate clasts in the so-called conglomerate measures (Pashin et al., 1995), and thus provides significant new information on the source terranes for the upper parts of the Pottsville Formation in this part of the Appalachian foreland basin. This study develops a more comprehensive model for the evolution of the southern Appalachians, including tectonic and geomorphic changes that controlled sediment routing into the Cahaba depocenter during the later stages of the Alleghenian continent-continent collision.

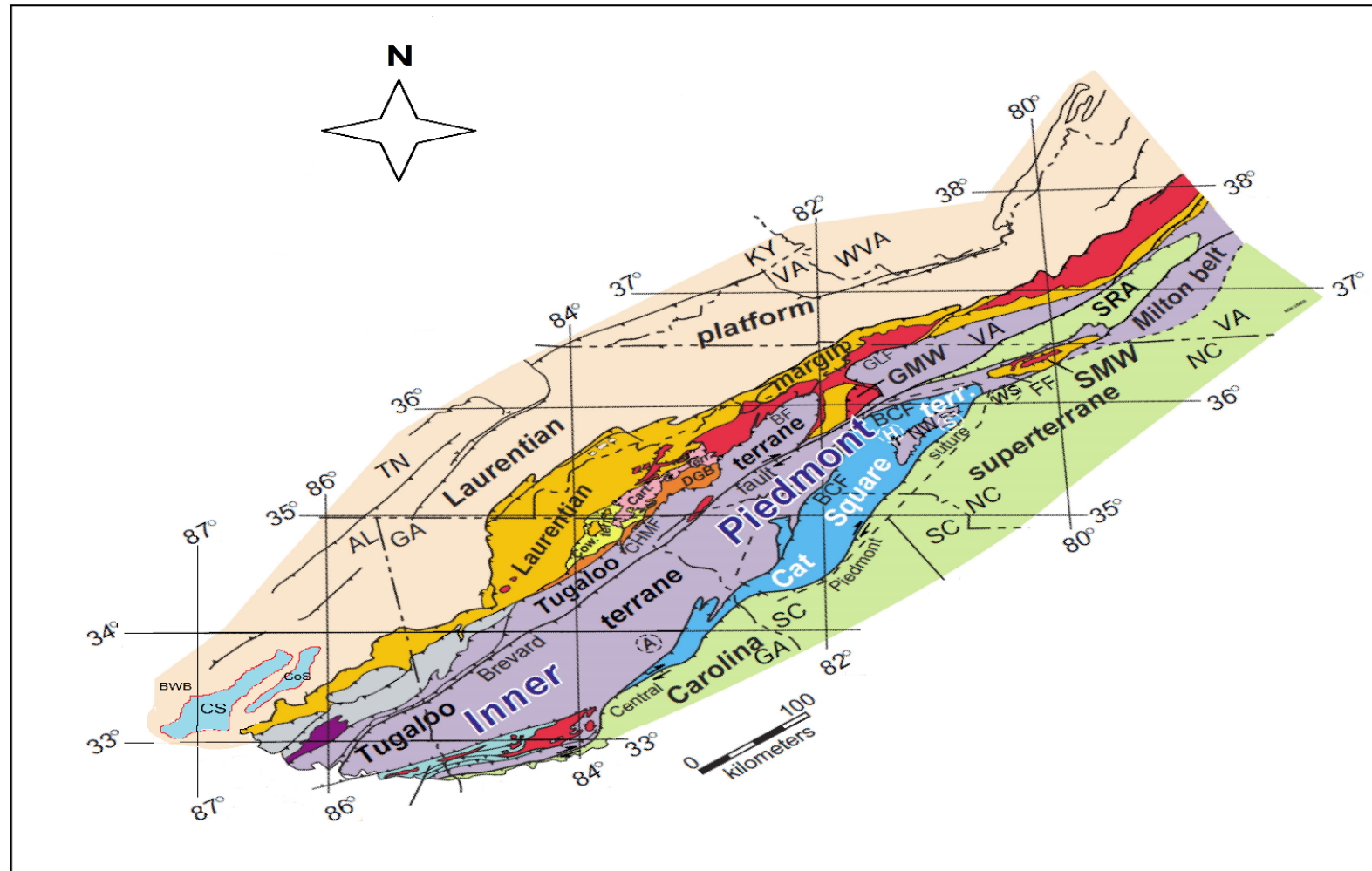


Figure 1: Map of the southern Appalachian region showing the location of Appalachian lithotectonic units including Piedmont and Carolina superterrane. BWb, CS, and CoS show the locations of Black Warrior basin, Cahaba synclinorium and Coosa synclinorium, respectively (modified after Merschat, 2009).

1.2 Provenance Study of Conglomerate

Provenance studies of sedimentary sequences deposited on the flanks of mountain belts can provide important information on mountain-building processes and the unroofing history of mountain belts (Uddin and Lundberg, 1998). Syntectonic sediments also record the unroofing history of related thrust systems (Da'vila and Astini, 2007; Graham et al., 1986; DeCelles et al., 1987; Beck et al., 1988; DeCelles, 1988). Provenance studies of foreland strata provide valuable information on both location and composition of adjacent source areas and on the pathways of transport from source to basin (Graham et al., 1975; Basu, 1985; DeCelles et al., 1993). Synorogenic sediments provide a unique opportunity to reconstruct paleogeography and tectonic setting of orogenic belts (Da'vila et al., 2004). These sediments are important for paleogeographic reconstructions, constraining lateral displacements in orogens, characterizing crust that is no longer exposed, testing tectonic models for uplift at the fault block or orogen scales, mapping depositional systems, sub-surface correlation, and predicting reservoir quality (Haughton et al., 1991). Thus, provenance data can aid in paleogeographic reconstructions and in modeling tectonic exhumation in adjacent uplands (Graham et al., 1986; DeCelles, 1994).

Over the last two decades, studies of clastic sediment provenance have undergone significant advances via the use of single-crystal isotope-dating techniques (Wandres et al., 2004). Many attempts have been made to determine the provenance of sedimentary rocks using sand-sized mineral grains (Ireland, 1992; Pell et al., 1997; Adams and Kelley, 1998; Ireland et al., 1998; Cawood et al., 1999; Sircombe, 1999;

Pickard et al., 2000). However, in some cases, sand- and mud-sized sediment may be transported over thousands of kilometers, resulting in potential problems and ambiguities in provenance studies (Bassett, 2000).

Coarse-grained rocks, notably conglomerates, reflect transport over comparatively short distances and, therefore, their composition may be more reflective of proximal sources (Kodama, 1994; Ferguson et al., 1996). Conglomerates contain clasts that are direct relicts of their source rocks and may not have traveled far from their source areas. Hence, these coarser clastic deposits can provide significant information about source terrains. However, most previous investigations of the Pottsville Formation have been restricted to the lower parts, in sequences that lie below the conglomerate measures of the Cahaba Basin, and thus most existing Pottsville provenance data have been obtained from studies of sandstones. The main stage of classic ‘molasse’ sedimentation expressed in the upper Pottsville Formation, including the abundant and thick alluvial deposits with coarse polymict conglomerates, has not been well studied. This current study focused on the conglomerate measures of the upper Pottsville Formation, with the goal of providing information on the orogenic history of the southeastern parts of the Appalachians.

1.3 Study Area

The Appalachian Foreland Basin includes three sub-basins with regard to the three Appalachian depocenters: (1) the northern Appalachian depocenter—the Dunkard Basin in Pennsylvania, Ohio and northern West Virginia; (2) the central Appalachian depocenter—the Pocahontas Basin in Virginia and southern West Virginia; and (3) the southern Appalachian depocenter—the Black Warrior basin,

Cahaba, and Coosa basins in Alabama and Mississippi. The latter three basins are together known as the Greater Black Warrior basin (GBWb) (Fig. 2).

The Black Warrior basin is a roughly triangular Carboniferous foreland basin located at the southern extremity of the Appalachian mountain belt and is flanked on the southeast by the folded and faulted Appalachian belt (Demko and Gastaldo, 1996). The GBWb consists of three sub-basins; the Black Warrior basin, the Cahaba basin and the Coosa basin (Fig. 3). The Cahaba basin, also known as the Cahaba synclinorium, is centered in eastern Bibb and southwestern Shelby counties, Alabama (Fig. 3). The basin is filled up by the southeast-thickening Mississippian and Lower Pennsylvanian sediments. Most of the Pennsylvanian rocks are assigned to the Pottsville Formation, which is ~ 2500 m thick in the central part of the basin (Hewitt, 1984). The Pottsville Formation overlies the Upper Mississippian-Lower Pennsylvanian Parkwood Formation throughout the Cahaba basin. It is locally unconformably overlain by the Upper Cretaceous Coker Formation of the Tuscaloosa Group (Pashin and Carroll, 1999). The accumulation of Pottsville strata occurred over a very short geologic interval. Gillespie and Rheams (1985) reported entire Pennsylvanian sequence to be Westphalian A (Moscovian) based on the record of plant fossils.

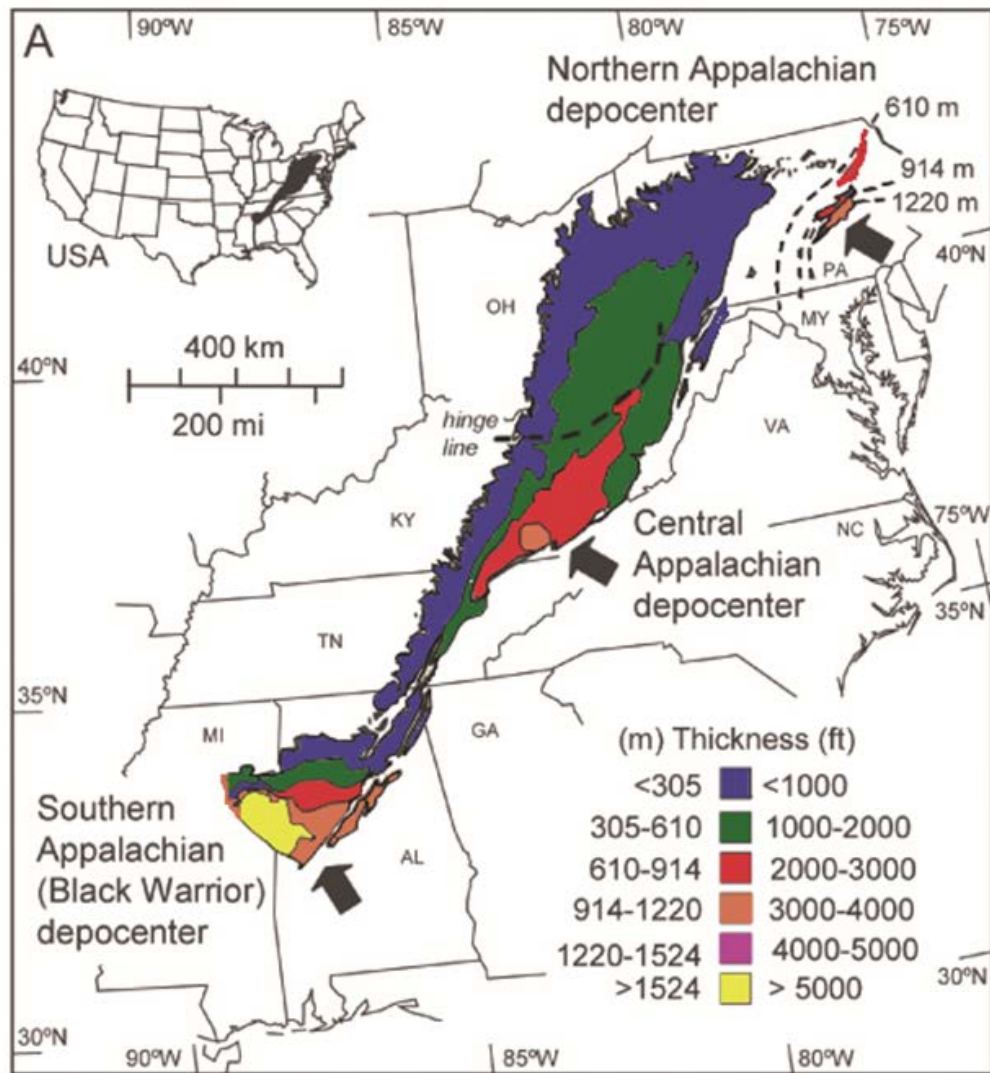


Figure 2: Map of Pennsylvanian paleogeography of Appalachian depocenters showing the thickness of Pottsville sediments in different Appalachian foreland basins (after Greb et al., 2008).

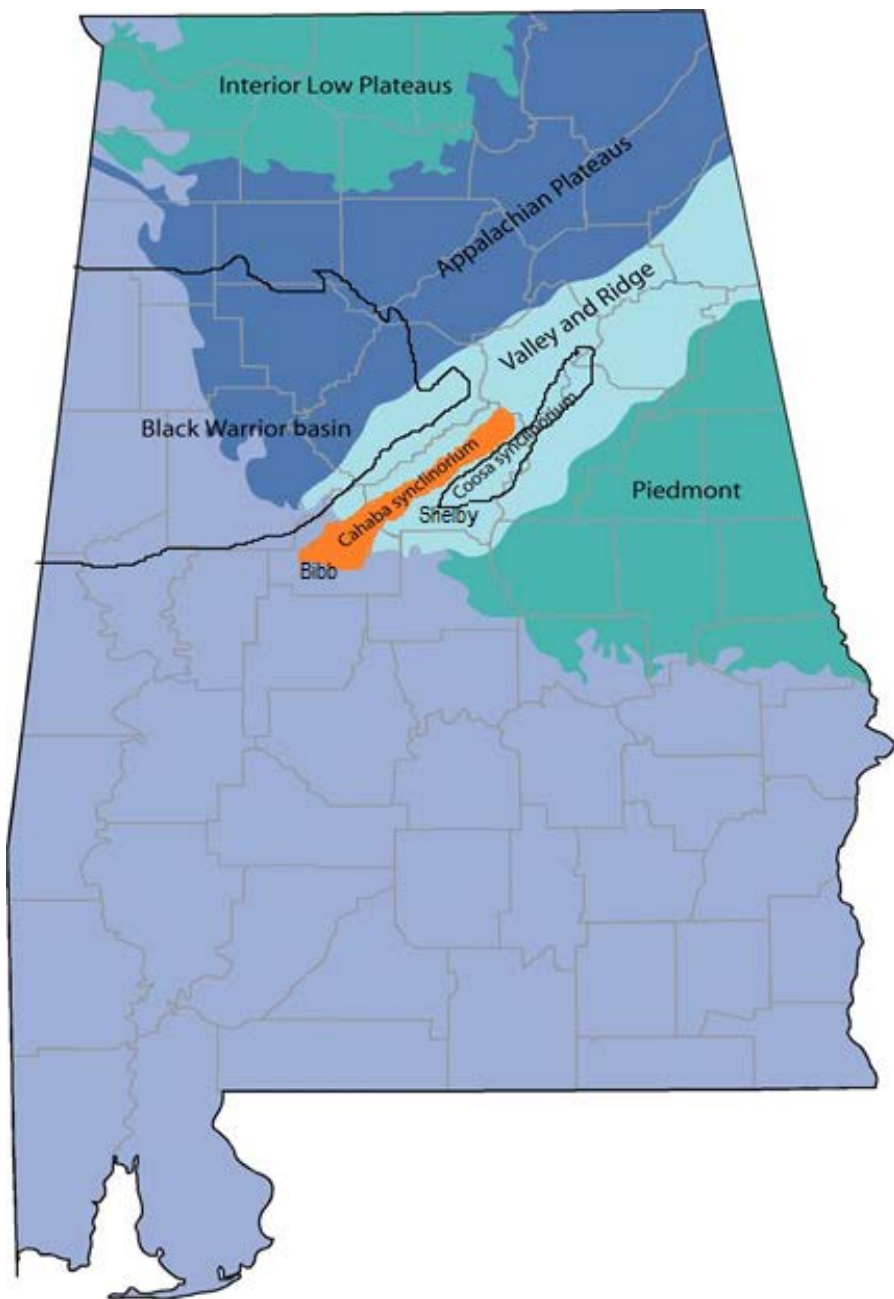


Figure 3: Location map of the Black Warrior basin, Cahaba synclinorium and Coosa synclinorium in central Alabama (not to scale).

1.4 Previous Studies

The depositional environments of the Pottsville Formation in Alabama have been reported by many as braid-delta fluvial plain/barrier bar/beach to upper delta plain

(Hobday, 1974; Demirpolat, 1989). In Cahaba basin, these cyclothemic clastic wedges are subdivided into three magnafacies based on their dominant lithology (Pashin et al., 1995). The upper unit, dominated by conglomerates, is known as the conglomerate measures. The lowermost conglomerate deposits of the conglomerate measures belong to the Straven Conglomerate (Fig. 4), located between the Gholson coal zone and the Thompson coal zone. The Straven Conglomerate is interpreted to represent bedload-dominated fluvial deposits (Osborne 1988, 1991). Petrological (provenance) studies of the Straven Conglomerate of the Pottsville Formation within the Cahaba basin indicate that the source area consisted of sedimentary rocks composed primarily of chert, carbonates, and sandstones with some volcanic, granitic, and metamorphic rocks presumably derived from the inner part of the Appalachian Piedmont (Osborne, 1988).

Although the Pottsville conglomerates are thought to be derived from early Alleghenian highlands, a previously unrecognized abrupt change in paleocurrent and sediment dispersal direction was documented by Robinson and Prave (1995) in central Pennsylvania in the central Appalachian foreland basin. They studied the paleocurrent pattern and stratal geometry and found older units display uniform northwest sediment transport, while younger units display a southwest transport direction. Based on asymmetric ripple marks and cross-bedding orientations, Demirpolat (1989) studied selected sandstones and conglomerates in the southern part of the Cahaba basin and suggested that sediment was transported from the southeast, which was probably the up-slope direction at the time of deposition. Schlee (1963) measured several hundred orientations of cross-beds in the basal Pennsylvanian Pottsville sandstone in the southern Appalachian mountains and, based on sediment-dispersal direction, inferred

an Appalachian source. Mack et al. (1983) mainly worked in the Black Warrior basin and found rock fragments containing foliated quartz-mica, unstable polycrystalline quartz, and polycyclic monocrystalline quartz, and concluded that the source-rock province was a low-grade metamorphic and sedimentary fold and thrust belt to the southwest (Ouachita). Using structural cross sections of the Pottsville Formation, Pashin and Carroll (1999) provided evidence for an Appalachian source (Fig. 5).

Some recent studies (e.g., Peavy, 2008; Moore, 2012) reported upper-grade metamorphic source terranes for the Pottsville Formation in Cahaba basin and Black Warrior basin, respectively. Moore (2012) also reported that the conglomerates in upper part of the basin were derived from proximal sources in Valley and Ridge, Piedmont, and Blue Ridge provinces. Peavy (2008) and Moore (2012) also reported $^{40}\text{Ar}/^{39}\text{Ar}$ single-crystal muscovite ages from several levels of the Pottsville that suggest cooling ages reflecting all three Appalachian orogenic events. Moore (2012) also found evidence of long-distance channels delivering sediments from the central and northern Appalachians to the Black Warrior basin. Gomes (2012) worked on sequence stratigraphy and petrofacies of the Pottsville Formation in the Cahaba basin and noted an increase in feldspar and lithic fragments in the upper part of the Pottsville Formation and suggested recycled orogenic source terranes to southeast (Appalachian).

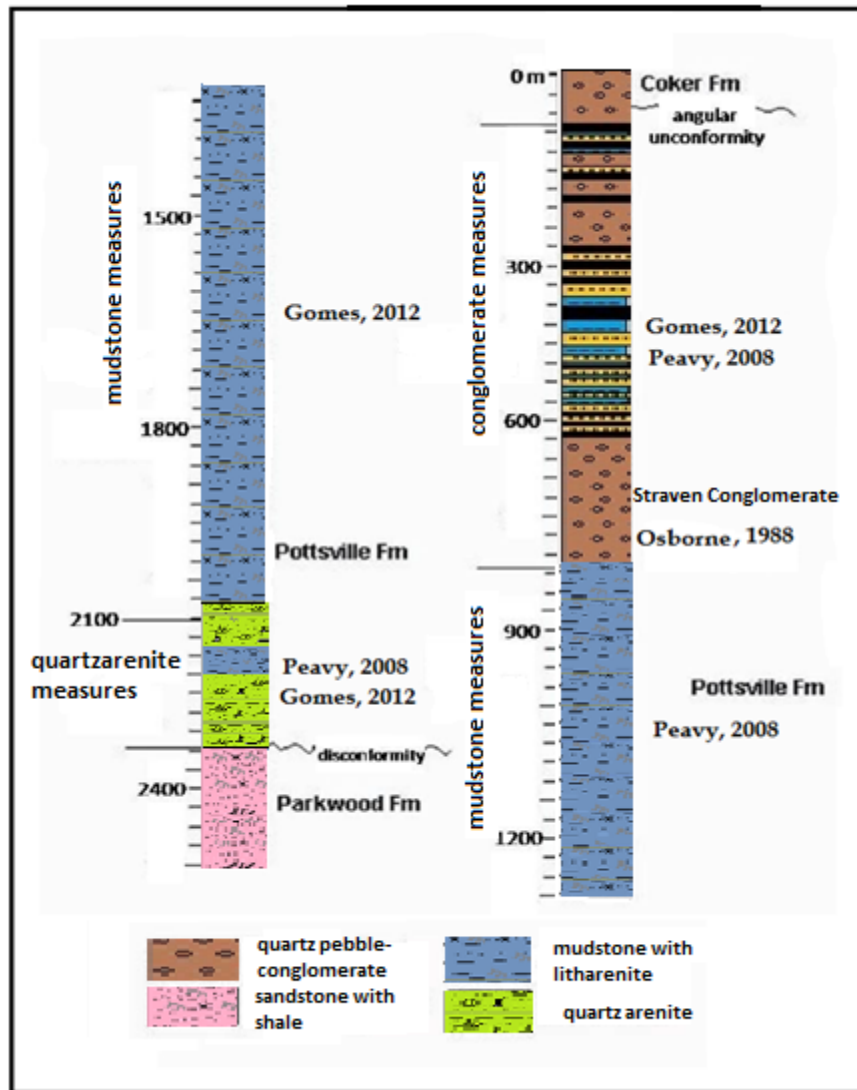


Figure 4: Generalized stratigraphic column of the Pottsville Formation in the Cahaba basin showing stratigraphic intervals examined by previous researchers (modified from Pashin et al., 1995; Peavy, 2008).

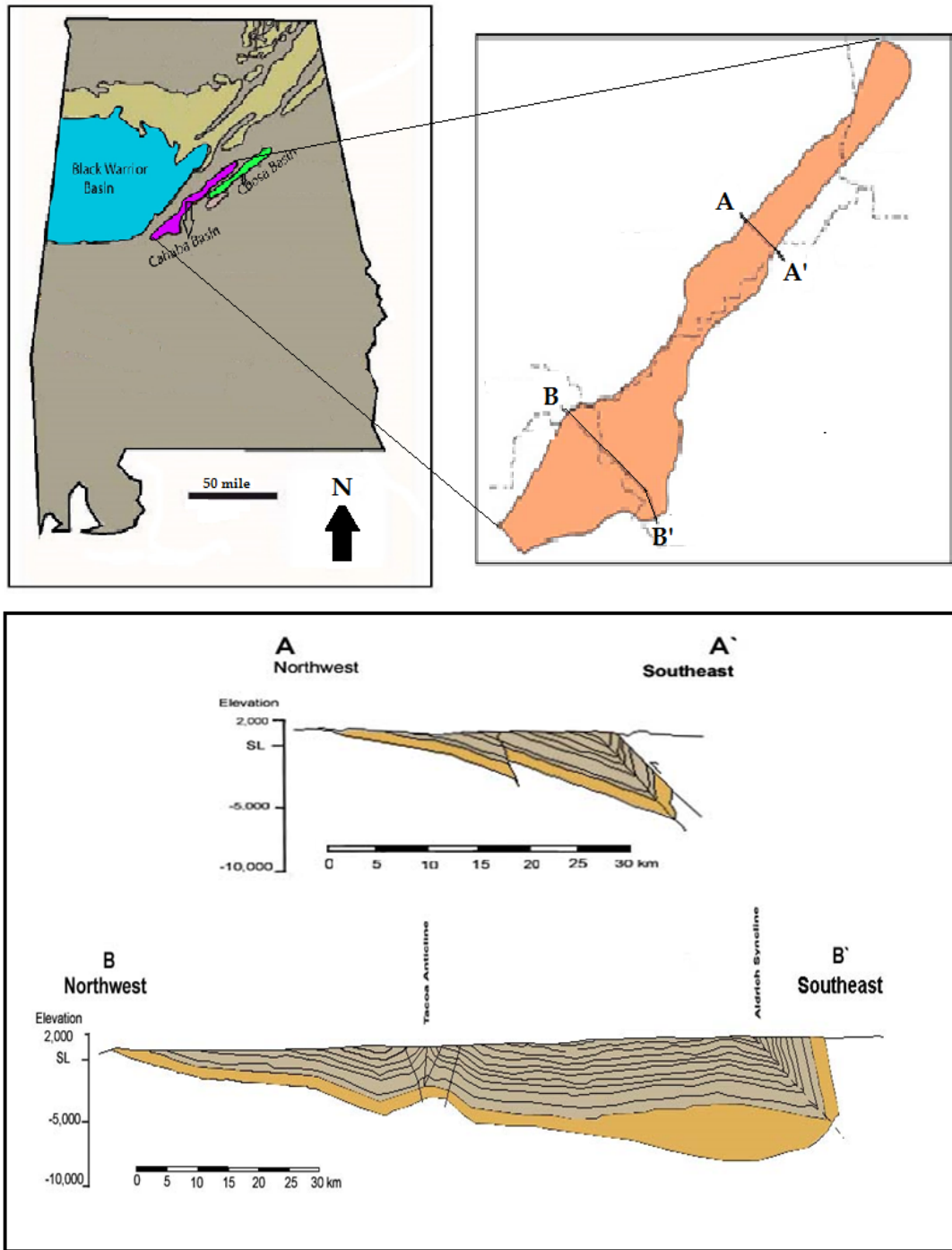


Figure 5: Structural cross sections of the Pottsville Formation in the Cahaba basin. The clastic wedge thickens to the southeast, indicating a source area located to the southeast (modified from Pashin and Carroll, 1999).

CHAPTER 2: REGIONAL TECTONIC SETTING AND FORMATION OF CAHABA BASIN

2.1 Introduction

The eastern margin of North America experienced two complete Wilson cycles; (i) the Proterozoic assembly and break up of Rodinia and (ii) the assembly and break up of Pangea (Thomas, 2005). During various phases of the assembly of Pangea various foreland basins developed along the convergent margin of the Laurentian craton, in response to three orogenies (Thomas, 1976; Chesnut, 1991). The first orogenic event, the Taconic orogeny, occurred during Middle Ordovician when an active volcanic arc collided with and was thrusted upon the eastern margin of Laurentia. The second orogenic event, the Acadian orogeny, occurred during Middle Devonian when the Avalonian microcontinent collided with Laurentia. The third and final orogenic event, the Alleghenian orogeny, occurred during the Pennsylvanian-Permian, when part of Gondwana collided with Laurentia and formed the Appalachian and Ouachita mountains (Figs. 6 and 7).

The Appalachian-Ouachita orogenic belt records all three successive orogenies (Drake et al., 1989; Hatcher et al., 1989). The collision of southern Laurentia with a Gondwanan arc-system during the Late Devonian-Pennsylvanian resulted in the formation of the Ouachita mountain range (Graham et al., 1975; Poole et al., 2005). The Appalachian foreland basins were formed due to episodic thrusting and orogenic sediment loading during these successive orogenies (Fig. 7). The Greater Black Warrior basin is in the southern Appalachian foreland basin that formed in response to the Alleghenian-Ouachita orogeny during the Mississippian-Pennsylvanian.



Figure 6: The rotational transpressive collision of Gondwana with Laurentia to form the supercontinent Pangea at the end of the Paleozoic. Features in red were active at the time indicated (after Hatcher, 2002).

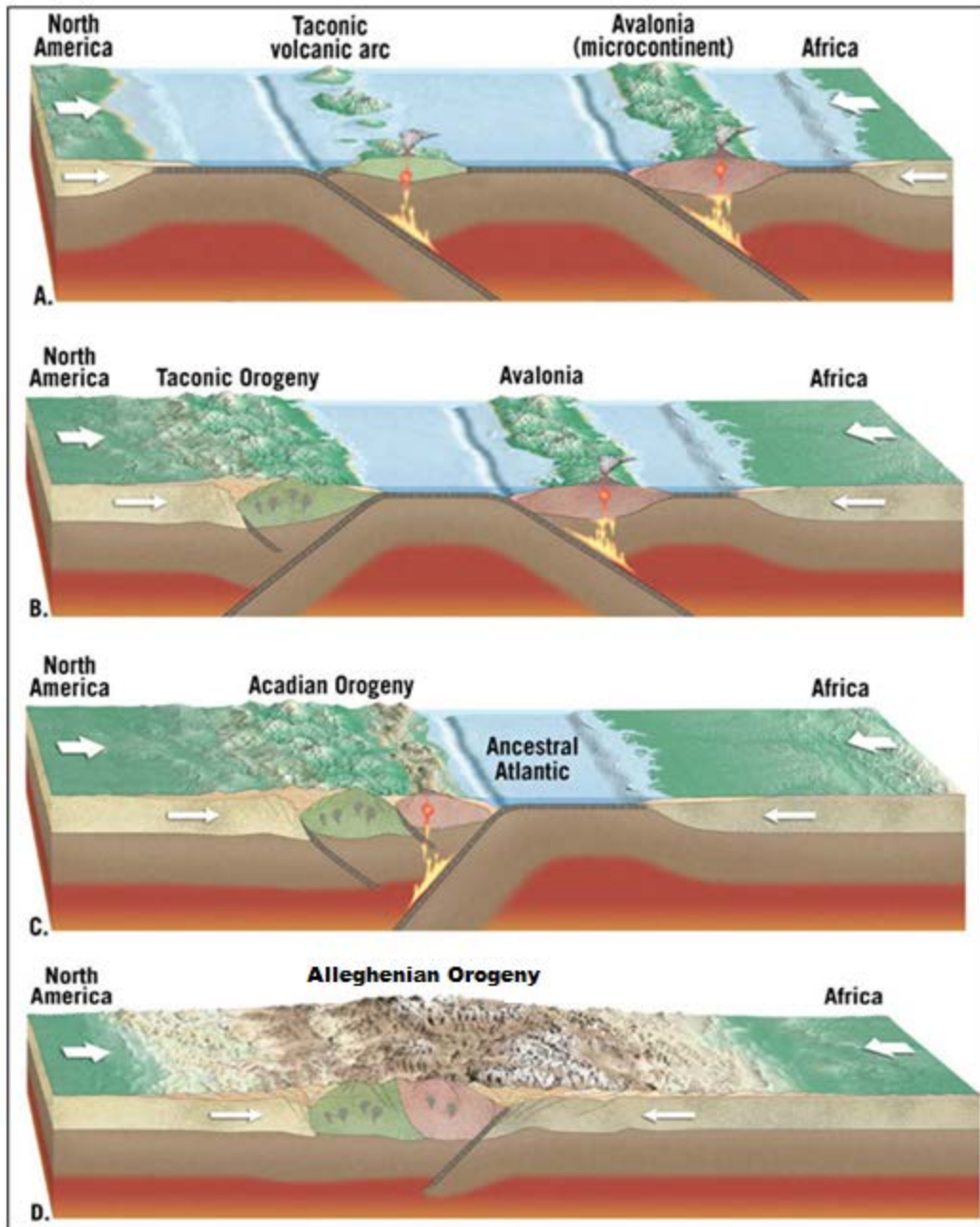


Figure 7: Tectonic models of Appalachian orogenies (from Lutgens and Tarbuck, 2015). (A) Pre-Taconic event when a volcanic arc, the microcontinent Avalonia, and Africa were converging towards North America. (B) Collision between a volcanic arc and North America (Taconic orogeny). (C) Collision between the microcontinent Avalonia and North America (Acadian orogeny). (D) Final collision between Africa and North America (Alleghenian orogeny).

2.1.1 Taconic Orogeny

The Taconic orogeny was the first of three mountain-building events that influenced formation of the Appalachian mountains in eastern North America. The Taconic orogeny was diachronous; earlier collision began in the southern Appalachians and younger deformation occurred in the central Appalachians (Hatcher, 2005). Subduction along the Laurentian margin resulted in the obduction of several oceanic and arc assemblages onto the margin during the Taconic orogeny (Figs. 7A and 7B). The Cowrock, Cartoogechaye, and Tulagoo terranes were emplaced in the southern Appalachians, and the Chopawamsic, Potomac, and Baltimore terranes were emplaced in the central Appalachians (Hatcher, 2002).

From the Cambrian to Early Ordovician, the eastern margin of North America was a carbonate platform flanked to the east by a continental slope and rise. An eastward thickening, shallow-water carbonate sequence was deposited in the platform area, whereas continental slope and rise were characterized by deep water argillaceous and arenaceous sediments with minor volcanics, carbonates, and cherts (Rowley and Kidd, 1981). During Middle Ordovician to Early Silurian, the closing of the Iapetus Ocean triggered the convergence of Laurentia and an arc terrane (Fig. 7B) (Drake et al., 1989; Horton et al., 1989). During the Taconic orogeny, the carbonate platform was drowned, followed by the obduction of slope/rise allochthons and large ophiolite sheets (Bradley, 1989). Convergence also caused igneous intrusion and regional metamorphism, subduction of oceanic crust, obduction and arc accretion in the northern and southern Appalachians between 455-470 Ma. High-precision U/Pb zircon dating of felsic volcanics from Hillabee Greenstone of NE Alabama and Dahlonega gold belt of NE Georgia indicate a ~470 Ma

age (McClellan and Miller, 2000). During the Taconic collisions, flexure of North America also produced deep sedimentary basins that accumulated up to 300 meters of sediment in some areas; e.g., the Queenston Delta in New York and the Blount Group in eastern Tennessee.

2.1.2 Acadian Orogeny

The entire Appalachian orogen from Newfoundland to Alabama was affected by the Middle Devonian Acadian orogeny with varying intensities of deformation and metamorphism (Faill, 1985, 1997). After the Taconic collision, subduction along the Laurentian margin continued and the microcontinent called Avalonia was moving towards Laurentia (Fig. 7B). The Avalonia terrane was a composite of several terranes and made up of Late Precambrian to Early Paleozoic rocks. The collisions between Laurentia and various arc terranes between ca. 400-360 Ma are responsible for the Acadian orogeny, which was responsible for the formation of several Acadian foreland basins; i.e., the Michigan, Illinois, and Appalachian basins (Fig. 7C). The subsidence of Taconic foreland basin was also reactivated during the Acadian events. The Acadian orogeny also metamorphosed the Laurentian margin sediments (Hatcher et al., 2007).

Absolute age dating on several Appalachian terranes documents the metamorphism and magmatism associated with Acadian tectonism. The Cat Square Terrane and Carolina Superterrane were accreted to eastern Laurentia circa 400-360 Ma, during the Acadian orogeny (e.g., Hatcher et al., 2007). Miller et al. (2006) document plutonism of Acadian (377 Ma) age in the Eastern Blue Ridge of the southern Appalachians. Carrigan et al. (2001) and Bream (2003) also found zircons from the Blue Ridge and Tugaloo terranes

that contain metamorphic rim ages of 360-350 Ma, with deformation at 366 Ma. The effects of the Acadian orogeny and its role in the history of the southern Appalachians are poorly preserved due to the overprinting by plutonic and metamorphic activity, development of complex structural features, and lack of stratigraphic continuity (Osberg et al., 1989). Acadian rocks are also poorly exposed in the southern Appalachians and more easterly sections are covered by Coastal Plain sediments.

2.1.3 Alleghenian Orogeny

The Alleghenian orogeny is the youngest and most pervasive event that affected the Appalachians. The Alleghenian orogeny occurred when northwest Africa, a part of the supercontinent Gondwana, collided with the eastern part of North America, closing the Proto-Atlantic oceans (Fig. 7D). The Alleghenian collision resulted in several associated orogenies. These include: the Mauritanide, the complementary orogeny on the Africa continent opposite to the Alleghenian; the Ouachita, formed by the collision of South America with the Gulf Coast region; and the Hercynian, formed by the collision between Gondwana and southern Europe. During the Alleghenian orogeny, the hinterland of Africa was thrust up over the margin of North America.

Due to large-scale thrusting during the Alleghenian orogeny, considerable deposition and subsequent deformation of clastic sediments occurred in the central and southern Appalachian foreland basins (Thomas, 1976; Hatcher et al., 1989; Hatcher, 2002). The Pennsylvanian Pottsville Formation represents the Alleghenian clastic-wedge in the southern Appalachian basin, the deposition of which began during the early Alleghenian and continued up to the final faulting and folding stages of orogenies (Hatcher et al., 1989;

Thomas, 2005; Hatcher et al., 2007). Stratigraphic and structural data also suggest that low-relief synsedimentary structures formed in the Paleozoic rocks over basement structures and that basement faults subsequently influenced the position and geometry of large-scale Alleghenian thrust ramps (Osborne and Guthrie, 1986). Metamorphism and plutonism were also associated with the Alleghenian orogeny.

2.2 Cahaba Synclinorium

The Greater Black Warrior basin (GBWb) consists of three sub-basins; the Black Warrior, Cahaba, and Coosa basins. Initially, the GBWb was formed due to the flexural subsidence associated with the Ouachita orogeny during the Mississippian. A thick succession of Mississippian sediments was deposited and were latter unconformably overlain by Pennsylvanian Pottsville sediments (Thomas, 1976; Thomas and Mack, 1982). Thrusting and folding during the Alleghenian orogeny later separated the GBWb into several smaller structural basins, including the Black Warrior basin, Cahaba basin/synclinorium, and Coosa basin/synclinorium. During the Alleghenian orogeny the subsidence of the Black Warrior basin increased to the southeast (Figs. 5 and 8) (Pashin and Carroll, 1999; Pashin, 2004).

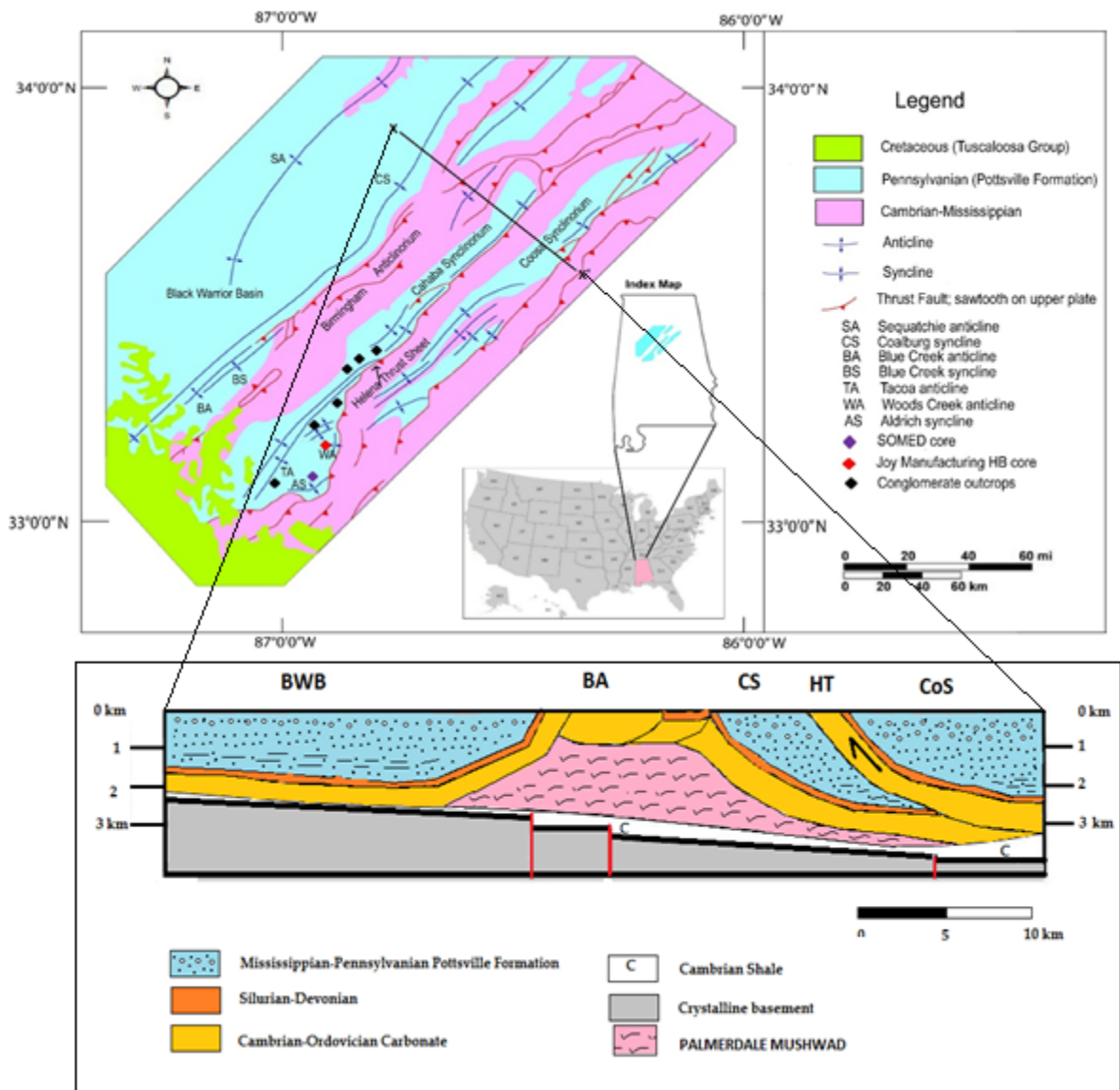


Figure 8: Generalized geologic map of Cahaba and adjacent basins and cross section along the Black Warrior basin (BWB) through the Coosa basin (CoS). The BWB and Cahaba synclinorium (CS) are separated by the Birmingham anticlinorium (BA), and the Cahaba and Coosa synclinoria are separated by the Helena thrust (HT). The inset map shows the location of Cahaba and Coosa synclinorium in central Alabama (modified from Thomas and Bayona, 2005; Pashin et al., 2010).

The Cahaba synclinorium is located in the Valley and Ridge province in central Alabama. The Valley and Ridge province in Alabama corresponds in part to the fold and thrust belt of the southern Appalachian orogen (Raymond et al., 1988). The fold and thrust belt in Alabama is subdivided into three domains; a northwestern domain, a central domain, and a southeastern domain (Thomas and Neathery, 1980; Thomas, 1982; Neathery and Thomas, 1983). In the central domain, the Birmingham anticlinorium shares a common limb with the Cahaba synclinorium on the southeast. Structurally, the Cahaba synclinorium consists of a series of anticlines and synclines (Squire, 1890). It is bounded by the Birmingham anticlinorium to the northwest, and by the regionally extensive Helena Fault to the southeast (Fig. 8).

Smith (1979) suggested that the Black Warrior and Cahaba basins, which are now separated today, were connected during Pennsylvanian. Outcrops of pre-Pennsylvanian rocks along the Birmingham anticlinorium separate the Pottsville Formation in the Cahaba basin from the Pottsville Formation to the northwest in the Black Warrior basin. However, there is disagreement as to whether the Black Warrior and Cahaba basins were separated during the deposition of the Pottsville Formation. Cooper (1964) concluded that the Black Warrior basin must have been separated from the Cahaba basin by a broad anticlinal swell during Pottsville time. Smith (1979) stated that several coal fields in Alabama, the Warrior, Plateau, Cahaba, and Coosa coal fields, were more or less continuous during Pennsylvanian time. The Helena fault involves at least 3000 m of stratigraphic displacement as it places Cambrian and Ordovician formations over the rocks of the upper part of the Pennsylvanian Pottsville Formation (Butts, 1940). Regionally the Pottsville Formation is overlain by upper Cretaceous Tuscaloosa Formation (Fig. 9).

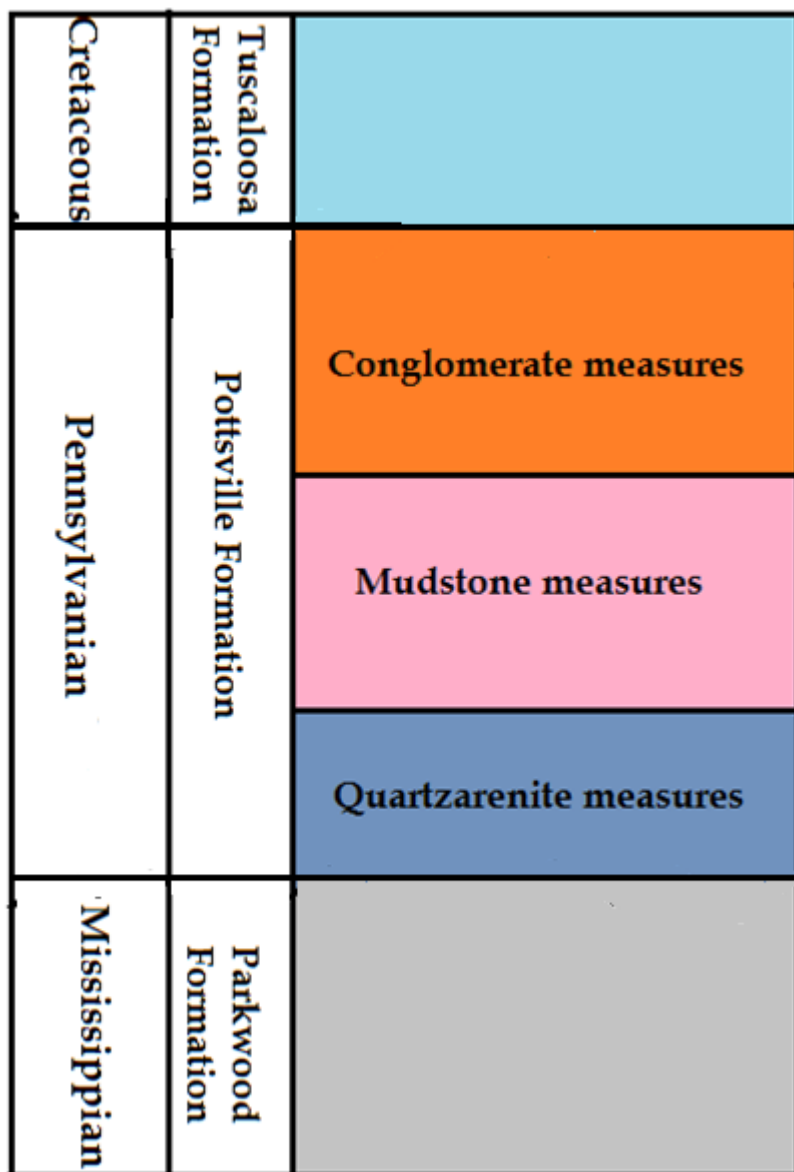


Figure 9: Generalized stratigraphic column of Cahaba basin.

2.3 Pottsville Formation

2.3.1 Introduction

Pennsylvanian Pottsville sediments extend from New York to Alabama and were deposited in all three Appalachian depocenters (Fig. 2). The maximum preserved thickness of Pottsville sediments is in the southern Appalachian or Greater Black Warrior depocenter (Greb et al., 2008). The Cahaba basin, a northeast-southwest orientated sub-basin of the Greater Black Warrior basin, holds a maximum of 2.5 km of Pottsville Formation. The Pennsylvanian Pottsville Formation is a clastic wedge deposited in the eastern United States in response to the collision of Laurentia and Gondwana. Sequences in the Pottsville Formation are cyclothemetic and consist of alternating sandstone, siltstone, claystone, shale, coals and conglomerates (Mack et al., 1983). Pashin et al. (1995) subdivided the cyclothemetic clastic wedges of the Cahaba basin into three major magnafacies (Fig. 10): (1) the lower sandstone-dominated quartzarenite measures; (2) the middle mudstone-dominated mudstone measures; and (3) the upper conglomerate-dominated conglomerate measures.

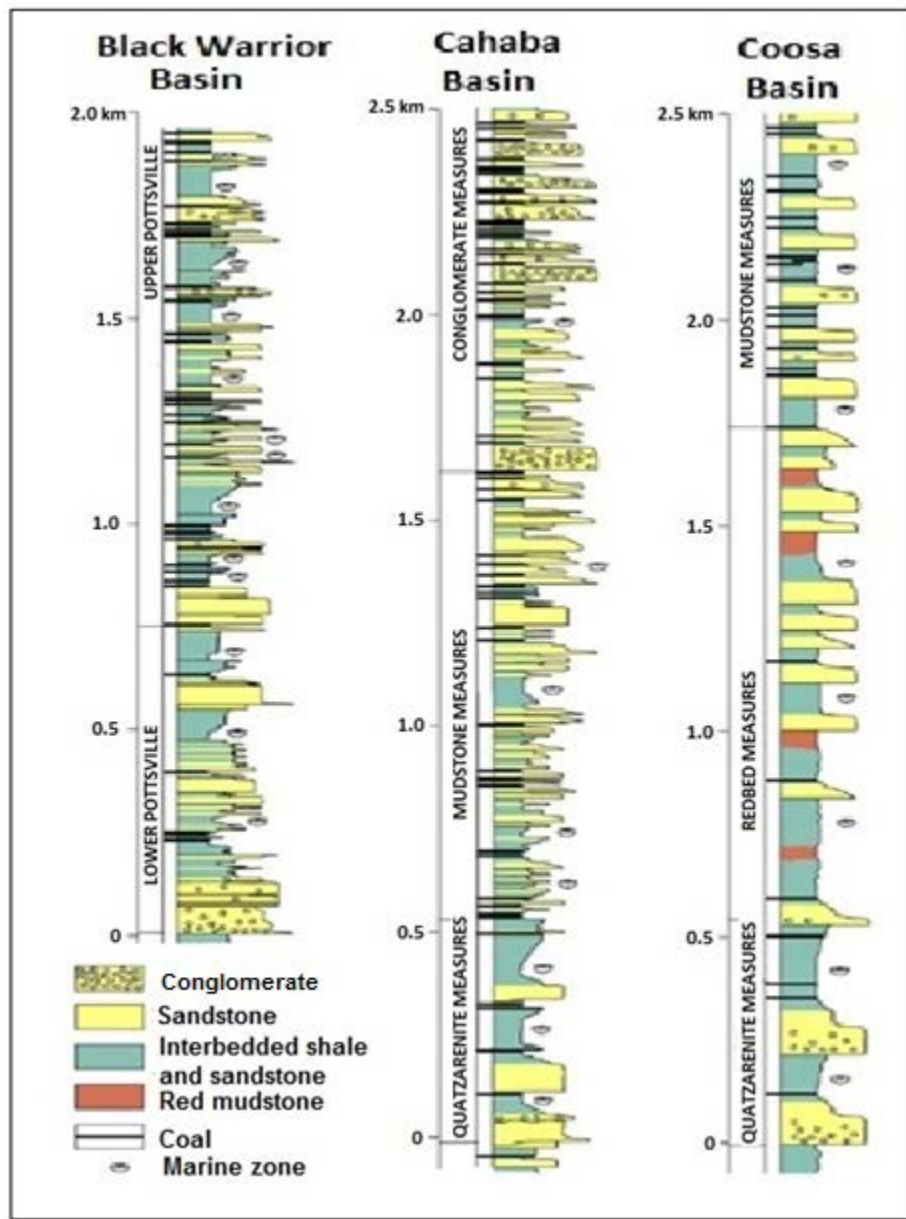


Figure 10: Composite stratigraphic section for the Cahaba synclinorium and adjacent basins. Three magnafacies of the Pottsville Formation—lower quartzarenite measures, middle mudstone measures, and upper conglomerate measures—were delineated in the Cahaba basin by Pashin et al. (1995).

2.3.2 Conglomerate Measures

The conglomerate measures, the focus of the current study, is up to ~800 m thick and consists mainly of conglomerate, sandstone, shale and coal. The lowermost conglomerate unit of the conglomerate measures is called the Straven Conglomerate located between the Gholson and Thompson coal zones (Fig. 11). The Straven Conglomerate Member is the lowermost widespread conglomerate in the Pottsville Formation and is used as a key marker for mapping and correlation (Butts 1927, 1940).

Coarse clastic rocks of the conglomerate measures include extraformational conglomerates with lithoclasts of chert, schist, gneiss, and volcanics and intraformational conglomerates with clasts of mudstone, siderite, sandstone, coal, and fossil logs (Osborne, 1988, 1991; Demirpolat, 1989; Pashin et al., 1995).

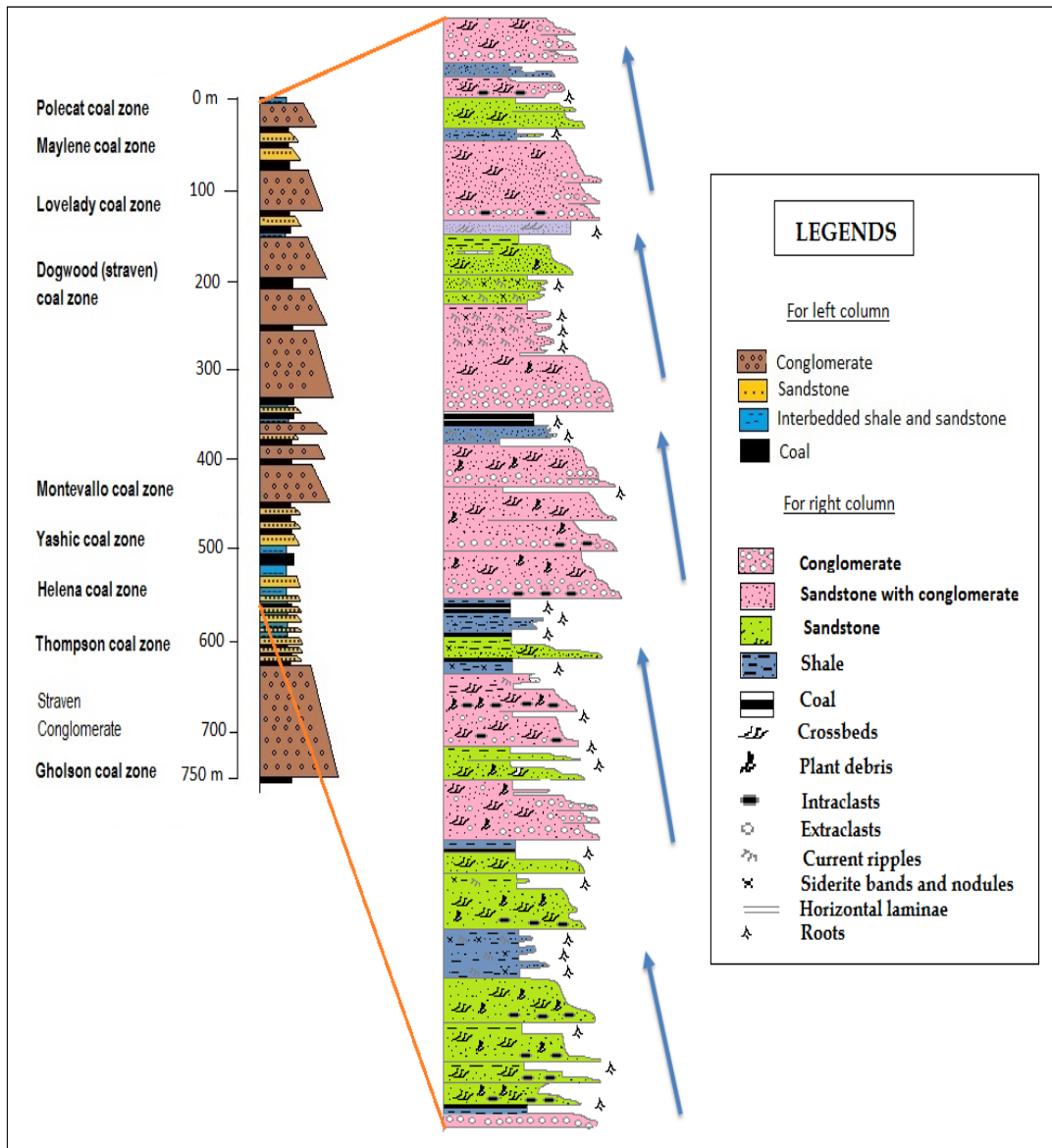


Figure 11: The right column shows the generalized stratigraphic column of the conglomerate measures of the Pottsville Formation in Cahaba synclinorium. The left column shows the cyclothem sequences measured from Helena through Maylene coal zones in the Joy Manufacturing H.B (JMHB) core. Blue arrows show fining upward sequences that indicate long-term aggradation in fluvial systems (modified from Pashin et al., 1995).

2.3.3 Depositional Environment of Conglomerate Measures

The conglomerate measures is the product of braidplain-anastomosis cycles in which aggradation of widespread bedload-dominated fluvial systems led to the development of anastomosed fluvial systems and, ultimately, major peatlands represented by the coal seams. The lower Pottsville sediments primarily consist of orthoquartzitic sandstone and was deposited in a prodelta/barrier/back-barrier system, whereas the upper coal-bearing strata were deposited in a fluvial-dominated deltaic system (Smith, 1979; Horsey, 1981; Rheams and Benson, 1982). The depositional environments of the Pottsville Formation in Alabama have been reported by many as braid-delta fluvial plain/barrier bar/beach to upper delta plain (Hobday, 1974; Demirpolat, 1989). Osborne (1988, 1991) interpreted the Straven Conglomerate as bedload-dominated fluvial deposits.

The abundance of extraformational conglomerate indicates continued unroofing and extensive alluvial plain deposition. The overall fining upward sequence (Fig. 11) also indicates long-term aggradation of fluvial systems and a transition from a coarser-grained braided plain to a finer-grained braidplain (Pashin et al., 1995). Coal beds in the conglomerate measures accumulated in interfluvial swamps. The thick, finer-grained succession above the Straven Conglomerate member, which includes the Thompson, Helena, and Yeshic coal zones (Fig. 11), indicates a partial return to coastal-plain conditions (Pashin et al., 1995). Cross-bed and pebble-imbrication paleocurrent data from the conglomerate measures suggest an eastern to southeastern source (Osborne, 1988; Demirpolat, 1991). The presence of marine strata between the Yeshic and Helena coal zones document a short-lived marine transgression (Fig. 11).

2.3.4 Core Locations

Conglomerate samples were collected from the two drill cores—the Joy Manufacturing H.B. (JMHB) and School of Mines and Energy Development (SOMED) cores—both achieved at the Geological Survey of Alabama in Tuscaloosa. The latitude and longitude of Joy Manufacturing H.B. core is approximately 33°11' N and 86°53' W. The location of SOMED is SE1/4, SW1/4, SE1/4, NE1/4, Sec 15, T22S and R4W in Pea Ridge Quadrangle, which is approximately 33°07' N latitude and 86 °56' W longitude. Figure 12 shows the location of JMHB and SOMED drill wells, and Figures 13 and 14 show the representative core from which samples were collected.

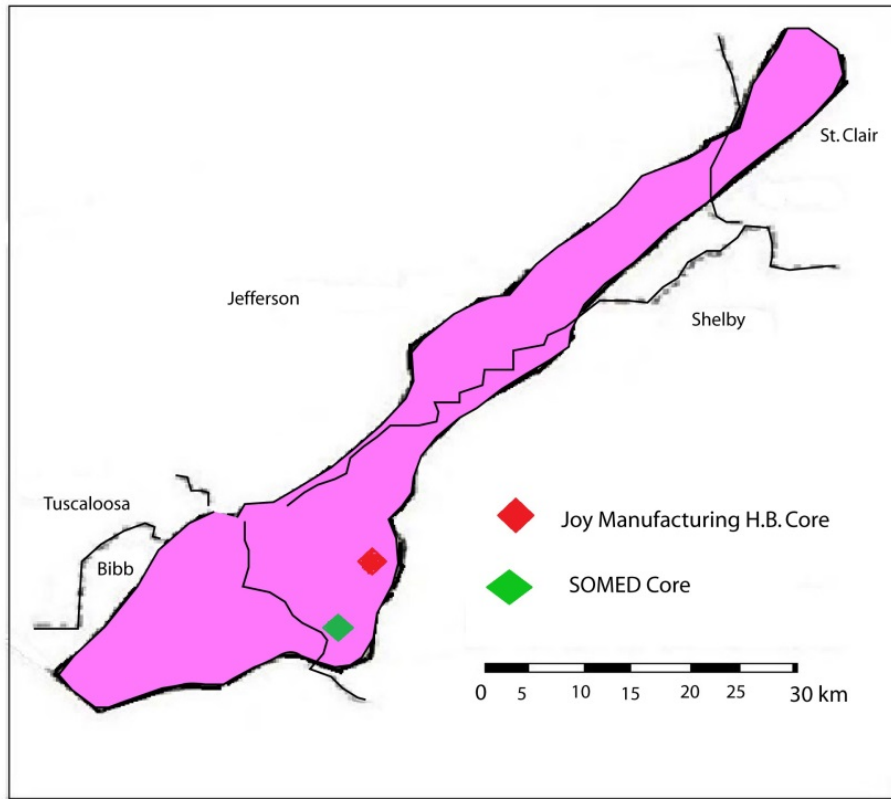


Figure 12: Location of the two drill cores in the Cahaba basin (purple). Green diamond shows the location of SOMED core and red diamond shows the location of Joy Manufacturing H.B. core.



Figure 13: Cores of the Pottsville conglomerate measures, Joy Manufacturing H.B. core.



Figure 14: Representative core samples of the Pottsville conglomerate measures collected from SOMED core.

CHAPTER 3: CONGLOMERATE PETROGRAPHY

3.1 Introduction

Qualitative petrographic study provides important information on the nature of the source areas. In order to decipher the provenance of sedimentary deposits, sedimentary petrologists identify and quantify the mineralogic and textural constituents of a rock. Extensive work has been done on analysis of sandstones (e.g., Basu et al. 1975; McBride, 1985; Uddin and Lundeberg, 1998) in order to delineate mineralogy of source rocks. Sandstone petrography is widely used to infer the paleotectonic setting and provenance of ancient clastic sequences. Relationships between sandstone modal analysis and tectonic setting are well established (Dickinson and Suczek, 1979; Ingersoll and Suczek, 1979; Dickinson, 1985). Conglomerates contain clasts that are direct relicts of the source rocks and that may not have traveled far from source areas. Conglomerate clasts typically are small pieces of the source rock, as opposed to the individual mineral grains. Hence, they are useful for delineating source materials (Moore, 2012).

In this chapter, the petrography and modal analysis of conglomerates of the upper Pottsville Formation from the Cahaba basin is described. This analysis mainly focuses on detailed petrography and quantification of the constituent lithic clasts and sand-sized grains (matrix) of Pottsville conglomerates to evaluate the provenance of these siliciclastic sediments.

3.2 Methodology

Twenty-five conglomerate samples were collected from intervals between the Gholson to Thompson coal zones and between the Yashic to Polecat coal zones in two cores; thirteen samples were collected from the Joy Manufacturing H.B (JMHB) core and twelve samples were collected from the SOMED core. Core samples were collected from the upper conglomerate magnafacies defined by Pashin and Carroll (1999). The generalized stratigraphic column of the conglomerate measures with the coal zones and the core locations are shown in figures 11 and 12. Core samples were processed in the Department of Geosciences rock processing laboratory at Auburn University, and conglomerate slices were sent to Spectrum Petrographic Inc. for thin-section preparation.

Standard 30-micron-thick thin sections were made for petrographic analysis. The clast types and matrix were identified in each of the conglomerate samples. The size and shape of the pebbles also were documented. Since conglomerate contains original clasts of the source rocks, the quantification of percentages of various clasts was important to infer the sediment-source terranes. To quantify the volume percentages of various clast types versus the volume of matrix, a grid technique was used (Fig. 15). To calculate clast percentages, a total of twenty equal-area squares (grids) were plotted on a highly transparent plastic film similar in size to the thin sections. Each of the square grid represents five percent (5%) of the total thin-section area. Conglomerate thin sections were studied under a petrographic microscope to identify the clasts and matrix compositions and then the film was put on top of the thin sections to calculate the percentage of different clast types. Clasts percentage was counted in each of the grids and then added together to get the total percentage of each type of clast in the thin section. The following compositional

parameters were distinguished among both clasts and sand matrix as appropriate: monocrystalline quartz (Qm); polycrystalline quartz (Qp); sedimentary lithics (Ls) and their types; metamorphic lithics (Lm); volcanic and plutonic lithics (Lv and Lp) and their types; metamorphic lithic fragments (Lm); plagioclase; k-feldspar; chert; and calcite. Special care was paid to the classification of lithic fragments and feldspar types (Pettijohn et al., 1987; Uddin and Lundberg, 1998).

To determine the provenance fields of the sand-sized grains, modal compositions of sands in the conglomerate matrix were plotted on standard ternary diagrams (Qt-F-L, Qm-F-Lt, Qm-P-K, and Qp-Lv-Ls etc.) following the approach of Dickinson and others (Dickinson, 1970, 1985; Dickinson and Suczek, 1979). Detrital framework grains of sandstones, plotted on different ternary diagrams, can be used to discriminate various tectonic settings and to interpret plate interactions in the geologic past (Graham et al., 1976; Dickinson and Suczek, 1979). The provenance fields of the sand-sized grains (matrix) were compared with previous provenance analyses of sandstones from other parts of the Pottsville Formation. Deformation textures are also documented in metamorphic clasts and used to delineate provenance. Table 1 shows the compositional parameters used to draw ternary diagrams.

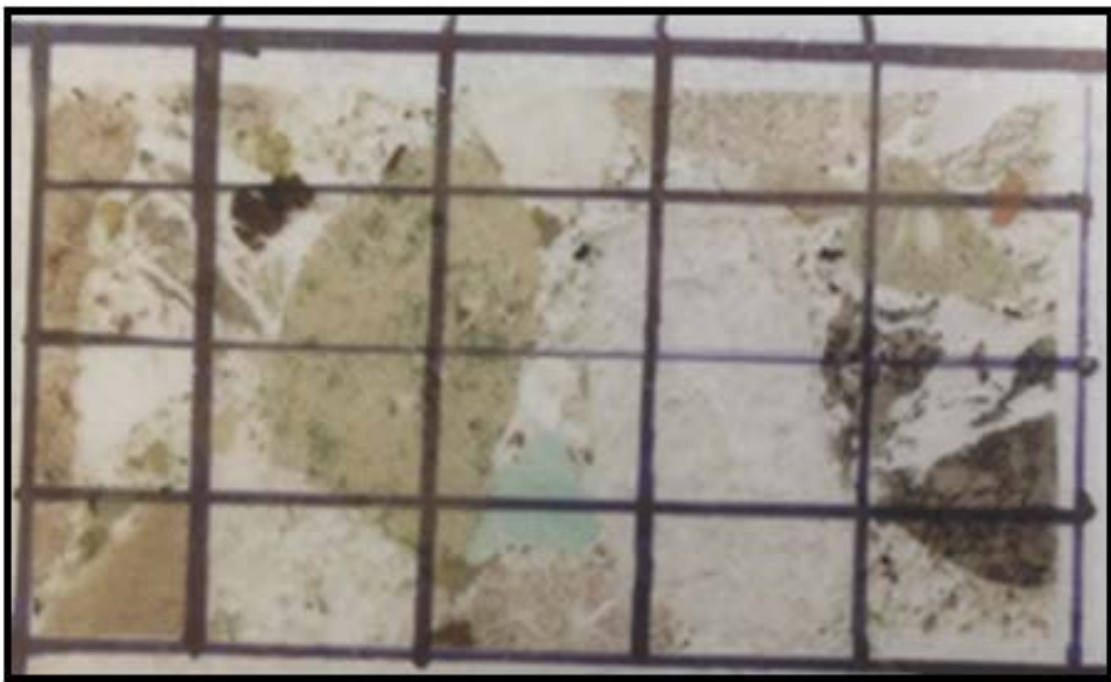


Figure 15: Grid technique used to quantify the volume percentage of various clast types versus the volume of matrix in the conglomerate thin sections. Each of the square grids represents five percent (5%) of the total thin-section area. Clast percentage was counted in each of the grids and then added to get the total percentage of each type of clast in the thin section.

Table 1: Recalculated compositional parameters for sand-sized grains (matrix) used in this study. Primary parameters are after Graham et al. (1976), Dickinson and Suczek (1979), Dorsey (1988), and Uddin and Lundberg (1998).

Qt = Qm + Qp , Where, Qt = total quartzose grains Qm = monocrystalline quartz (> 0.625 mm) Qp = polycrystalline quartz (including chert)
Feldspar Grains (F=P+K) , where, F = total feldspar grains P = plagioclase feldspar grains K = potassium feldspar grains
Unstable Lithic Fragments (Ls, Lv , Lm) , where, Lt = total unstable lithic fragments and chert grains Lv = volcanic/metavolcanic lithic fragments Ls = sedimentary lithic fragments Lm = metamorphic lithic fragments

3.3 Conglomerate Clast Petrography

Conglomerates are the dominant lithology in the conglomerate measures of the upper Pottsville Formation. Clasts in conglomerates of the upper Pottsville Formation mainly consist of chert, sedimentary (sandstone and mudrock) and metasedimentary (phyllite, schist, quartzite) lithic fragments, and volcanic and plutonic rock fragments (e.g., andesite and tonalite). Clasts are usually large and sub-rounded to well-rounded and mostly granule to pebble sized (Figs. 13 and 14). The composition of Pottsville conglomerates varies with stratigraphic position (Figs. 16 and 17). Chert and sedimentary lithic fragments are the dominant clast types present in the conglomerate samples (>50%). However, they become less abundant up-section as the contribution of metamorphic clasts (about 5-30%) increases. After chert, sedimentary lithics (i.e., sandstone and shale) are the most common clasts type present in the conglomerate. Conglomerate clasts in the conglomerate samples from stratigraphically lower intervals overwhelmingly consist of quartzose sandstone lithics, with lesser amount of metamorphic and igneous clasts. These quartzose grains are mostly chert, polycrystalline quartz, or vein quartz. The percentage of igneous clasts (5-12%) remains almost constant throughout the conglomerate measures.

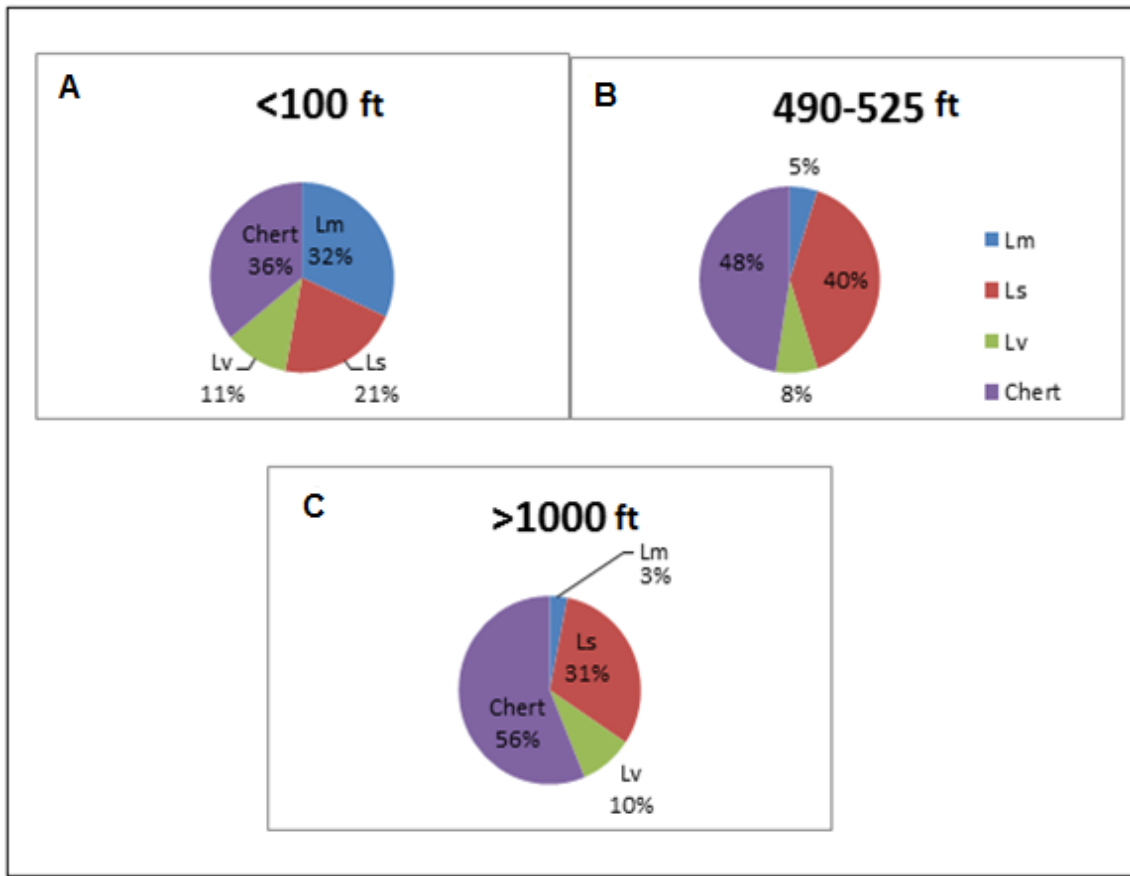


Figure 16: Pie diagrams showing the average percentages of different clasts in conglomerate samples with stratigraphic position (core depth) in the conglomerate measures from both cores. (A) Percentages of clasts from depths less than 100 ft, (B) Percentages of clasts in the depth range of around 500 ft, and (C) Clast percentages at depths greater than 1000 ft. (Lm = metamorphic clasts, Ls = sedimentary clasts, Lv = volcanic clasts).

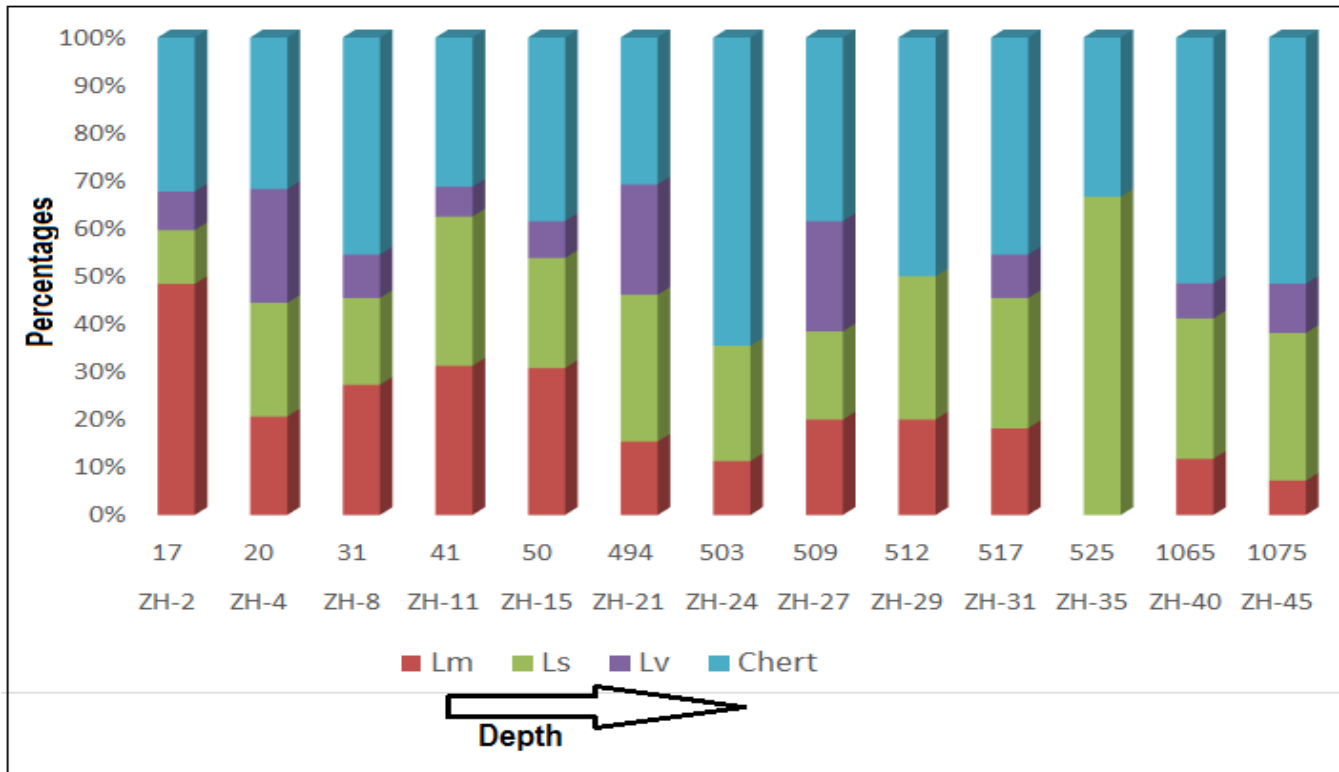


Figure 17: Bar diagrams showing the percentages of different clast types in conglomerate samples with depth (in feet) in Joy Manufacturing H.B core.

3.3.1 Igneous Clast Lithology and Petrography

Igneous clasts are less abundant among the clasts present in conglomerate samples of the upper Pottsville conglomerate measures. Igneous clasts, both volcanic and plutonic, comprise only 5-12% (average = 7%) of total clasts in the studied conglomerates. Volcanic clasts are mostly andesite and tonalite with minor dacite. Volcanic clasts exhibit a texture of plagioclase laths, and most of the volcanic clasts contain phenocrysts of feldspar and/or quartz (Fig. 18). Plagioclase crystals are acicular and mostly 0.1 mm to 0.3 mm long. A few metavolcanic clast also were observed and these contain the relict texture of plutonic igneous rocks. Igneous clasts have a brownish appearance in plane-polarized light and are dark to dark brown under crossed polarized light. The sizes of the igneous clasts are relatively small compared to the other clast types. They are sub-rounded, indicating a long travel distance. No pyroclastic textures were observed and the presence of smaller plagioclase crystals suggest a rapid cooling.

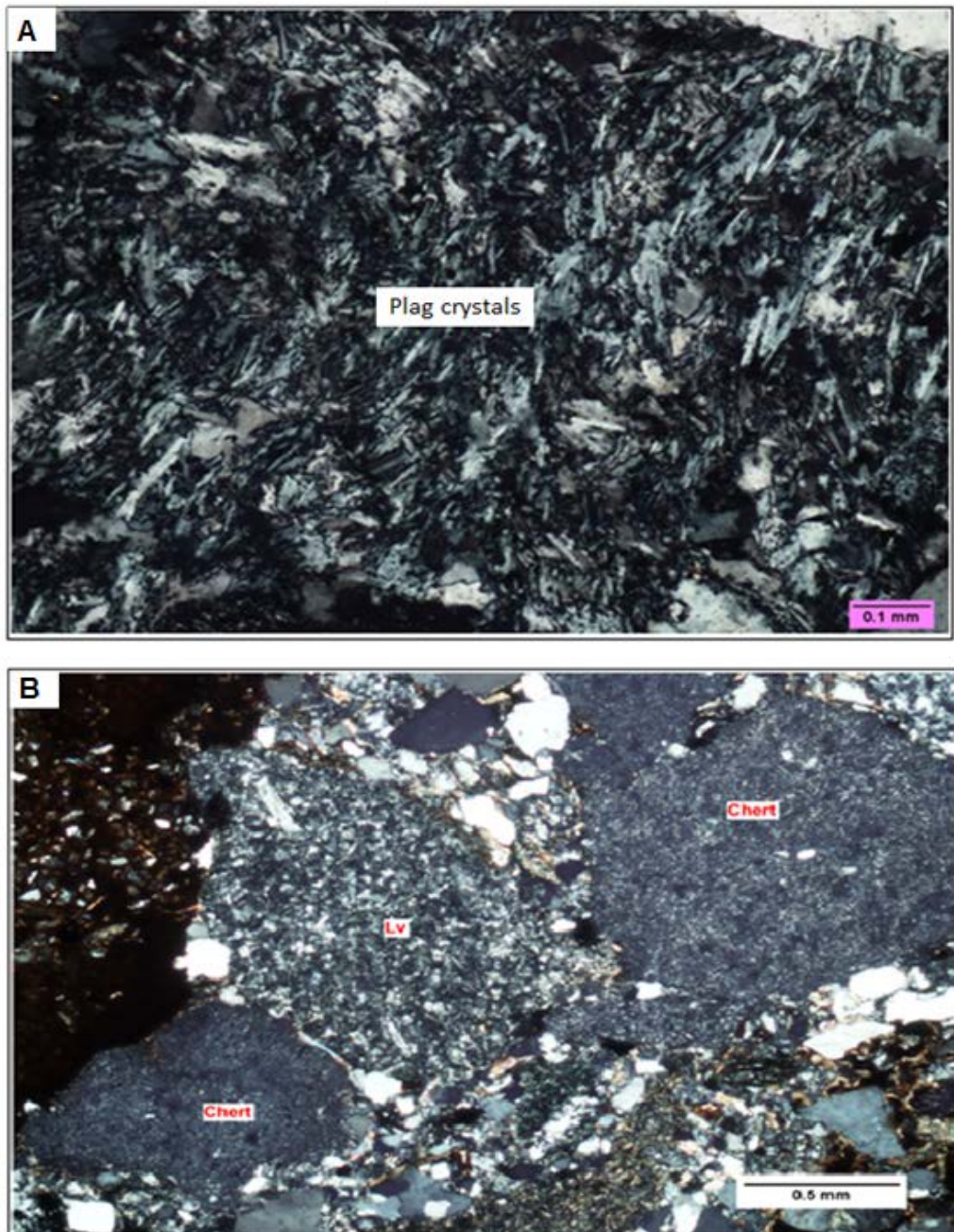


Figure 18: Representative photomicrographs from conglomerate samples showing volcanic clasts and other clast types in the Pottsville conglomerate measures. Most of the feldspar lacks observable twinning, however, polysynthetic and simple twins are visible in a minority of crystals suggesting both plagioclase and sanidine are present. (A) Laths of plagioclase and sanidine crystals. (B) Volcanic clast (Lv) and chert. Volcanic clasts are mainly dacite and andesite.

3.3.2 Metamorphic Clast Lithology and Petrography

Metamorphic clasts are the second most dominant lithology after sedimentary lithic fragments in the conglomerate measures. The percentage of metamorphic lithics varies with depth. Metamorphic lithics become more abundant upward through the conglomerate measures. Metamorphic clasts constitute about 5% of the conglomerate in the lower samples but increase up to 32% in upper samples. Metamorphic clasts dominantly consist of quartzite and low grade- to medium-grade metasedimentary rocks (i.e., phyllite and schist etc.) (Figs. 19 and 20).

Quartzites are the most common metamorphic clast types present in the conglomerates. They mostly consist of polycrystalline quartz (Qp), are white to light gray, sub-rounded to well-rounded, and vary from 1.0 cm to 3.0 cm. Some of the quartzite clasts show schistosity along with other metamorphic fabrics. Several deformation textures are observed in metaquartzite indicative of medium- to high-grade metamorphism. Both dynamically recrystallized and static state recrystallized textures were found (Fig. 19). Quartz deformation textures in quartzite consist of strain free grains, sub-grain rotation (SGR), lobate, serrated and minor bulging grain boundaries, all of which are indicative of dynamic recrystallization. Replacement of relict crystals by newly recrystallized larger grains, known as grain boundary area reduction, which results in an increase in grain size and straightening of irregular grain boundaries, suggests static state deformation. Grain boundaries with triple junctions at angles of ~120° also provide an evidence of static state deformation (Trepmann and Stöckhert, 2003). The presence of undulose extinction in quartz can be interpreted to reflect retrograde metamorphism that occurred after peak metamorphism (McQueen and Jonas, 1975). Bulging recrystallization in quartz is

dominant in temperature between $\sim 280^{\circ}\text{C}$ to $\sim 400^{\circ}\text{C}$, whereas sub-grain rotation and grain boundary migration are common in temperature between $\sim 400^{\circ}\text{C}$ - 500°C and $\sim 500^{\circ}\text{C}$ respectively (Stipp et al., 2002). Quartz-mica schist is the second dominant metamorphic clasts present in the conglomerates. These clasts are elongate, show a well-developed schistosity, and mostly contain quartz, muscovite and lesser amount of biotite (Fig. 20). Medium- to upper medium-grade metamorphic lithic fragments are dominant over the low-grade metamorphic lithics.

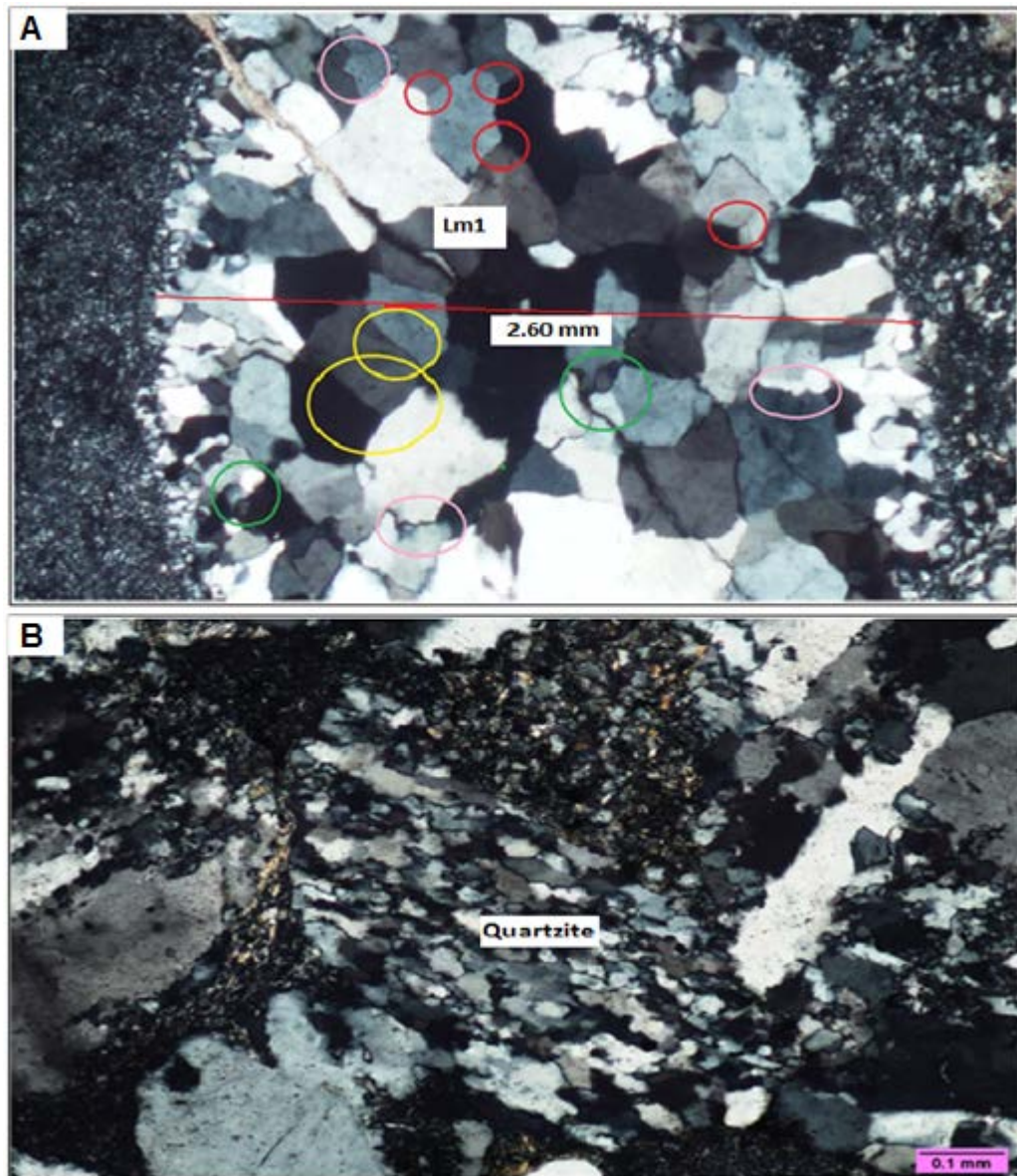


Figure 19: Representative photomicrographs of quartzite clasts in the Pottsville conglomerate measures. (A) Quartzite (Lm1) grain with metamorphic fabric from sample ZBH-11. Red circles show triple junctions at $\sim 120^\circ$, green circles show subgrains, yellow circles show straight grain boundaries, pink circles show serrated and bulged grain boundaries. (B) Typical fabric of dynamically recrystallized quartz formed by SGR (sample ZBH-2).

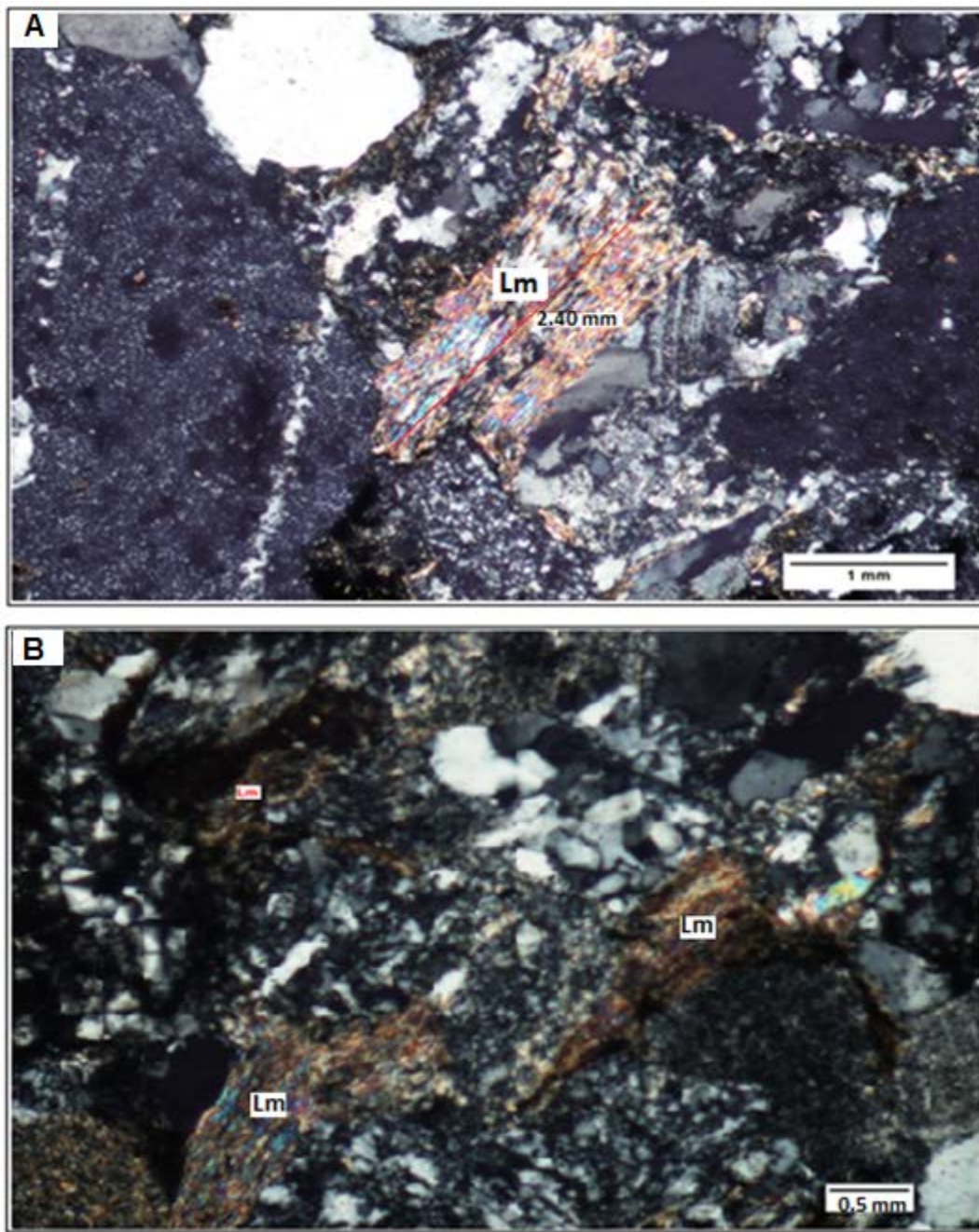


Figure 20: Representative photomicrographs of metamorphic clasts (Lm) in the Pottsville conglomerate measures, including low-grade phyllites with a parallel arrangement of quartz and muscovite crystals in sample ZBH-10 (A) and sample ZBH-2 (B).

3.3.3 Sedimentary Clast Lithology and Petrography

Sedimentary clasts comprise >50% of the upper Pottsville conglomerate clast populations and consist of chert, sandstone, siltstone, mudstone, and less common carbonates (Figs. 21-24). The abundance of sedimentary lithic fragments decreases upsection as the abundance of metamorphic lithics increases (Figs. 16 and 17). Among the sedimentary clasts, chert is the dominant type, followed by sandstone and siltstone. Cherts are usually dark black to brown and show mosaic textures of interlocking microcrystalline quartz. The size of chert clasts varies from 1 cm up to a few centimeters (Fig. 21A). Most of the chert clasts contain quartz veins that contain polygonal and strain free grains (Fig. 21B). Some of the chert contains chalcedony, a cryptocrystalline form of quartz, composed of very fine grained intergrowth of silica (Fig. 22A). Dolomite crystals are also observed in same chert clasts in few samples (Fig. 22B). No macro- or microfossils were observed in any of the chert clasts.

Sandstone and siltstone clasts, the second most common sedimentary clast types, are light gray to gray, matured and well sorted. Sandstone clasts widely vary in size and include some cobbles. They consist mostly of fine sand- to silt-sized monocrystalline quartz grains (Fig. 23A). Siltstones are also dominated by quartz grain (Fig. 23B). Mudstone clasts are extraformational and contain very fine sand- to silt-sized quartz. Mudstone clasts are white to reddish gray to brown under crossed polarized light and some of the mudrock clasts are ~4 mm (Fig. 24).

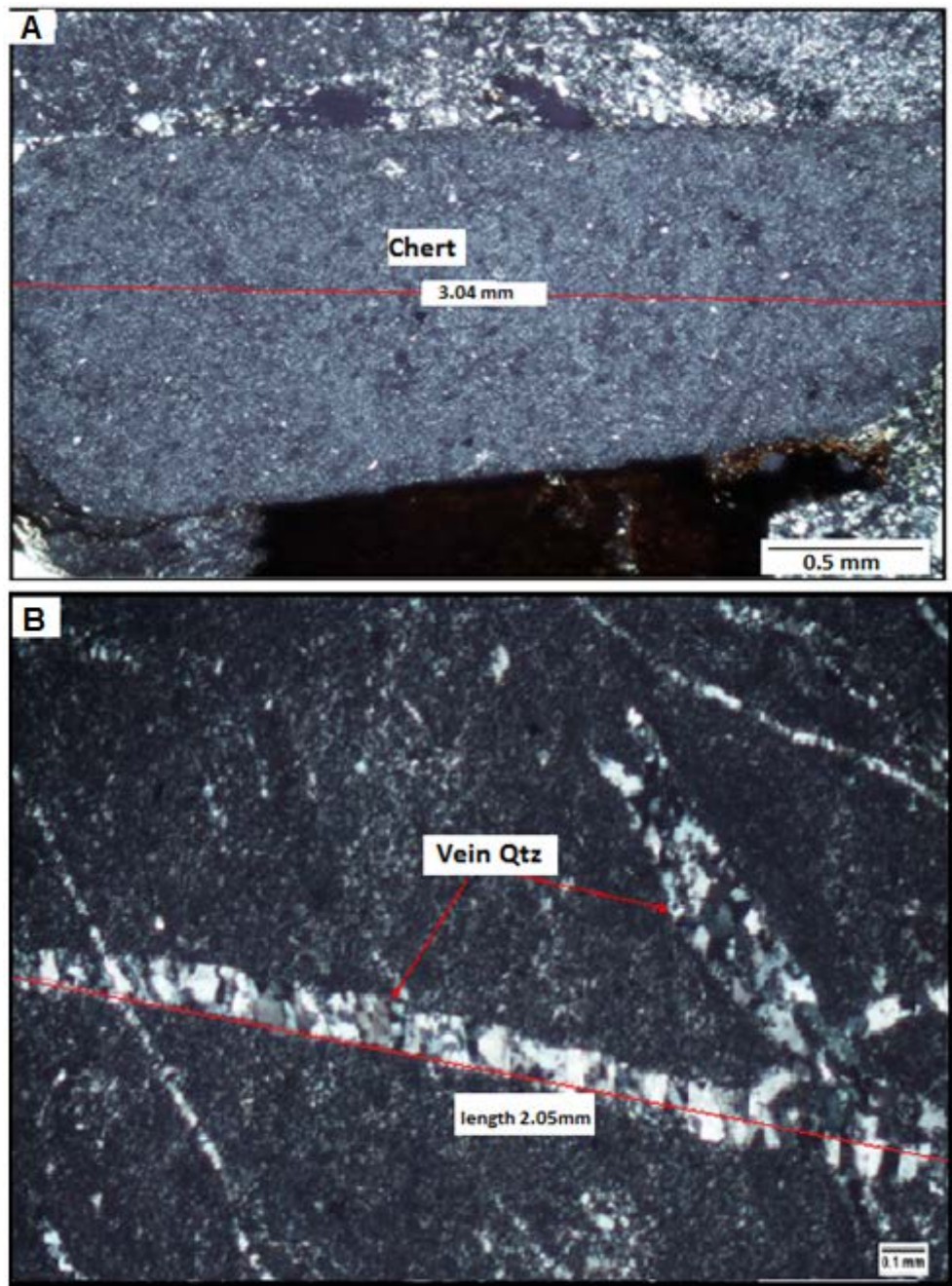


Figure 21: Representative photomicrographs of chert clasts in the upper Pottsville conglomerates. (A) Dark black to light black chert clast with mosaic textures formed due to the interlocking microcrystalline quartz (crossed polarized light). (B) Chert clast with quartz veins. Quartz crystals are polygonal in shape and strain free. Qtz = Quartz.

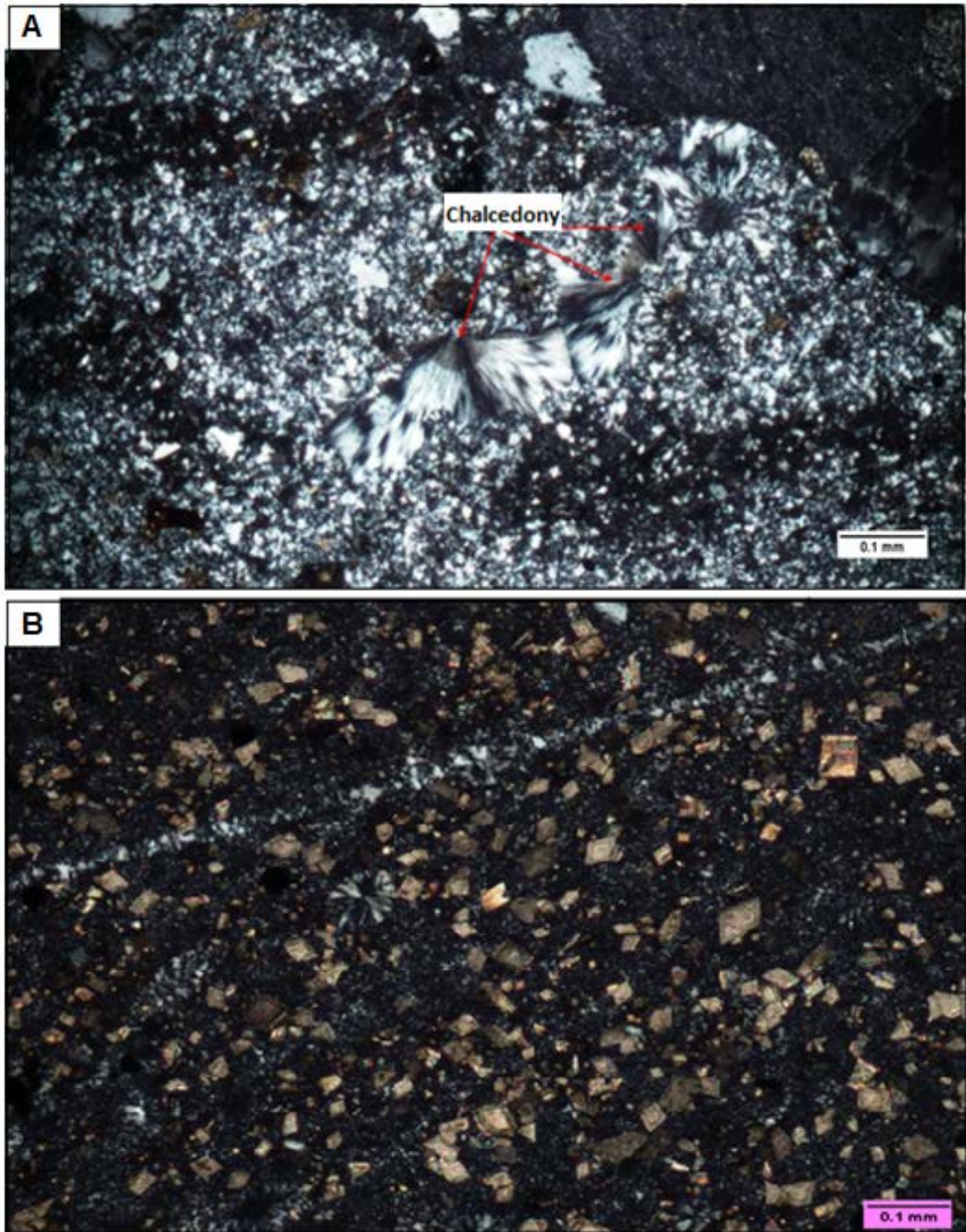


Figure 22: Representative photomicrographs of chert clasts in the upper Pottsville conglomerate. (A) Microcrystals of quartz with a chalcedony. (B) Chert with dolomite rhombs.

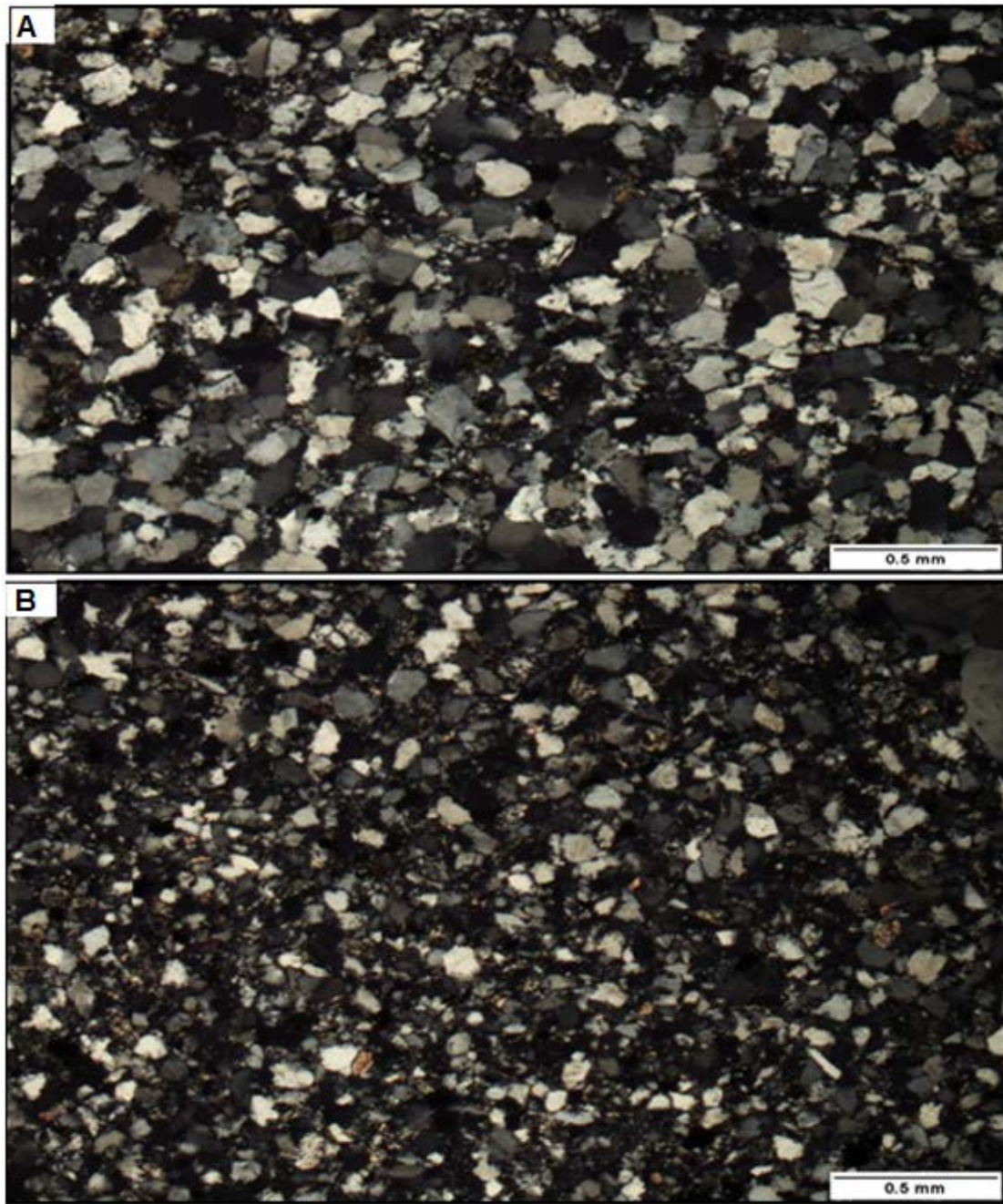


Figure 23: Representative photomicrographs of sedimentary lithic clasts. (A) Sandstone clast dominated by quartz (sample ZHS-1). (B) Sandy siltstone clasts dominated by monocrystalline quartz (sample ZHS-3).

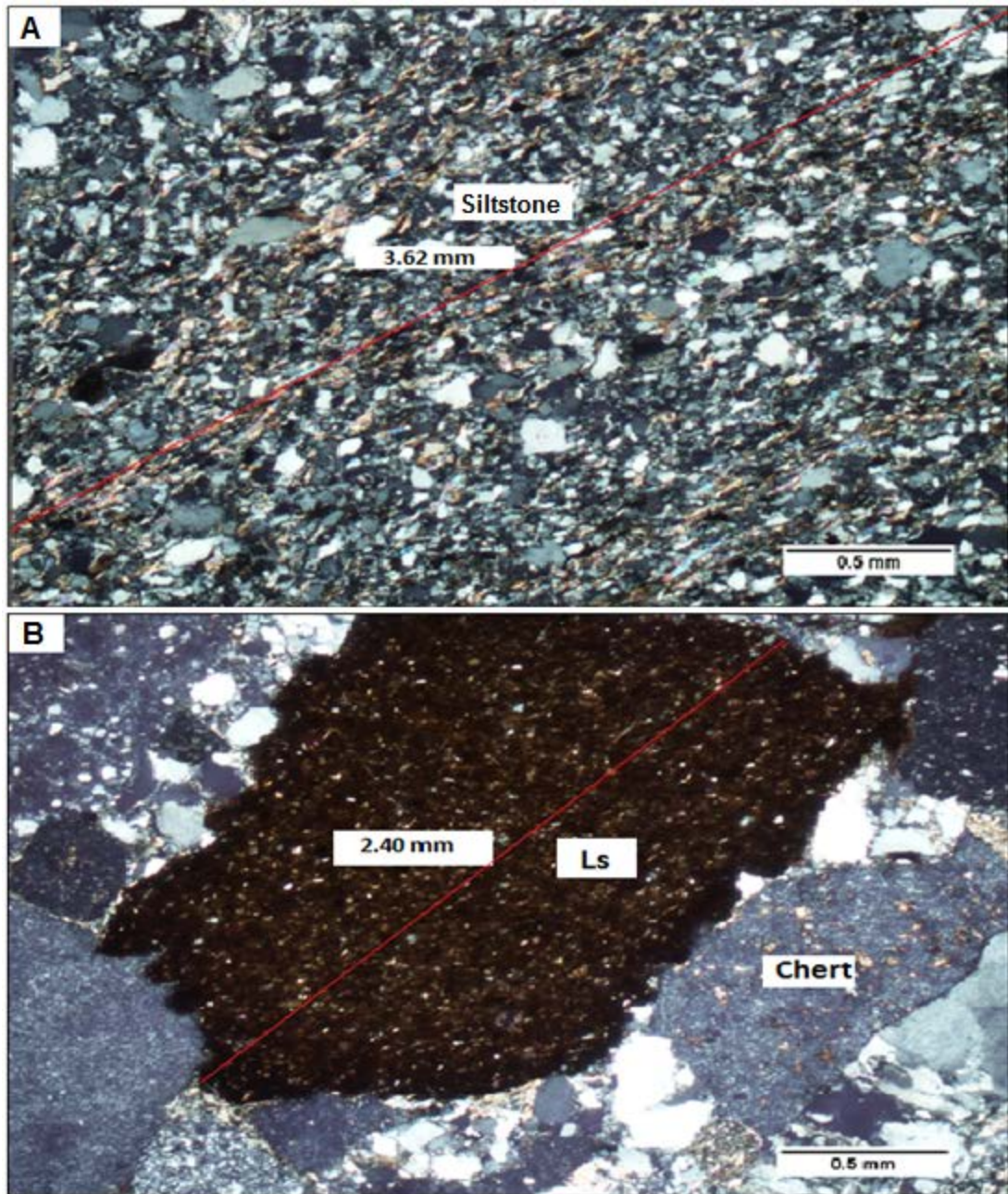


Figure 24: Representative photomicrographs of fine-grained sedimentary lithic clasts in the Pottsville conglomerate measures. (A) Siltstone clast with fine sand-sized quartz. (B) Fine-grained mudstone clast (Ls).

3.3.4 Sand Grain (matrix) Point Counting

Sand-sized matrix comprises 30-60% of the conglomerate samples examined in thin sections. Grains in the matrix contain medium to coarse sand consisting of a mixture of chert, sedimentary lithics, metamorphic lithics, volcanic lithics, polycrystalline quartz, monocrystalline quartz, and lesser amount of feldspars (Fig. 25). Polycrystalline quartz dominates over monocrystalline grains. Normalized modal composition of sand-sized matrix from the SOMED and JMHB cores is shown in Table 2. The provenance fields for these sands are shown in Qt-F-L, Qm-F-Lt, Qp-Lv-Ls and Qm-P-K ternary plots in figures 26 through 29. The red and pink polygons show the provenance fields for sand from SOMED and JMHB cores, respectively. Both Dickinson (1985) and Weltje (2006) provenance fields were used to delineate the provenance of matrices in conglomerates.

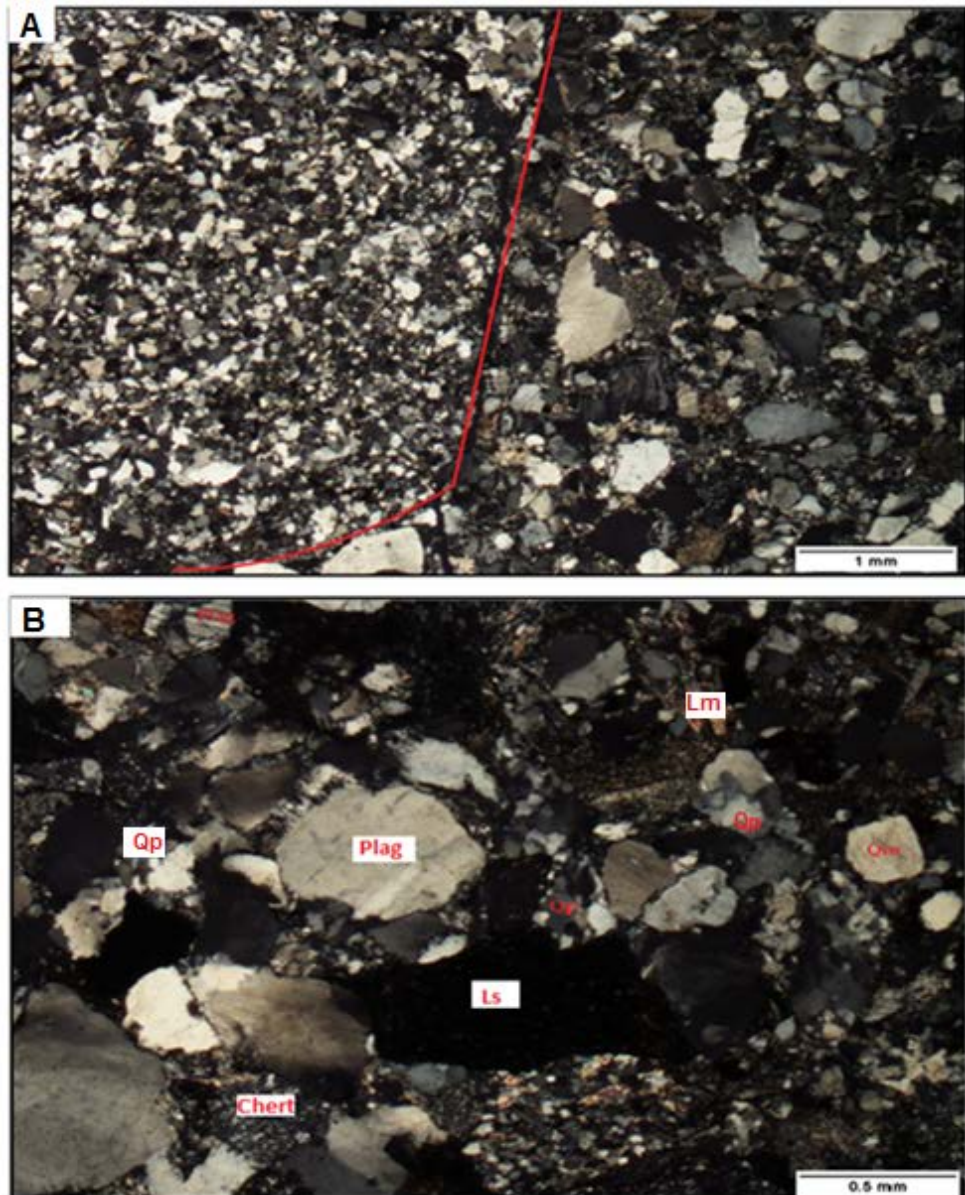


Figure 25: Representative photomicrographs showing sedimentary lithic pebbles (siltsone and sandstone) and matrix in conglomerate. Sedimentary lithics are mature and consists of silt- and fine sand-sized grains of mostly monocrystalline quartz. In contrast, grains in the matrix are medium to coarse sand and consist of a mixture of chert, Ls, Lm, Qp, Qm and less common plagioclase. (A) Sedimentary lithic pebble (left) and matrix (right). (B) Matrix in Pottsville conglomerate consists of the mixture of chert, Ls, Lm, Qp, Qm and rare plagioclase.

Table 2: Normalized modal analysis of sand-sized grains from SOMED and JHMB cores from the upper Pottsville Formation in Cahaba synclinorium.

	QtFL (%)			QmFLt (%)			QmPK (%)			QpLvLs (%)		
SOMED core												
Sample no.	Qt	F	L	Qm	F	Lt	Qm	P	K	Qp	Lv	Ls
ZBH-1	48.4	5.4	46.2	5.4	5.4	89.2	50.0	0.0	50.0	63.5	4.8	31.7
ZBH-2	40.0	9.0	51.0	20.0	9.0	71.0	69.0	6.9	24.1	32.8	1.6	65.6
ZBH-3	37.0	5.0	58.0	5.0	5.0	90.0	50.0	20.0	30.0	58.2	5.5	36.4
ZBH-4	43.7	4.9	51.5	4.9	4.9	90.3	50.0	30.0	20.0	63.5	4.8	31.7
ZBH-5	26.3	5.3	68.4	5.3	5.3	89.5	50.0	20.0	30.0	40.0	10.0	50.0
ZBH-6	36.5	6.3	57.3	10.4	6.3	83.3	62.5	6.3	31.3	50.0	10.0	40.0
ZBH-7	48.9	6.5	44.6	21.7	6.5	71.7	76.9	3.8	19.2	49.0	2.0	49.0
ZBH-9	47.9	6.4	45.7	16.0	6.4	77.7	71.4	4.8	23.8	56.6	5.7	37.7
ZBH-10	42.6	4.3	53.2	3.2	4.3	92.6	42.9	14.3	42.9	55.2	7.5	37.3
ZBH-11	36.0	5.0	59.0	4.0	5.0	91.0	44.4	22.2	33.3	57.1	7.1	35.7
Mean	42.3	6.1	51.7	8.8	6.1	85.1	54.7	14.2	31.0	52.6	5.9	41.5
Std. Dev.	4.9	2.0	4.8	7.5	2.0	9.4	9.5	9.9	13.3	9.9	2.9	10.5
Joy Manufacturing H.B (JMHB) core												
ZH-2	52.2	7.5	40.3	14.9	7.5	77.6	66.7	20.0	13.3	67.6	13.5	18.9
ZH-4	52.1	3.1	44.8	26.0	3.1	70.8	89.3	3.6	7.1	45.5	27.3	27.3
ZH-8	56.0	8.3	35.7	17.9	8.3	73.8	68.2	22.7	9.1	68.1	10.6	21.3
ZH-11	54.9	4.9	40.2	12.2	4.9	82.9	71.4	21.4	7.1	66.0	5.7	28.3
ZH-15	54.6	4.1	41.2	8.2	4.1	87.6	66.7	25.0	8.3	69.2	7.7	23.1
ZH-21	43.5	7.6	48.9	5.4	7.6	87.0	41.7	41.7	16.7	50.0	21.4	28.6
ZH-31	77.9	9.1	13.0	26.0	9.1	64.9	74.1	18.5	7.4	80.0	0.0	20.0
ZH-35	46.1	4.9	49.0	6.9	4.9	88.2	58.3	16.7	25.0	44.4	0.0	55.6
ZH-40	58.5	4.3	37.2	5.3	4.3	90.4	55.6	11.1	33.3	62.5	6.3	31.3
ZH-45	58.8	5.2	36.1	7.2	5.2	87.6	58.3	25.0	16.7	58.8	11.8	29.4
Mean	53.8	5.9	40.3	17.8	5.9	76.3	73.9	16.9	9.2	61.2	10.4	28.4
Std. Dev.	1.9	2.4	3.7	6.0	2.4	5.2	10.5	9.9	2.9	11.5	8.7	10.5

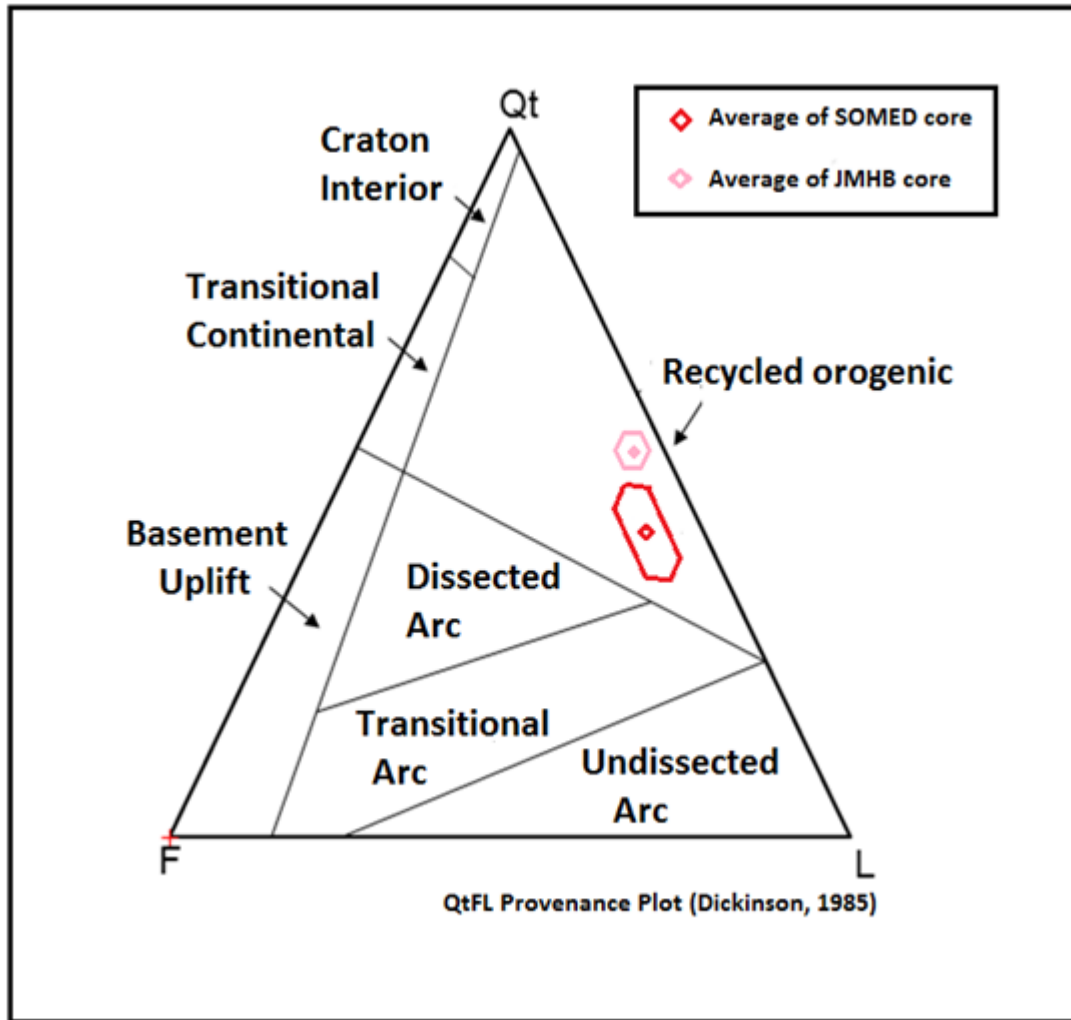


Figure 26: QtFL ternary diagram showing the provenance fields of sand-sized grains in upper Pottsville conglomerate samples. Standard deviation polygon is drawn around the mean (shown as red and pink diamond). Provenance fields are from Dickinson (1985). Qt = total quartz, F = total feldspar grains, L = lithic grains.

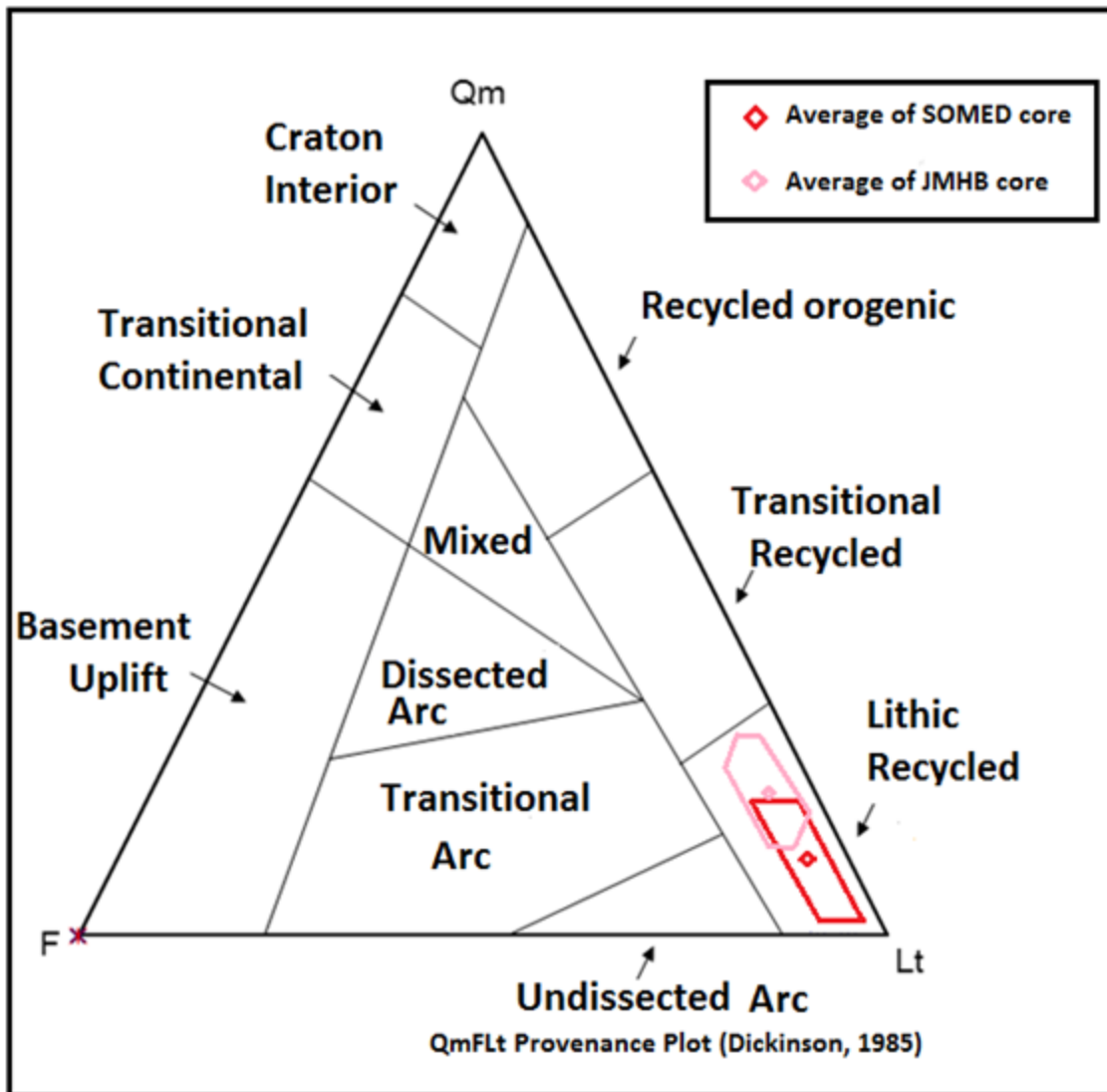


Figure 27: QmFLt ternary diagram showing the provenance fields of sand-sized grains in the upper Pottsville conglomerate samples. Standard deviation polygon is drawn around the mean (shown as red and pink diamond). Provenance fields are from Dickinson (1985). Qm = monocrystalline quartz, F = total feldspar grains, Lt = lithic grains and chert.

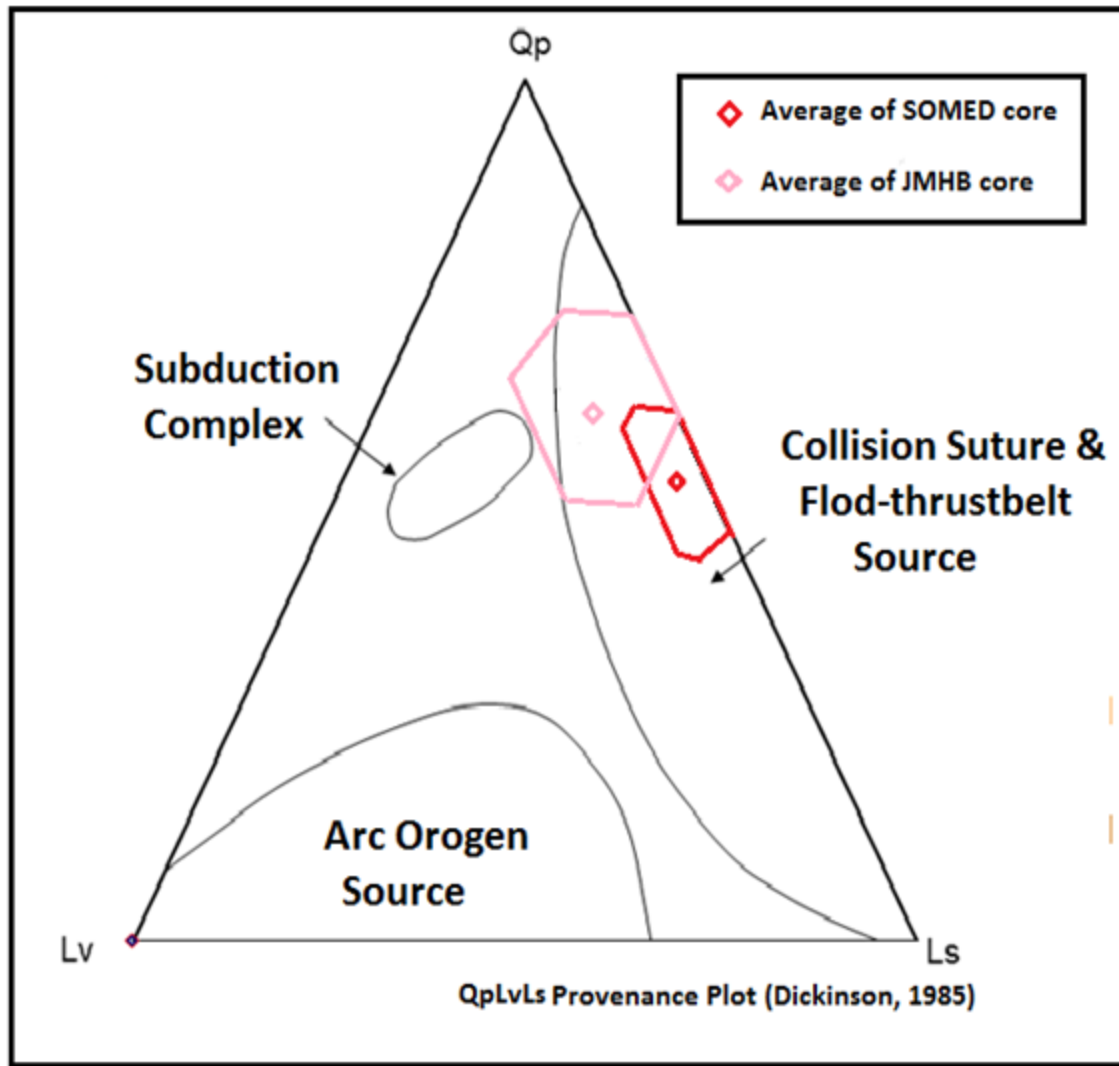


Figure 28: QpLvLs ternary diagram showing the provenance fields of sand-sized grains in upper Pottsville conglomerate samples. Standard deviation polygon is drawn around the mean (shown as red and pink diamond). Provenance fields are from Dickinson (1985). Qp = total quartz, Lv = volcanic lithic grains, Ls = sedimentary lithic grains.

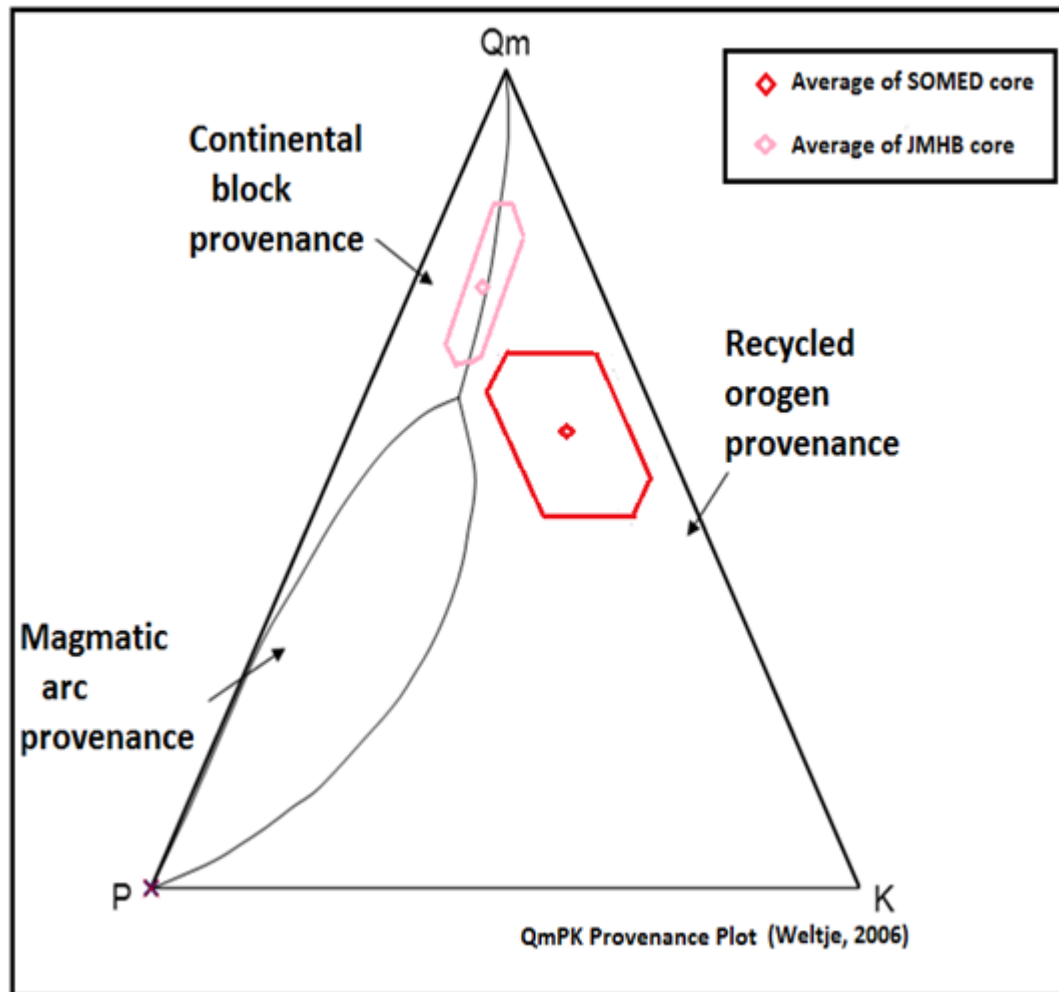


Figure 29: QmPK ternary diagram showing the provenance fields of sand-sized grains in upper Pottsville conglomerate samples. Standard deviation polygon is drawn around the mean (shown as red and pink diamond). Provenance fields are from Weltje (2006). Qm = monocrystalline quartz, P = plagioclase feldspar grains, K = potassium feldspar.

3.4 Interpretation of Conglomerate Petrography Data

Many of the clast types in the Pottsville conglomerates in the Cahaba basin are similar to the lithologies present in Cambrian, Ordovician, Devonian, and Mississippian sequences of the Appalachian fold and thrust belt and Piedmont of Alabama and Georgia (based on descriptions in Raymond et al., 1988; Steltenpohl, 2005). This suggests that the sediments were mostly derived from the southern Appalachians to the south-southeast. The large size of clasts, especially chert and mudstone clasts, indicate a nearby source. The modal analysis of sand-sized matrix in conglomerates suggest that sediments in upper Pottsville Formation were mostly derived from a recycled and collisional orogenic provenance.

Chert is the dominant clast type present in the conglomerates. One potential source of the chert could be the ridge-forming chert unit in the lower part of the Copper Ridge Dolomite of the Cambro-Ordovician Knox Group (Raymond et al., 1988). A second potential source of chert is the Mississippian Fort Payne Chert, which is dominated by bedded chert. Cherts and novaculites in the Ouachita orogenic belt maintain a constant lithology and faunal characteristics throughout the entire Ouachita structural belt and contain siliceous sponge spicules, radiolarians, spores, etc. (Goldstein, 1959). Given the apparent absence of such microfossils in the chert clasts of the Cahaba basin, the Ouachitas are not a likely source for the cherts present in the upper Pottsville Formation. Moreover, the large size of the chert clasts present in the upper Pottsville Formation indicates a relatively proximal source.

The character of metamorphic clasts also suggests a proximal Appalachian source. Rocks in the Ouachita orogen reached very low-grade metamorphic i.e., greenschist facies (Goldstein, 1959). However, the textures in the metamorphic clasts from the Cahaba basin indicate medium- to upper medium-grade metamorphic source terranes.

The volcanic clasts of the upper Pottsville conglomerate pose an interesting problem in interpreting provenance. The volcanic clasts have always been a mystery since there are no unmetamorphosed volcanics exposed in the southern Appalachians. Basalt, andesite, dacite and rhyolite are genetically related and can form from a magma due to the fractional crystallization (Eichelberger, 1975). Osborne (1988) documented that igneous clasts in the Straven Conglomerate consists of rhyolite, basalt, and granite. Igneous clasts in the upper Pottsville conglomerate measures are consisted of andesite, dacite and tonalite. The age of an andesite clasts found in this study from the Cahaba basin is ~323 Ma (Haque et al., 2015). The age data will be discussed in details in geochronology chapter of this thesis. Osborne (1988) suggested that basalts and rhyolites beneath Mesozoic sediments in southern Alabama could have been the source for the volcanic clasts present in Straven Conglomerate. There is no basaltic and rhyolitic clasts found in the upper Pottsville conglomerate in the Cahaba basin. The ~323 Ma age of an andesite clast suggests a volcanic source that is similar in age to inception of the Alleghenian orogeny in the Alabama Promontory. Several researchers have identified metamorphism that fall in Permian age range, but no volcanics in the Alabama and Georgia Piedmont (Steltenpohl, 1988). One possibility is that metavolcanics that were originally emplaced near the start of the Alleghenian orogeny (~323 Ma) could have been the source of the volcanic clasts

present in the Cahaba basin, or the volcanic clasts present in the upper Pottsville Formation in the Cahaba basin is yet to be discovered in the southern Appalachians.

CHAPTER 4: HEAVY MINERAL ANALYSIS

4.1 Introduction

Heavy minerals are those having specific gravities of 2.9 or higher. Heavy mineral analysis is one of the most commonly used techniques in provenance studies. Many heavy minerals are indicative of particular source rocks and, thus, are commonly used in foreland-basin studies (e.g., Uddin et al., 2007). Heavy minerals are among the most sensitive indicators of the nature of sediment-source areas, and over thirty common translucent detrital mineral species can be used as provenance indicators (Morton, 1985). Knowledge of the processes controlling the distribution of heavy minerals in sandstones recently has improved (Morton, 1985; Morton and Hallsworth, 1999; Uddin et al., 2007). Although heavy-mineral assemblages are greatly controlled by the provenance, they are also influenced by other extrabasinal and intrabasinal factors such as weathering, transport, deposition, and diagenesis (Morton, 1985; Morton and Hallsworth, 1999).

4.2 Methodology

For the heavy minerals analysis, ten sandstone samples (five samples from each core) were collected from the upper Pottsville Formation. The collected samples were disaggregated and oven-dried. Medium- to fine-grained sand samples were sieved using 4-Ø and 0-Ø screens, and representative 50-g subsamples were used for heavy-mineral separation. Heavy minerals were separated using 1, 1, 2, 2 tetrabromoethane, a liquid having a density of 2.96. Separated heavy minerals were washed with acetone and oven-dried (STABIL-THERM Gravity oven) at 100°C for 12 hours. Heavy minerals were then

reweighed to calculate the weight percentage of heavy minerals in each sample. A Frantz magnetic separator (Model- L-1) was used to separate heavy minerals into four subfractions according to their magnetic susceptibility (Hess, 1966). These subfractions are: (1) Group i- separated at 0.4 amps with side slope of 20° (strongly magnetic, SM); minerals include pyrrhotite, magnetite, garnet, olivine, hematite, chloritoid, chromite, and ilmenite; (2) Group ii- separated at 0.8 amps with side slope of 20° (moderately magnetic, MM); minerals include hornblende, hypersthene, augite, actinolite, biotite, and staurolite; (3) Group iii- separated by 1.2 amps with side slope of 20° (weakly magnetic, WM); common minerals in group-iii are tourmaline, muscovite, and tremolite; and (4) Group iv- weakly magnetic to non-magnetic minerals, including zircon, rutile, sillimanite, topaz, andalusite, and apatite. Polished thin sections were made from six of the ten samples for electron microprobe analysis.

4.3 Results

The abundance of heavy minerals in the upper Pottsville conglomerate measures is consistently low in samples from both cores. Samples from the upper Pottsville conglomerate measures contain heavy minerals less than 0.5 percent by weight, with the exception of sample ZHS-29, which contains 1.2% heavy minerals by weight (Fig. 30). The point-counting results of heavy minerals from upper Pottsville conglomerate measures are presented in table 3 and figure 31. Heavy minerals found in upper Pottsville conglomerate measures includes siderite, limonite, garnet, zircon, rutile, tourmaline, apatite, monazite, pyrite, chlorite, and iron rich biotite (Figs. 32 and 33). The overall dominant heavy minerals are garnet, zircon, tourmaline, rutile, and opaque grains. Overall shapes of the heavy minerals are sub-rounded to rounded, indicating a long travel distance.

Among the ultrastable minerals, rutile is the most abundant heavy mineral present in the upper Pottsville Formation.

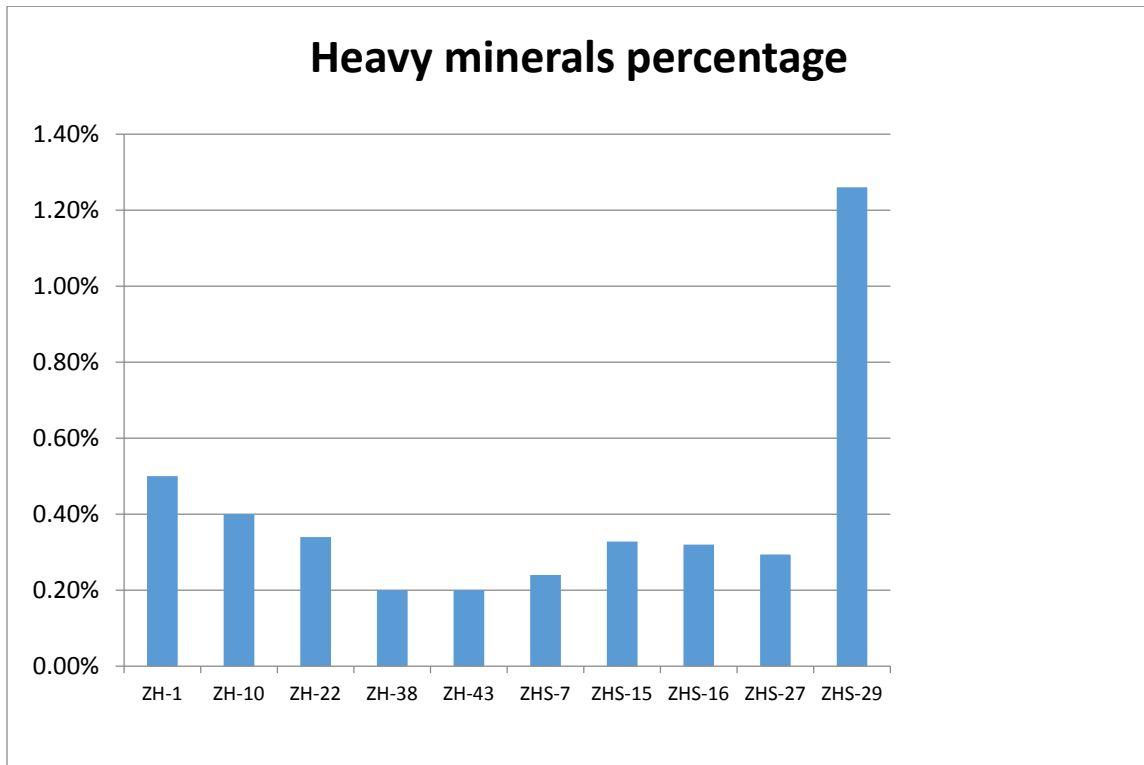


Figure 30: Bar diagram shows the weight percentages of heavy minerals in samples from the upper Pottsville conglomerate measure.

Table 3: Normalized abundances of heavy minerals of the upper Pottsville conglomerate measures, Cahaba Basin, Alabama.
 (ZTR- Zircon-Tourmaline – Rutile).

Upper Pottsville conglomerate measures										
	Heavy mineral percentages									
	ZH-1	ZH-10	ZH-22	ZH-38	ZH-43	ZHS-7	ZHS-15	ZHS-16	ZHS-27	ZHS-29
Zircon	4	3	6	7	5	4	4	3	5	5
Tourmaline	2	1	0	2	1	0	3	1	3	4
Rutile	10	17	22	18	15	22	17	15	12	13
ZTR%	16	21	28	27	21	26	24	19	20	22
Garnet	28	16	18	20	28	40	25	26	19	14
Chlorite		2	2	1	0	4	2	5	3	3
Apatite	8	0	1	4	2	0	1	1	0	2
Biotite	0	0	0	1	1	0	1	0		
Pyrite	4	2	2	3	2	8	1	1	3	2
Siderite	11	15	8	9	12	2	15	18	19	22
Limonite	0	5	3	5	7	2	3	0	2	5
Magnesite	3	2	0	0	1	1	0	0	2	0
Monazite	2	1	0	1	0	4	2	0	0	2
Opaque	28	36	39	29	27	13	26	40	31	32

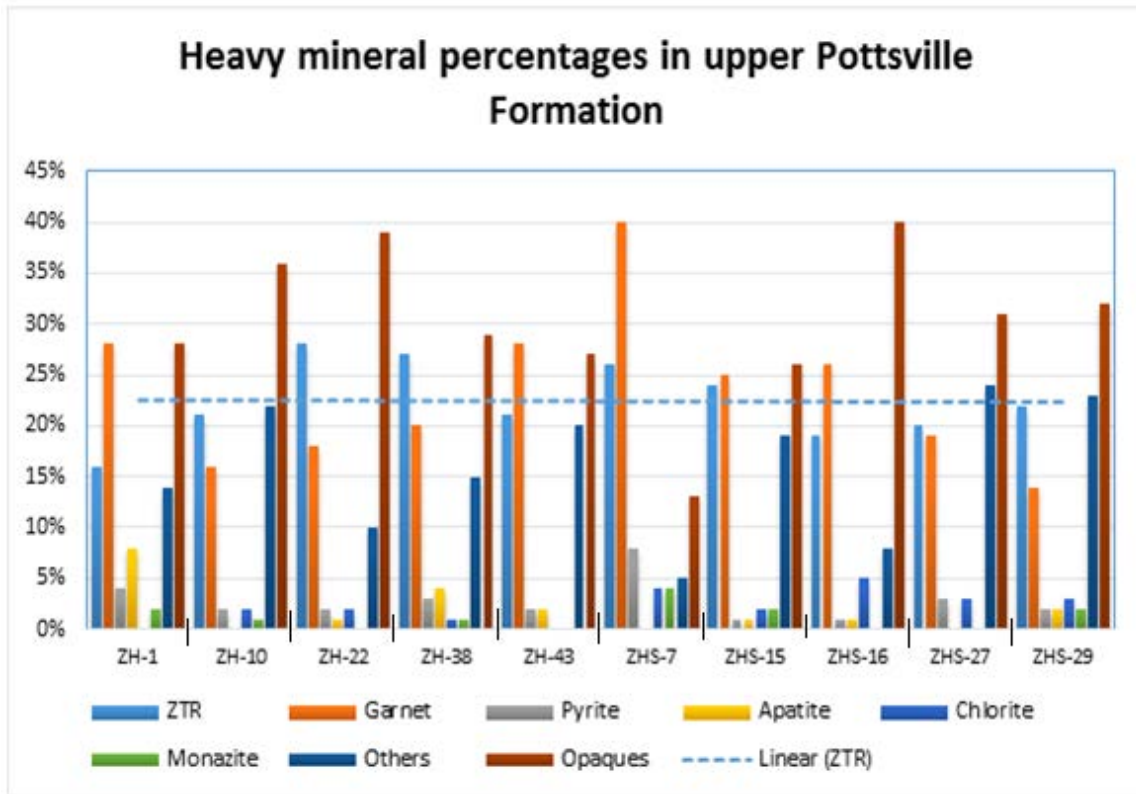


Figure 31: Bar diagram showing the distribution of the most common heavy minerals in the upper Pottsville conglomerate measures, Cahaba synclinorium, Alabama. Blue horizontal dashed line shows the average trend line of ZTR (ZTR- Zircon-Tourmaline-Rutile).

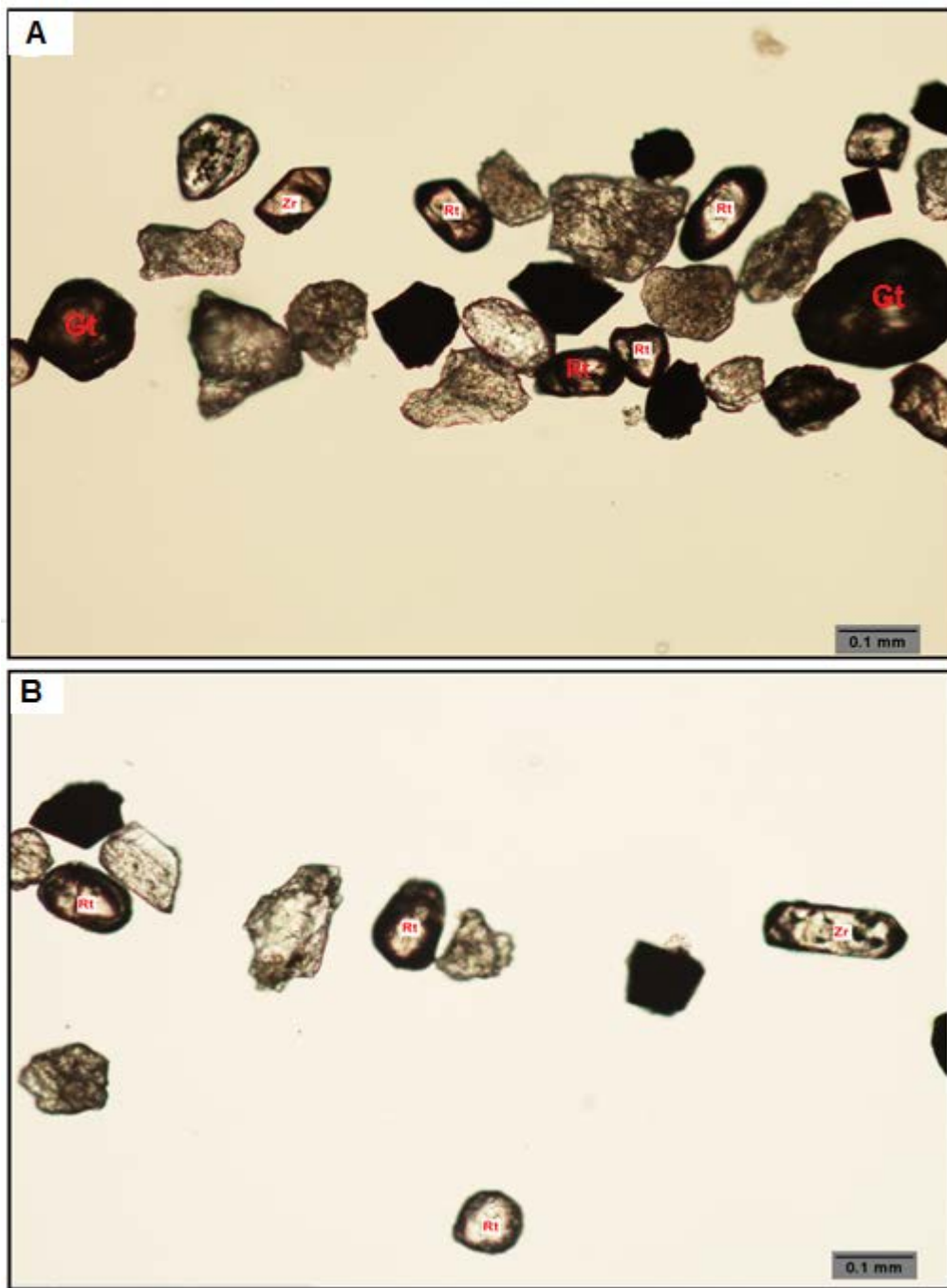


Figure 32: Representative photomicrographs of heavy mineral assemblages from the upper Pottsville conglomerate measures. (A) Rt = rutile, Zr = Zircon, Gt = Garnet, and other opaque minerals from sample ZH-10. (B) Rt = rutile, Zr = zircon, and other opaque minerals from sample ZHS-16. Both photos taken in crossed polarized light.

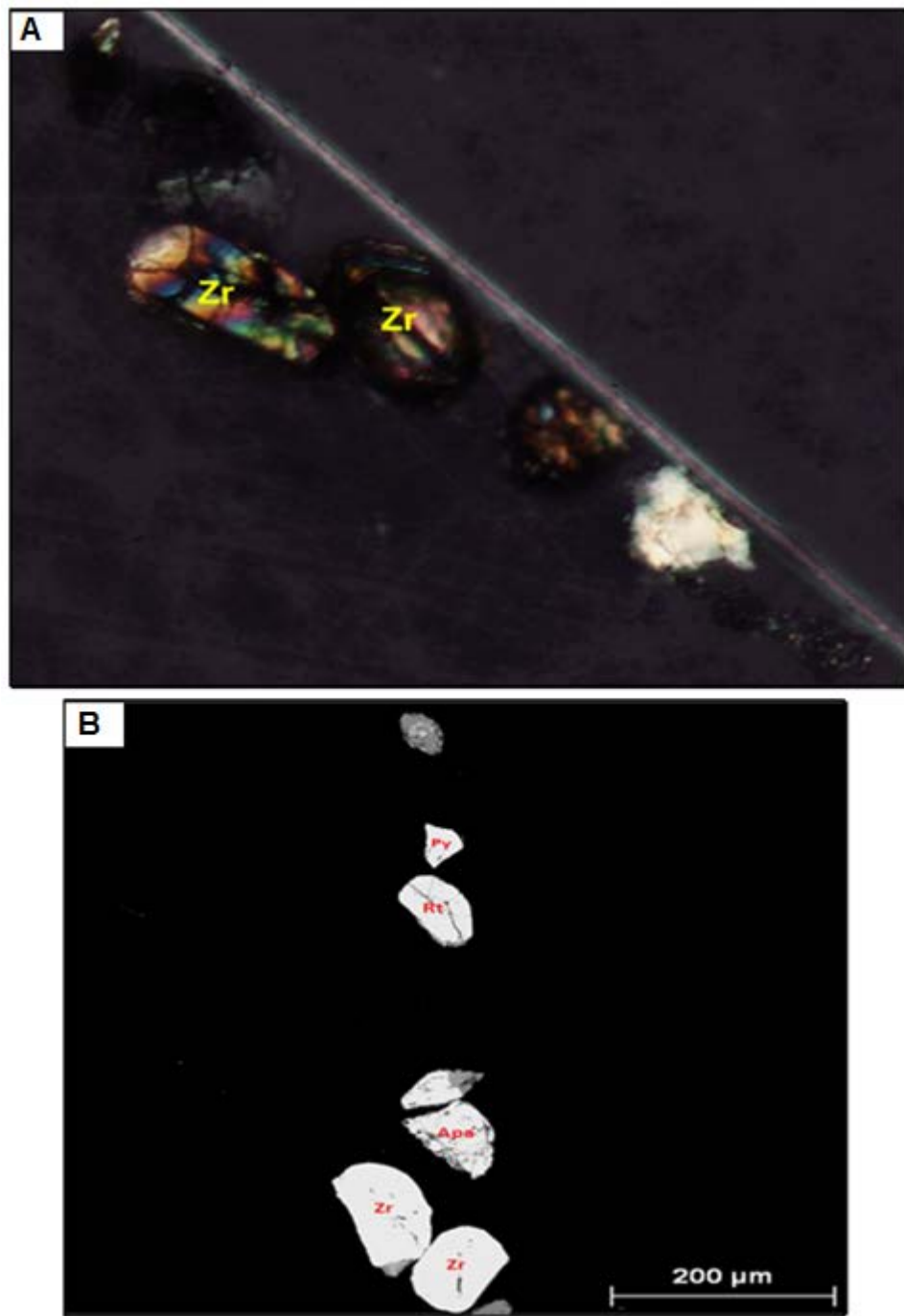


Figure 33: Representative photomicrographs of heavy mineral assemblages from the upper Pottsville conglomerate measures. (A) Zircons (Zr) in sample ZH-10. (B) Backscattered image of heavy minerals on which elemental analyses were performed. Rt = Rutile, Py = Pyrite, Zr = Zircon, Apa = Apatite.

4.4 Discussion

Among the non-opaque heavy minerals garnet is the most abundant heavy mineral followed by rutile, zircon, and apatite in the sandstones of upper Pottsville Formation. Rutile and garnet usually are associated with medium- to high-grade metamorphic sources (Mange and Maurer, 1992). The abundance of rutile and garnet suggests medium- to high-grade regionally metamorphosed source terranes for the upper Pottsville sediments in the Cahaba basin (Zack et al., 2004). As with the some metamorphic clasts in the conglomerates, regionally metamorphosed medium- to upper medium-grade rocks in the Appalachians (inner Piedmont and Western Blue Ridge terranes) could have been source for the metamorphic heavy minerals present in the sandstone of the upper Pottsville Formation in Cahaba basin.

The presence of ultra-stable minerals and low abundance of heavy minerals reflect intense chemical weathering and recycling during deposition of these sediments. Intense chemical weathering is also consistent with the inferred location of the basin near the paleo-equator during deposition of Pottsville (Thomas, 2005).

CHAPTER 5: GARNET CHEMISTRY

5.1 Introduction

In addition to the study of overall heavy-mineral suites, provenance analysis of clastic sediments also can be facilitated by chemical analyses of specific heavy mineral species; e.g., garnet, tourmaline, chrome-spinel (Henry and Guidotti, 1985; Morton, 1985; Henry and Dutrow, 1990; Morton and Taylor, 1991; Nanayama, 1997; Zahid, 2005 and Peavy, 2008). The composition of heavy minerals is related to the formative conditions of their parent rocks. Garnets commonly occur in metamorphic and certain igneous rocks and comprise a group of silicates with the general formula $A_3B_2(SiO_4)_3$ in which A = Ca, Fe²⁺, Mg, Mn²⁺; B = Al, Cr, Fe³⁺, Mn³⁺, Si, Ti, V, Zr; and Si may be replaced partly by Al, Ti, and/or Fe³⁺. Nearly all natural garnets exhibit extensive substitution; solid-solution series and the name of the end-members that make up the largest percentage of any given specimen is usually applied. The common rock-forming garnet end members composition and their typical sources are shown in table 4. The rock-forming garnets are most common in metamorphic rocks but a few occur in igneous rocks, especially granites and granitic pegmatites (Mange and Maurer, 1992). Garnets derived from such rocks occur sporadically in clastic sediments and sedimentary rocks.

Table 4: End-member compositions and typical sources of the common rock-forming garnets (Mange and Maurer, 1992).

Name	Formula	Subgroup	
Pyrope (Py)	$Mg_3Al_2(SiO_4)_3$	Pyralspite	
Almandine (Al)	$Fe_3Al_2(SiO_4)_3$		
Spessartine (Sp)	$Mn_3Al_2(SiO_4)_3$		
Grossular	$Ca_3Al_2(SiO_4)_3$	Ugrandite	
Andradite	$Ca_3Fe_2(SiO_4)_3$		
Uvarovite	$Ca_3Cr_2(SiO_4)_3$		
End members	Common sources		
almandine	metamorphic rocks—especially mica schists, amphibolites, and granulites; granites, aplites, and granitic pegmatites.		
spessartine	granitic pegmatites; silica-rich skarns; metamorphosed manganese-bearing rocks		
grossular	impure calcite and dolomite marbles, especially those in contact metamorphic zones; amphibolites; basic igneous rocks		
andradite	large masses associated with tactites, some of which constitute ore deposits, in calcareous rocks of contact metasomatic origin		
pyrope	ultramafic rocks such as pyroxenites and peridotites and serpentinites derived from them; eclogites (high-pressure metamorphic rocks)		

Determination of the individual detrital garnet end-members may enhance the interpretation of provenance as demonstrated in number of previous studies (Morton, 1986; Morton and Taylor, 1991; Zhang et al., 2003; Li et al., 2004). Early studies in chemical zoning in garnet showed that the ratio of $(\text{Fe}^{2+} + \text{Mg}^{2+})/(\text{Ca}^{2+} + \text{Mn}^{2+})$ increases with increasing metamorphic grade. More modern studies show a decrease in $\text{Fe}/(\text{Fe} + \text{Mg})$ reflecting the increase in pyrope content with increasing temperature (Spear and Cheney, 1989).

Electron-microprobe analysis provides a complete micrometer-scale quantitative chemical analysis of inorganic solid materials. To constrain provenance, the chemical composition of garnets from the Pottsville conglomerate measures were assessed via microprobe analysis.

5.2 Electron Microprobe Methodology

Electron microprobe analysis (EMPA), also called electron probe microanalysis (EPMA), is an analytical technique that is used to determine the composition of small areas on the surface of solid samples. In the EMPA technique, a beam of an accelerated electrons is focused on the surface of a specimen using a series of electromagnetic lenses, and these energetic electrons produce characteristic X-rays within the small volume (typically 1 to 9 cubic microns) of the specimen. The characteristic X-rays are detected at particular wavelengths, and their intensities are measured relative to standards to determine concentrations. Each element has a specific set of X-rays that it emits and, using EPMA, all elements (except H, He, and Li) can be detected (Armstrong, 1988). Additionally, the electron microprobe also can function like a scanning electron microscope (SEM) and obtain highly magnified secondary- and backscattered-electron images of a sample.

Six polished heavy mineral samples were analyzed using a JEOL 8600 electron microprobe, with 15 KV accelerating voltage and 15 nA beam current, at the University of Georgia EMPA lab. Mineral grains were qualitatively identified using a Bruker 5010 Silicon Drift Detector (SDD) and energy-dispersive x-ray (EDS) detector controlled by a Bruker Quantax energy-dispersive system. Quantitative analyses were performed with wavelength dispersive spectrometers (WDS) automated with Advanced Microbeam, Inc. electronics and Probe for EPMA software, using 10-second counting times, and natural and synthetic mineral standards. Analyses were calculated using Armstrong's (1988) Phi-Rho-Z matrix correction model. Backscattered electron images (BEI) were acquired using imaging software of the Quantax analysis system (Fig. 34). Appropriate standards were

used to obtain standard X-ray intensities of the materials measured during microprobe analysis, and different standards were used for different solids (See appendix-A for details).

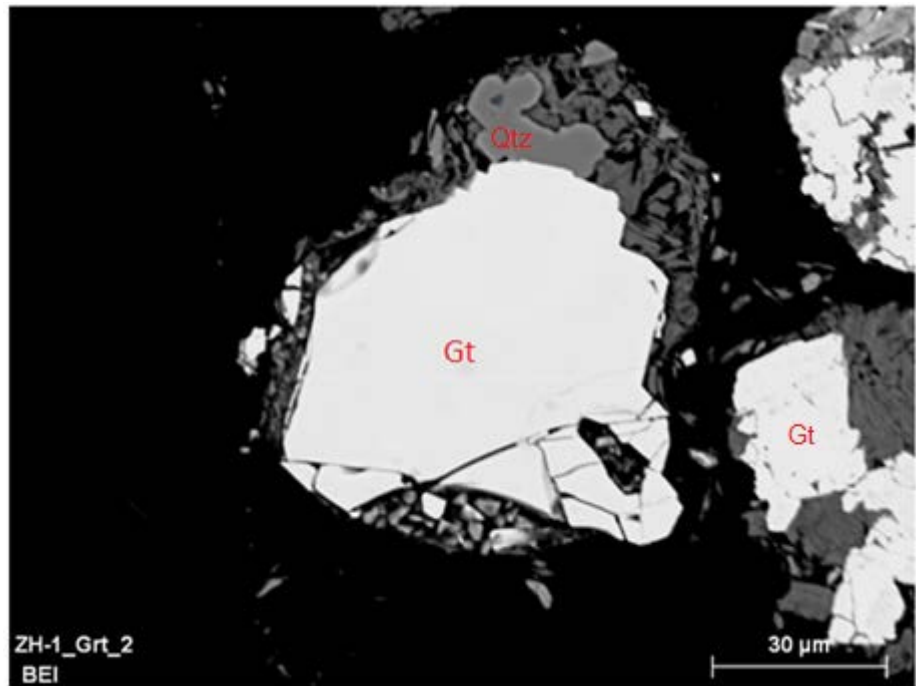


Figure 34: Representative backscatter electron image of garnet grains (Gt) and a quartz grain. Due to the higher atomic number garnet grains are bright compare to the surrounding quartz grain. Garnet grains are subrounded and uniform brightness of the garnet grains suggest uniform atomic distribution.

5.3 Results

Source composition and P-T conditions during the crystallization control the chemical composition of garnets. A total of thirteen garnet samples were analyzed and garnet end-member compositions were calculated to constraint sediment provenance. Table 5 shows the percentage of almandine, spessartine, pyrope and grossular in the garnet samples. The end members were calculated from the data obtained by EMPA, and these end members are plotted on various ternary diagrams reflecting chemical composition (Figs. 35-38).

Ternary plots of garnet end-member composition suggest that garnets from the upper Pottsville Formation of Cahaba basin are predominantly almandine types (average 75%, maximum 83%). Pyrope content ranges from 4-17% and grossular content ranges from ~3 to 17%. Spessartine content in the garnets of the upper Pottsville conglomerate measures in Cahaba basin is generally less than 6%, only one has spessartine content ~12%. Table 5 shows the calculated Fe/Fe+Mg ratio in all the garnet samples. The range in Fe/Fe+Mg ratios of the Pottsville garnet grains is 0.82-0.94. Assuming that the garnet was in equilibrium with biotite for pelitic compositions and either Barrovian (medium-pressure, high temperature) or Buchan (low pressure) facies, Fe/Fe+Mg ratios can be used to estimate temperature condition (Spear and Cheney, 1989). The estimated temperature ranges for the upper Pottsville garnets are ~500-750°C (Fig. 39).

Table 5: End member percentages and Fe/Fe+Mg ratios. Samples ZH-1 and ZH-10 are from Joy Manufacturing H.B core and samples ZHS-7, 16, 22, and 29 are from SOMED core. (See appendix-B for the full data table).

Sample	Depth (in ft)	Almandine	Spessartine	Pyrope	Grossular
ZH-1_Grt_2	10.00	75.03	1.23	15.43	8.32
ZH-1_Grt_4	10.00	83.45	0.24	9.75	6.56
ZHS-16_s2_grt_2	10.00	77.50	0.81	8.85	12.84
ZHS-16_s2_grt	40.00	67.01	12.70	8.59	11.71
ZHS-29_s2_grt	522.00	75.53	0.55	6.63	17.29
ZHS-29_s2_grt_2	626.00	75.34	1.24	9.82	13.60
ZHS-29_s2_grt_3	626.00	69.86	3.74	17.47	8.93
ZH-22_s_1_Grt	667.00	76.48	0.46	15.89	7.17
ZH-22_s_2_Grt	667.00	74.44	5.57	4.40	15.59
ZH-22_s_2_Grt_1	667.00	72.37	0.35	12.92	14.36
ZHS-7_Grt	2400.00	74.49	4.89	11.80	8.82
ZH-10_Grt_1	2400.00	79.70	2.28	7.36	10.66
ZH-1_Grt_3	2400.00	82.10	0.85	14.20	2.85

	ZH-1_Grt_2	ZH-1_Grt_4	ZHS-16_s2_grt_2	ZHS-16_s2_grt	ZHS-29_s2_grt	ZHS-29_s2_grt_2	ZHS-29_s2_grt_3	ZH-22_s_1_Grt	ZH-22_s_2_Grt	ZH-22_s_2_Grt_1	ZHS-7_Grt	ZH-10_Grt_1	ZH-1_Grt_3
Fe	2.26	2.52	2.32	2.05	2.27	2.24	2.10	2.33	2.25	2.21	2.25	2.41	2.46
Mn	0.04	0.01	0.02	0.39	0.02	0.04	0.11	0.01	0.17	0.01	0.15	0.07	0.03
Mg	0.46	0.29	0.26	0.26	0.20	0.29	0.52	0.48	0.13	0.39	0.36	0.22	0.43
Fe+Mg	2.73	2.82	2.58	2.31	2.47	2.54	2.62	2.81	2.38	2.60	2.61	2.63	2.89
Fe/Fe+Mg	0.83	0.90	0.90	0.89	0.92	0.88	0.80	0.83	0.94	0.85	0.86	0.92	0.85

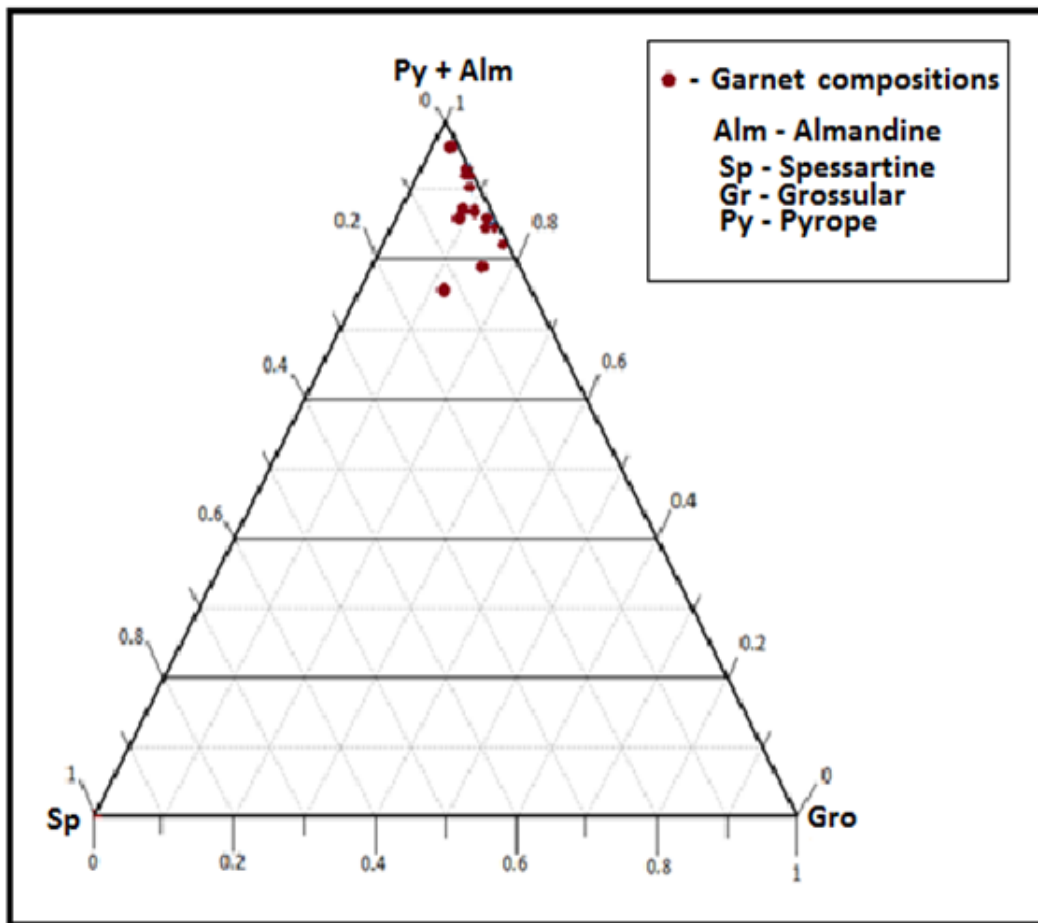


Figure 35: Chemical composition of garnets from upper Pottsville Formation in Cahaba basin plotted on (Py+Alm)-Sp-Gro ternary diagram (adapted from Nanayama, 1997).

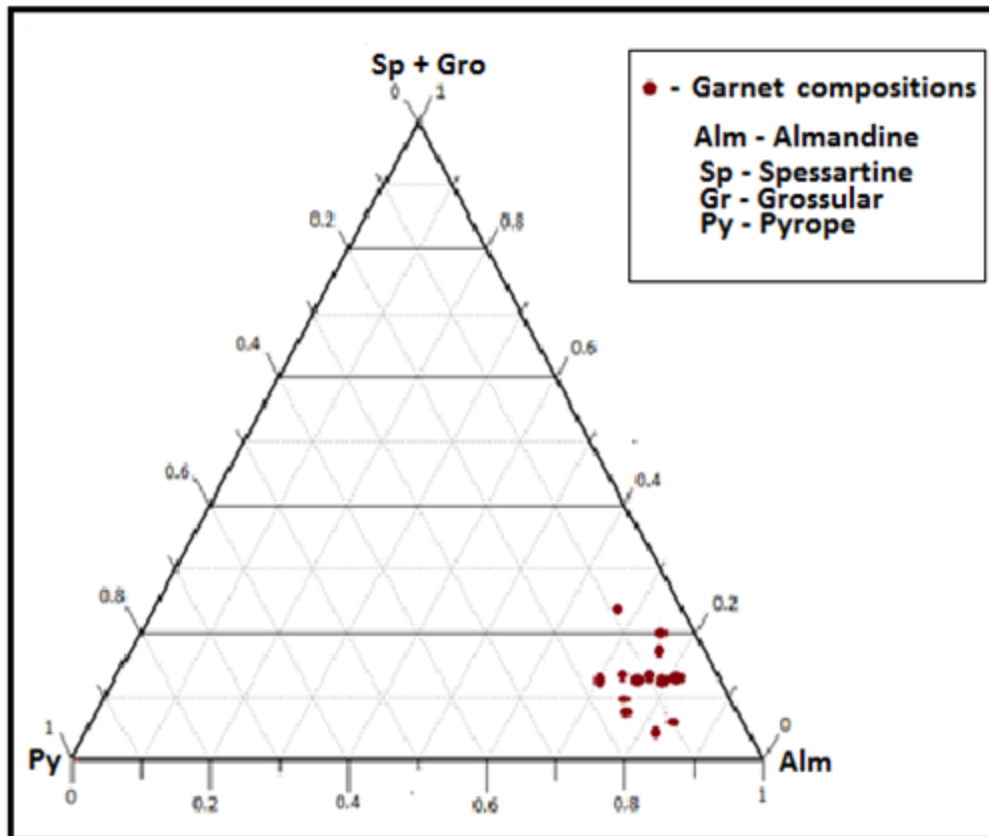


Figure 36: Chemical composition of garnets from upper Pottsville Formation in Cahaba basin plotted on (Sp+Gro)-Py-Alm ternary diagram (adapted from Nanayama, 1997).

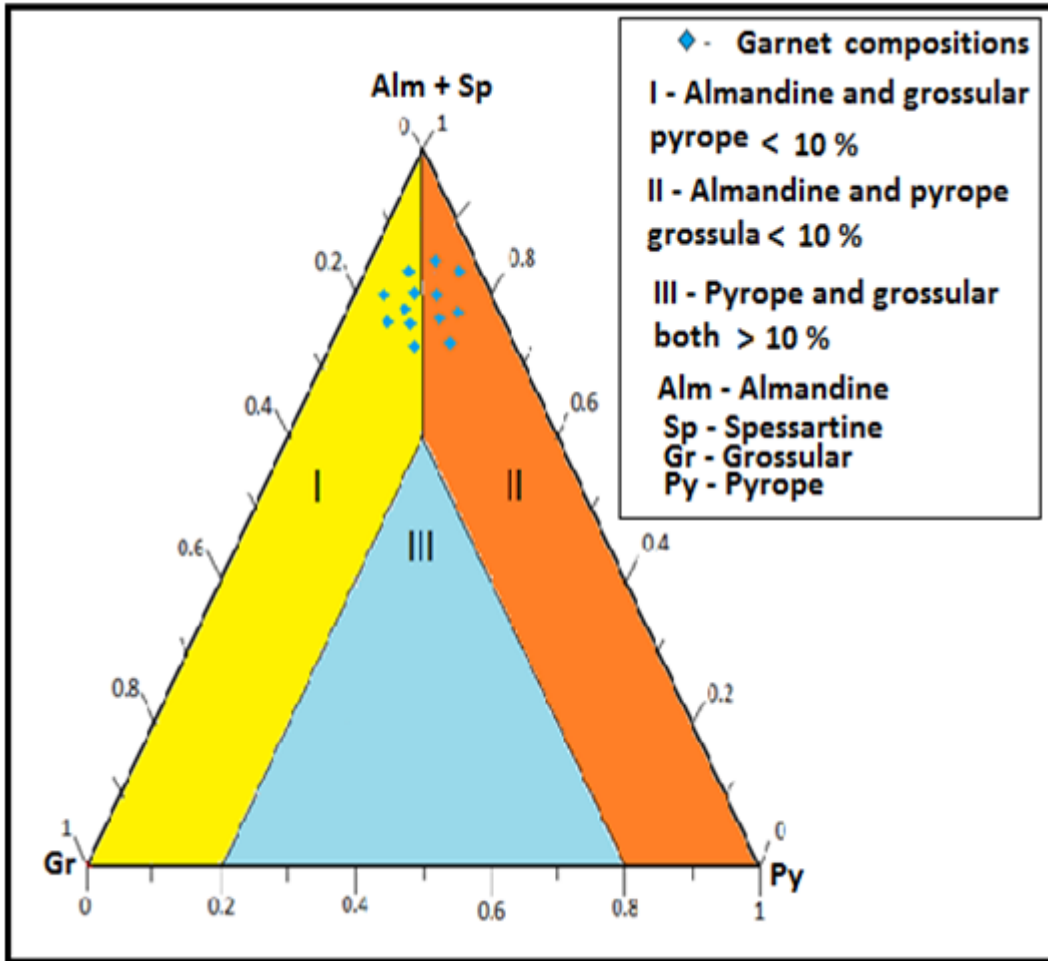


Figure 37: Chemical composition of garnets from upper Pottsville Formation in Cahaba basin plotted on (Alm+Sp)-Gr-Py ternary diagram (adapted from Nanayama, 1997).

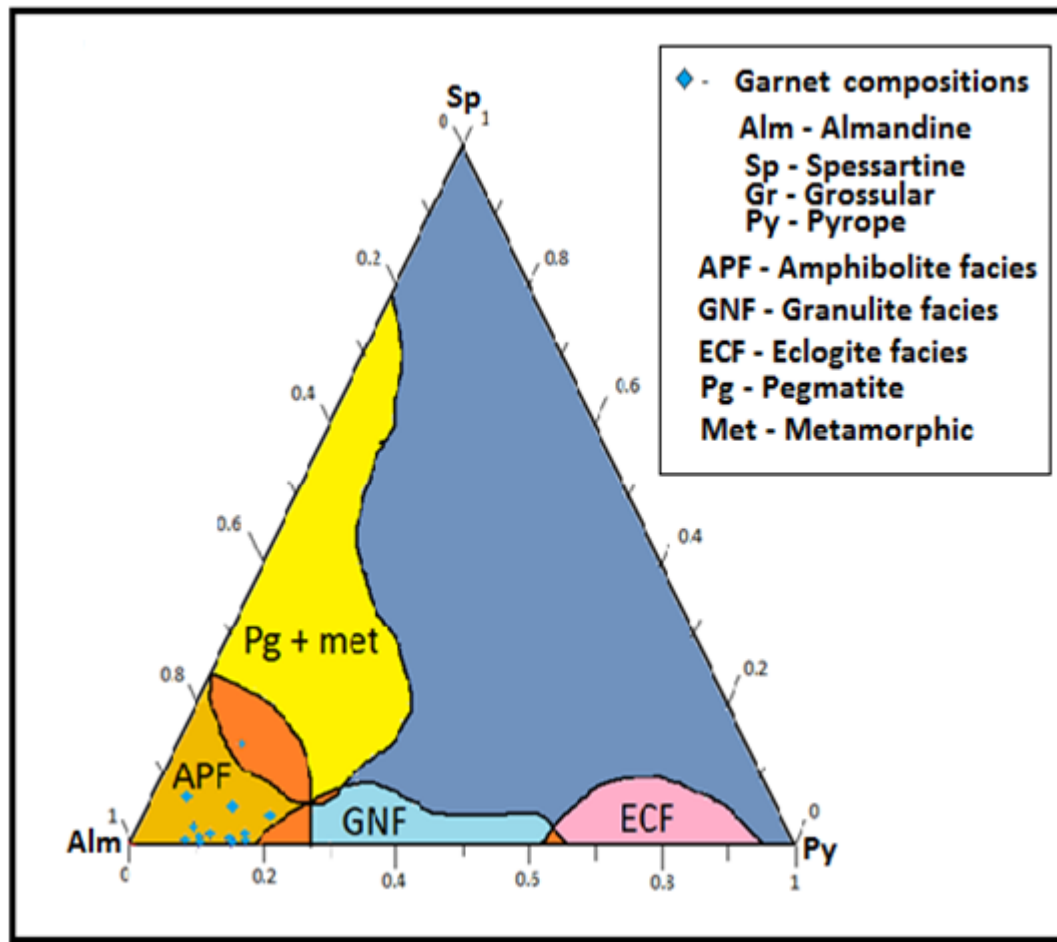


Figure 38: Chemical composition of garnets from upper Pottsville Formation in Cahaba basin plotted on Sp-Alm-Py ternary diagram (adapted from Nanayama, 1997).

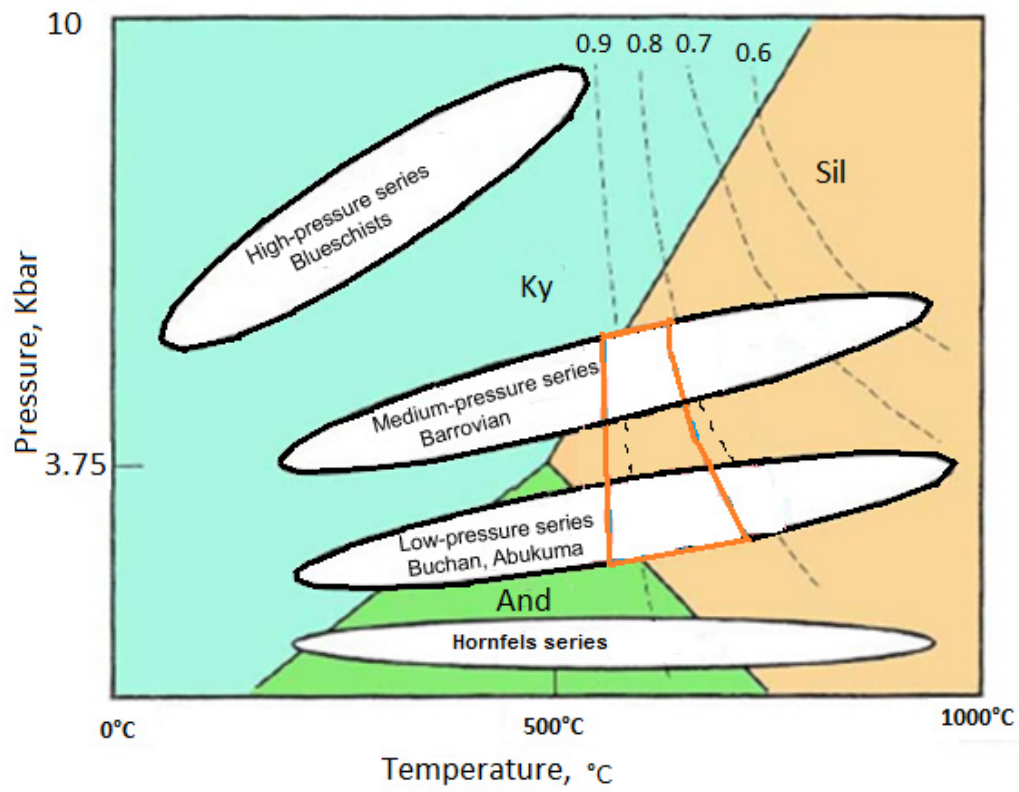


Figure 39: Relationship between Pottsville garnet chemistry and metamorphic pressures and temperatures. Dashed black lines are isopleths of constant $\text{Fe}/(\text{Fe}+\text{Mg})$ calculated assuming that the garnet was in equilibrium with biotite for pelitic compositions and either Barrovian (medium-pressure, high temperature) or Buchan (low pressure) facies (from Spear and Cheney, 1989).

5.4 Interpretations

Most of the garnet grains from the upper Pottsville Formation are high in almandine but low in other garnet end members. The high percentage of almandine content suggests that the garnet grains are mostly derived from a medium grade metamorphic facies. The ternary plot of chemical compositions of garnets in the Sp-Alm-Py ternary diagram also suggest an amphibolite facies provenance.

Rocks in the Ouachita orogeny primarily consists of folded and deformed Paleozoic sandstones, shales, novaculites, and cherts (Engel, 1952; Goldstein, 1959). Localized contact metamorphism of the Ouachita rocks reached very low- to low-grade metamorphism, mainly greenschist facies (Goldstein, 1959; Flawn et al., 1961; Richards et al., 2002). In the Appalachians, the inner Piedmont and Western Blue Ridge terranes reached medium-to high-grade metamorphism. Hence, the garnets of the upper Pottsville Formation in the Cahaba basin were most likely sourced from the Piedmont and Western Blue Ridge of the Appalachians.

CHAPTER 6: $^{40}\text{Ar}/^{39}\text{Ar}$ GEOCHRONOLOGY

6.1 Introduction

$^{40}\text{Ar}/^{39}\text{Ar}$ dating is one of the widely used techniques to understand the structural evolution of fold and thrust belts and to measure the numerical age of crystallization of minerals. The half-life of ^{40}K is 1250 million years, which makes this isotopic technique suitable for the study of geological events of most of earth's history. Volcanic clasts that preserve their high-temperature mineralogy without significant alteration can provide useful information about the timing of eruption and cooling. Fresh and well-crystallized volcanic rocks provide material for $^{40}\text{Ar}/^{39}\text{Ar}$ dating, as the high temperature mineral phases retain radiogenic argon at temperatures experienced in the upper crust. This chapter focuses on $^{40}\text{Ar}/^{39}\text{Ar}$ dating of volcanic clasts separated from the conglomerate samples from upper Pottsville Formation.

6.2 $^{40}\text{Ar}/^{39}\text{Ar}$ Dating

The nuclei of naturally occurring ^{40}K atoms are unstable and decay at a constant rate to produce stable daughter isotopes of ^{40}Ar . In the $^{40}\text{Ar}/^{39}\text{Ar}$ dating technique, the sample is irradiated along with a standard of a known age. This transforms a portion of the ^{39}K atoms to ^{39}Ar . The ratio of $^{40}\text{Ar}/^{39}\text{Ar}$ is proportional to the ratio of $^{40}\text{Ar}/^{40}\text{K}$, and therefore is proportional to age (McDougall and Harrison, 1999). To release argon isotopes five samples are placed in a sealed chamber and heated to fusion, and the argon isotopes measured in a mass spectrometer. The measured $^{40}\text{Ar}-^{39}\text{Ar}$ ratio is used to calculate age with following equation:

$$t = \frac{1}{\lambda} \ln\left(\frac{^{40}\text{Ar}}{^{39}\text{Ar}} J + 1\right) \quad (\text{Merrihue and Turner, 1966}).$$

In this equation, t = age of the sample, λ = decay constant, and J = proportionality constant determined by analysis of the monitors with known age.

6.3 Methodology

For $^{40}\text{Ar}/^{39}\text{Ar}$ age dating, two plagioclase-rich volcanic clasts—a fresh andesite (at ~500 feet depth in the JMHB core) and a metatonalite (at 20 feet depth in the JMHB core)—were extracted from the upper Pottsville conglomerate. Figure 40 shows the stratigraphic position of the samples in the upper Pottsville Formation in the Cahaba basin. Conglomerate core samples were sliced in the rock-cutting laboratory of the Geosciences department at Auburn University (Fig. 41). Each of the conglomerate slices were investigated under a microscope to identify volcanic clasts (Figs. 42 and 43). Standard polished thin sections were made from the volcanic clasts to look at the primary texture of the grains, and qualitative microprobe analysis were performed to determine the overall composition of the clasts. Volcanic clasts also were subjected to XRD analysis to assess the mineralogical compositions of the clasts. Each crystalline solid has its unique characteristic X-ray diffraction pattern which may be used as a "fingerprint" for its identification. The X-ray diffraction pattern analysis of the metatonalite clasts reveals the dominant mineralogy of the clasts (Fig. 44).

Plagioclase can contain up to ~2 wt% K_2O . The $^{40}\text{Ar}/^{39}\text{Ar}$ ratio in plagioclase crystals is determined in a mass spectrometer and used in the age equation to determine the crystallization age of the plagioclase crystals. Considering some finely grained volcanic rocks where individual crystals of plagioclase are not large enough for separation, whole-

rock samples may be used for age determination (McDougall and Harrison, 1999). For the current study, plagioclase crystals were separated and used to date the metatonalite sample, and whole-rock samples were used to date the small andesite clasts. The $^{40}\text{Ar}/^{39}\text{Ar}$ dating was done at the Auburn Noble Isotope Mass Analysis Laboratory (ANIMAL) in the Department of Geosciences at Auburn University. Both samples were analyzed by the step-heating method.

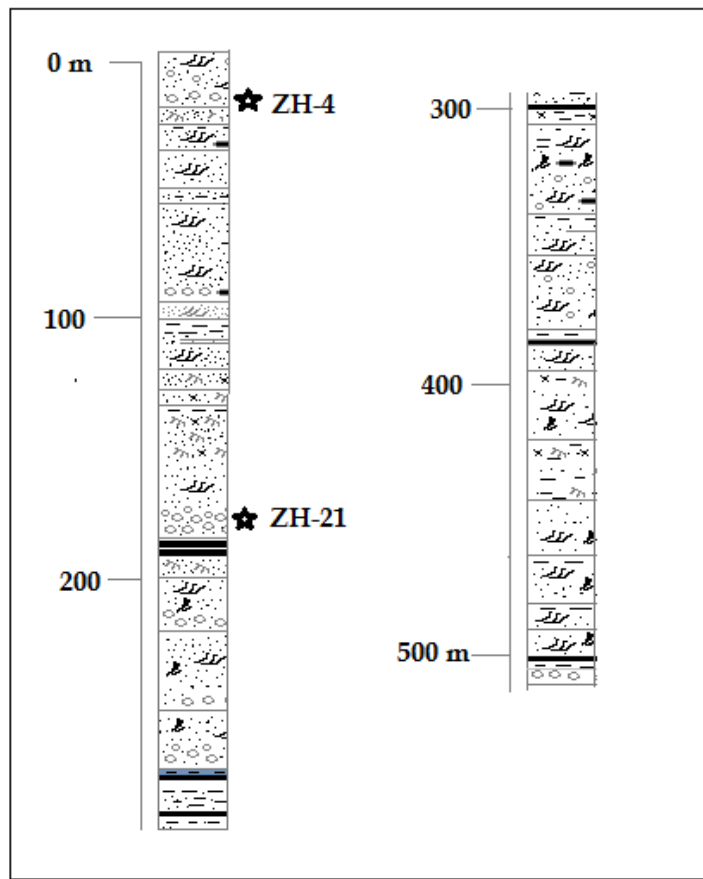


Figure 40: Lithologic column of Conglomerate measures in Joy Manufacturing H.B core with sample locations. ZH -4 is a metatonalite clast and ZH-21 is an andesite clast.

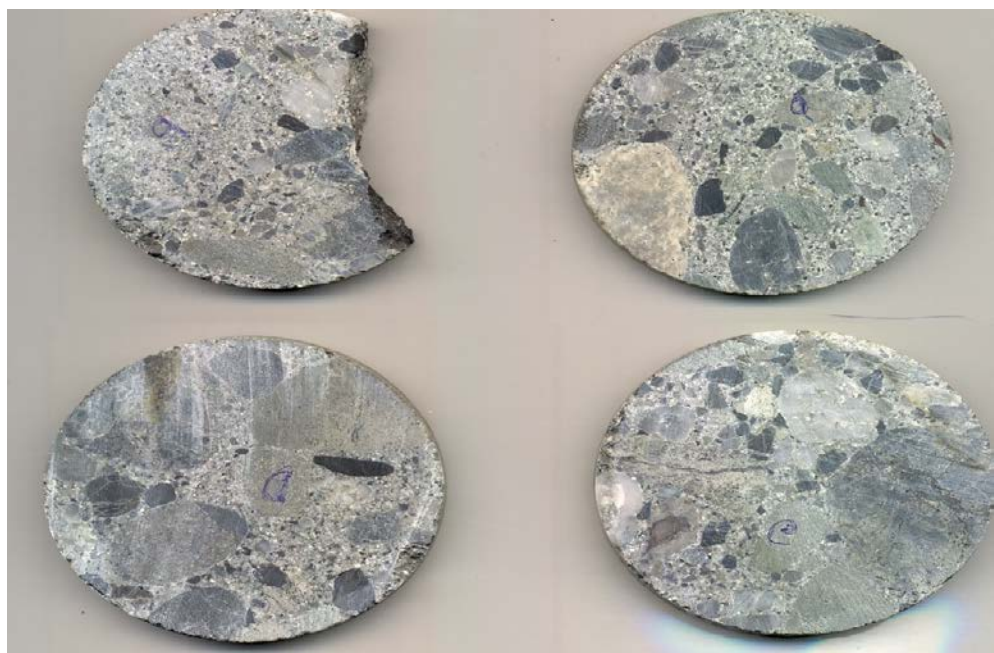


Figure 41: Examples of conglomerate slices used to identify and extract igneous clasts for $^{40}\text{Ar}/^{39}\text{Ar}$ analysis.

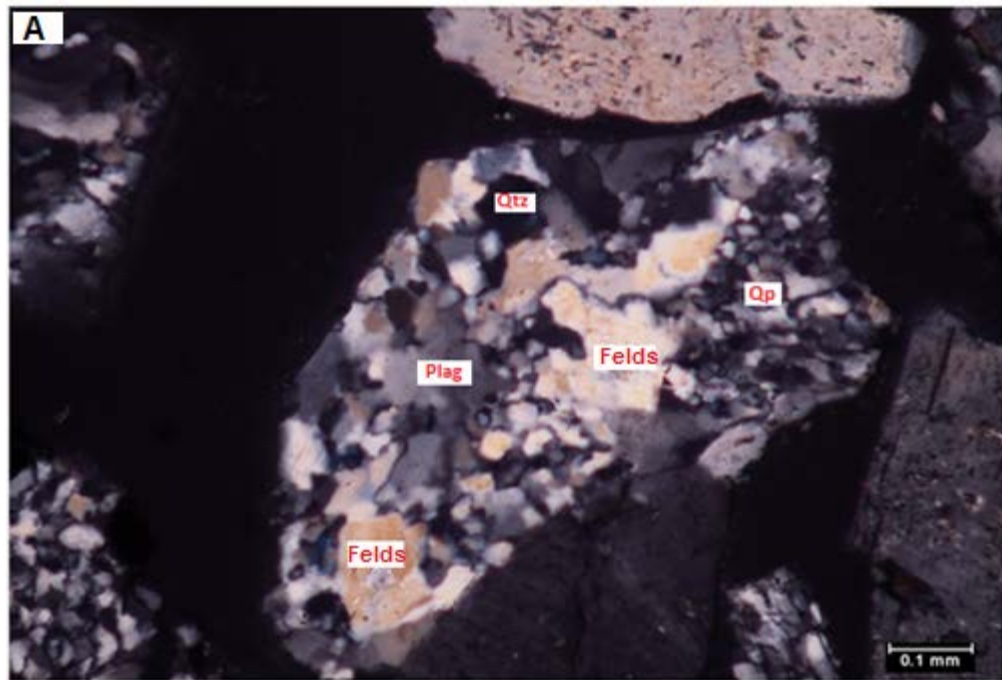


Figure 42: A representative photomicrograph of fragments of metavolcanic clast after crushing from sample ZH-4. (A) Showing few fragments of the clast containing feldspar (Felds) and quartz (Qtz) which has relict igneous texture.



Figure 43: A representative photomicrograph of fragments of volcanic clast after crushing from sample ZH-21. (A) Showing an andesite clast fragments containing feldspar (Felds) and plagioclase laths (Plag micro).

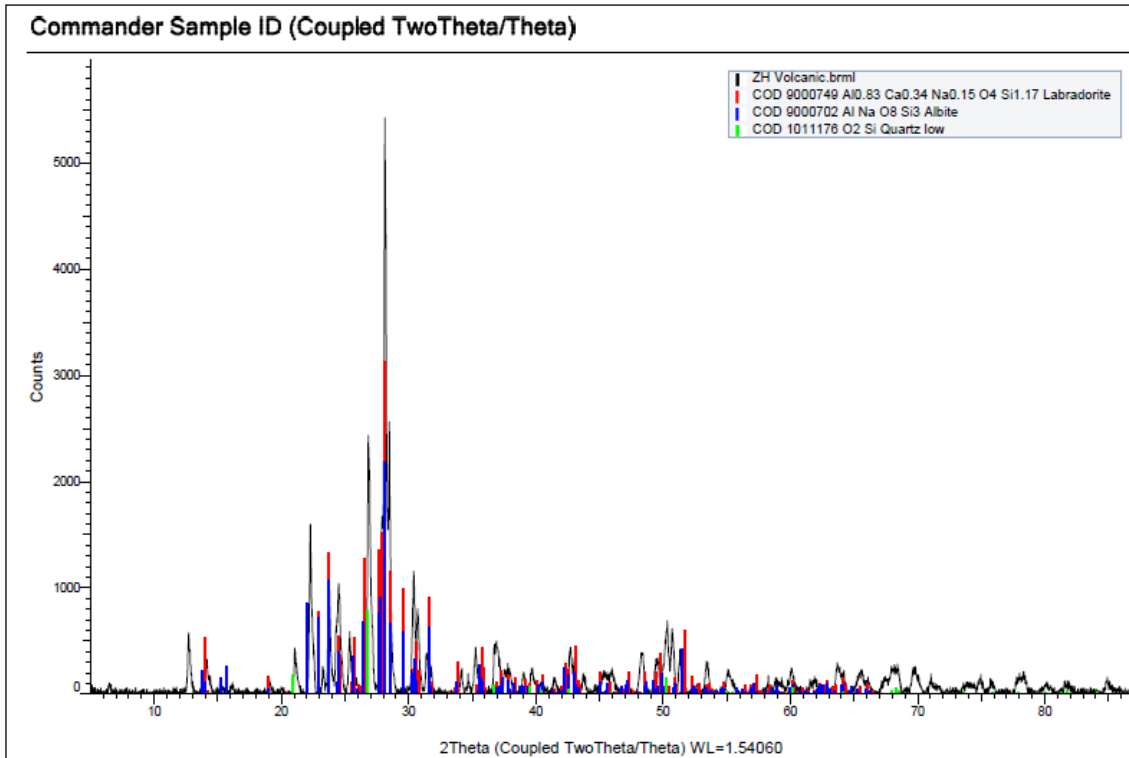


Figure 44: Characteristic X-ray diffraction pattern for metatonalite showing the bulk composition of sample ZH-4. The metatonalite sample is dominantly consists of labradorite, albite and quartz.

6.4 Results

The duplicate $^{40}\text{Ar}/^{39}\text{Ar}$ age spectra for two aliquots of fresh andesite separated from a single pebble gives an average age of ~ 323 Ma (320.2 ± 4.2 Ma and 325.7 ± 2.2 Ma) (Fig. 45). In the andesite samples, the age spectra initially yields a younger age followed by an increase and then a decrease in age over $\sim 10\text{-}30\%$ of the ^{39}ArK released. $^{40}\text{Ar}/^{39}\text{Ar}$ release pattern shows evidence of radiogenic argon loss from low retentivity K-rich sites and $^{40}\text{Ar}/^{39}\text{Ar}$ ratios enhanced by recoil effect of ^{39}Ar nuclei from the fine grained K-rich phase during neutron activation. Due to recoil redistribution of ^{39}ArK within the aphanitic matrix phases and in such cases, and in the absence of extraneous, non-atmospheric ('excess') argon, the total gas ages are preferred and interpreted to record the timing of mineral crystallization.

The age spectrum of metatonalite is complex; it reflects the release of unsupported 'excess' ^{40}Ar from a K-rich phase during the first $\sim 20\%$ of ^{39}ArK release (Fig. 46). Subsequent ages are interpreted to more closely reflect the argon isotopic composition and age of a Ca-rich phase (i.e., plagioclase). After releasing unsupported 'excess' ^{40}Ar from a K-rich phase, age spectra gives a minimum age of ~ 295 Ma and then over the major part of the release pattern of ^{39}ArK , the age spectra gives an age of ~ 320 Ma. The minimum age can be considered as a maximum estimate for the timing of a $^{40}\text{Ar}^*$ loss event recorded by the metatonalite of sample ZH-4. This loss event may have been cooling to a temperature sufficient for complete argon retention by ~ 295 Ma. This minimum age can be interpreted as the youngest permissible age of the Pottsville in the Cahaba basin. The release pattern of $^{37}\text{Ar}/^{39}\text{Ar}$ ratio from both samples also suggest that the later stages of the step heating argon gas was from Ca-rich phase.

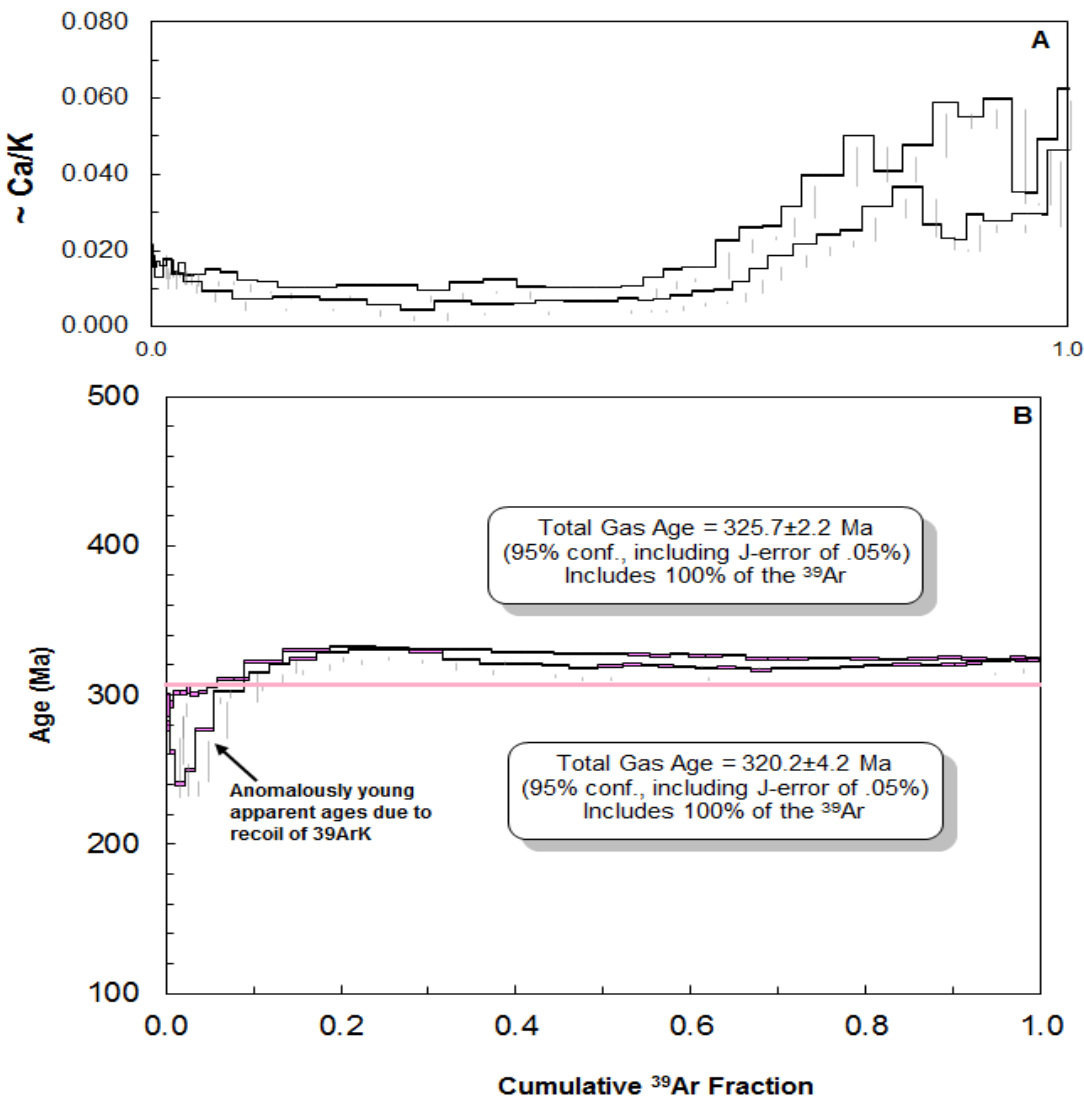


Figure 45: $^{40}\text{Ar}/^{39}\text{Ar}$ age spectra from an andesite clast separated from upper Pottsville Formation. (A) Release pattern of Ar37/39 from andesite sample. (B) Duplicate $^{40}\text{Ar}/^{39}\text{Ar}$ age spectra for two aliquots of fresh andesite separated from a single pebble. Over the major part of the release, the constant ($^{40}\text{Ar}/^{39}\text{Ar}$) ratio indicates a crystallization age of 325.7 ± 2.2 Ma and 320.2 ± 4.2 Ma for this sample (see appendix-C for raw data). Pink line shows the age of a volcanic ash bed (308.5 ± 1.5 Ma) reported by Uddin et al., (2010) for an upper marine section of the Pottsville Formation in Mississippi.

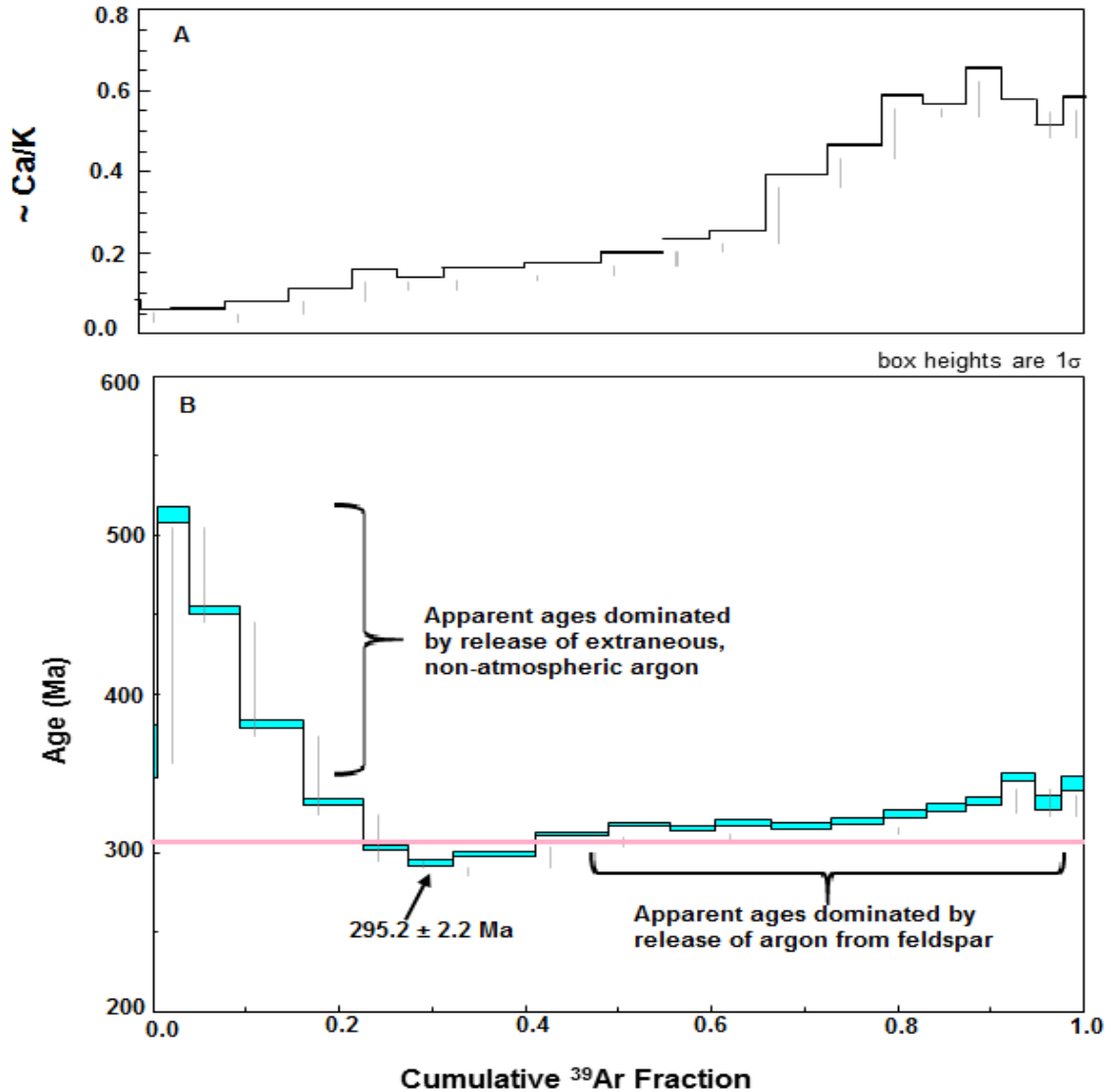


Figure 46: $^{40}\text{Ar}/^{39}\text{Ar}$ age spectra from a metatonalite clast separated from upper Pottsville Formation. (A) Release pattern of Ar37/39 from metatonalite. (B) $^{40}\text{Ar}/^{39}\text{Ar}$ age spectrum from an aliquot of plagioclase separated from metatonalite. $^{40}\text{Ar}/^{39}\text{Ar}$ release pattern shows evidence of unsupported excess argon in K-rich phase during the first ~20% ^{39}ArK release and then the following ages reflect age of Ca rich phase with a minimum age of ~295 Ma (see appendix-C for raw data). Pink line shows the age of a volcanic ash bed (308.5 ± 1.5 Ma) reported by Uddin et al., (2010) for an upper marine section of the Pottsville Formation in Mississippi.

6.5 Interpretation of $^{40}\text{Ar}/^{39}\text{Ar}$ Age Dates

The age of the andesite sample from the Cahaba basin records andesitic volcanism event at ~ 323 Ma. The timing of this volcanism corresponds to ages of fabric-forming metamorphic minerals in the regional Blue Ridge and Piedmont provinces, suggesting a causal relationship between crustal thickening of the Laurentian margin and andesitic volcanism during the Alleghenian orogeny. The minimum age of ~ 295 Ma for the metatonalite has significance for interpreting stratigraphy, as it can be interpreted as a maximum age for the timing of metamorphism of the protolith and a youngest permissible stratigraphic age for the conglomerate deposited in the Cahaba basin.

CHAPTER 7: DISCUSSION AND CONCLUSIONS

7.1 General Paleozoic Lithology of the Provinces in the Cahaba Basin Vicinity

Northern, northeastern and central Alabama consist of several physiographic provinces. From the east-southeast to west-northwest these are the Piedmont, Appalachian Valley and Ridge, Appalachian Plateau (also called Cumberland Plateau), and Highland Rim or Low Interior Plateau (Fig. 3). To the north and northeast of the Cahaba basin, the Appalachian and Interior Low Plateaus are underlain by Paleozoic (Cambrian to Pennsylvanian) sedimentary rocks that rest on crystalline basement of probable Precambrian age (Kidd, 1975; Sapp and Emplaincourt, 1975). The lowermost Paleozoic succession includes the Early and middle Cambrian Rome and Conasauga Formations (Raymond et al., 1988). The Rome Formation consists of fine-grained clastics with lesser amounts of carbonates and evaporites (Kidd, 1975; Neathery and Copeland, 1983). The overlying Conasauga Formation is a thick sequence of marine shale and limestone. The Conasauga Formation is overlain by a thick sequence of Late Cambrian to Late Ordovician shelf carbonates (cherty dolostones and limestones) of the Knox Group (Drahovzal and Neathery, 1971; Kidd, 1975; Benson and Mink, 1983). Mississippian rocks also are exposed in the Interior Low Plateaus, including shales of the Maury Formation and chert and cherty carbonates of the Fort Payne Chert.

In central and northeastern Alabama, the Valley and Ridge physiographic province consists of series of subparallel valleys and ridges trending generally northeast-southwest (Fenneman, 1938; Sapp and Emplaincourt, 1975; Raymond et al., 1988). Paleozoic rocks (Cambrian to Pennsylvanian) exposed in the Valley and Ridge province are grossly similar

to that in the Appalachian and Interior Low Plateaus. The sedimentary successions in the Valley and Ridge province may be subdivided into four major components that reflect different phases in the tectonic history of the southern continental margin of North America (Thomas, 1982). The deposition of carbonate-bank facies during the Cambrian-Early Ordovician indicates development of an extensive passive continental margin (Thomas, 1982). The carbonate rocks are equivalent to the Conasauga Formation in the Appalachian and Interior Low Plateaus and carbonates rocks of the Knox Group, which includes both chert-bearing formations and chert-free carbonate rocks. The rest of the Paleozoic sequence in the Valley and Ridge consists of mostly shallow marine shelf clastics deposited in response to various Appalachian orogenic events.

The Piedmont physiographic province, bordered to the northwest by unmetamorphosed sedimentary rocks of the Fold and Thrust belt, lies to the east and southeast of the Cahaba basin. The Piedmont province consists of metamorphosed crystalline rocks and is subdivided into three lithotectonic provinces; the Northern Piedmont, Inner Piedmont, and Southern Piedmont (Neathery et al., 1976). The Northern Piedmont is separated from the Valley and Ridge to the northwest by the Talladega fault system and from the Inner Piedmont to the southeast by the Brevard fault zone. The Northern Piedmont experienced a prograde Barrovian-style dynamothermal metamorphic event (M1). In some areas, intrusion of plutons resulted in complex pressure-temperature conditions (Muangnoichareon, 1975; Tull, 1978; Gibson and Speer, 1986).

Metamorphic grades in the Piedmont generally increases from low-grade greenschist facies in the northwest to high-grade migmatite facies in the southeast (Neathery, 1975; McConnel et al., 1986; Guthrie and Lesher, 1989). The northern

Piedmont is dominated by low-grade metasedimentary rocks and metavolcanic rocks, although high-grade metamorphic rocks with a local retrograde mineral assemblages and plutonic rocks also are present. To the southeast, the Northern Piedmont contains high-grade metasedimentary rocks, which are locally retrograded (Raymond et al., 1988). Rocks in the Northern Piedmont are mostly slate, phyllite, litharenite, quartzite, graphitic feldspathic mica schist, graphitic and garnetiferous quartzite, and garnet-mica schist and garnet-quartz-muscovite schist (Raymond et al., 1988 and Steltenpohl, 2005). The Wedowee Group of the Northern Piedmont is a heterogeneous sequence of metasedimentary rocks consisting of interlayered graphitic phyllite, garnet-biotite phyllite, biotite-chlorite-sericite phyllite, garnet-biotite metagrawacke, and garnet-feldspar gneiss (Neathery and Reynolds, 1975; Guthrie and Dean, 1989).

Rocks in the Inner Piedmont are subdivided into Dadeville Complex and Opelika Complex (Bentley and Neathery, 1970). Rocks in the Dadeville complex mainly consist of chlorite-actinolite schist, chlorite quartzite, muscovite schist, biotite-garnet-muscovite schist and amphibolite units. The Opelika Complex consists of Auburn Gneiss, kyanite-silimanite-muscovite schist, quartzite, and deformed granitic plutons. Rocks in the Southern Piedmont are highly metamorphosed and consist of highly deformed feldspathic schists and gneisses, the Hollis quartzite, Chewacla Marble, and a migmatitic metasedimentary sequence. K-Ar age determinations from the Phenix City Geniss and from a pluton in the Southern Piedmont range from 274 to 303 Ma, which constrain the last major deformational or metamorphic event in the region (Wampler et al., 1970; Russell, 1978). Figure 47 shows the major lithologies in the Northern and Inner Piedmont.

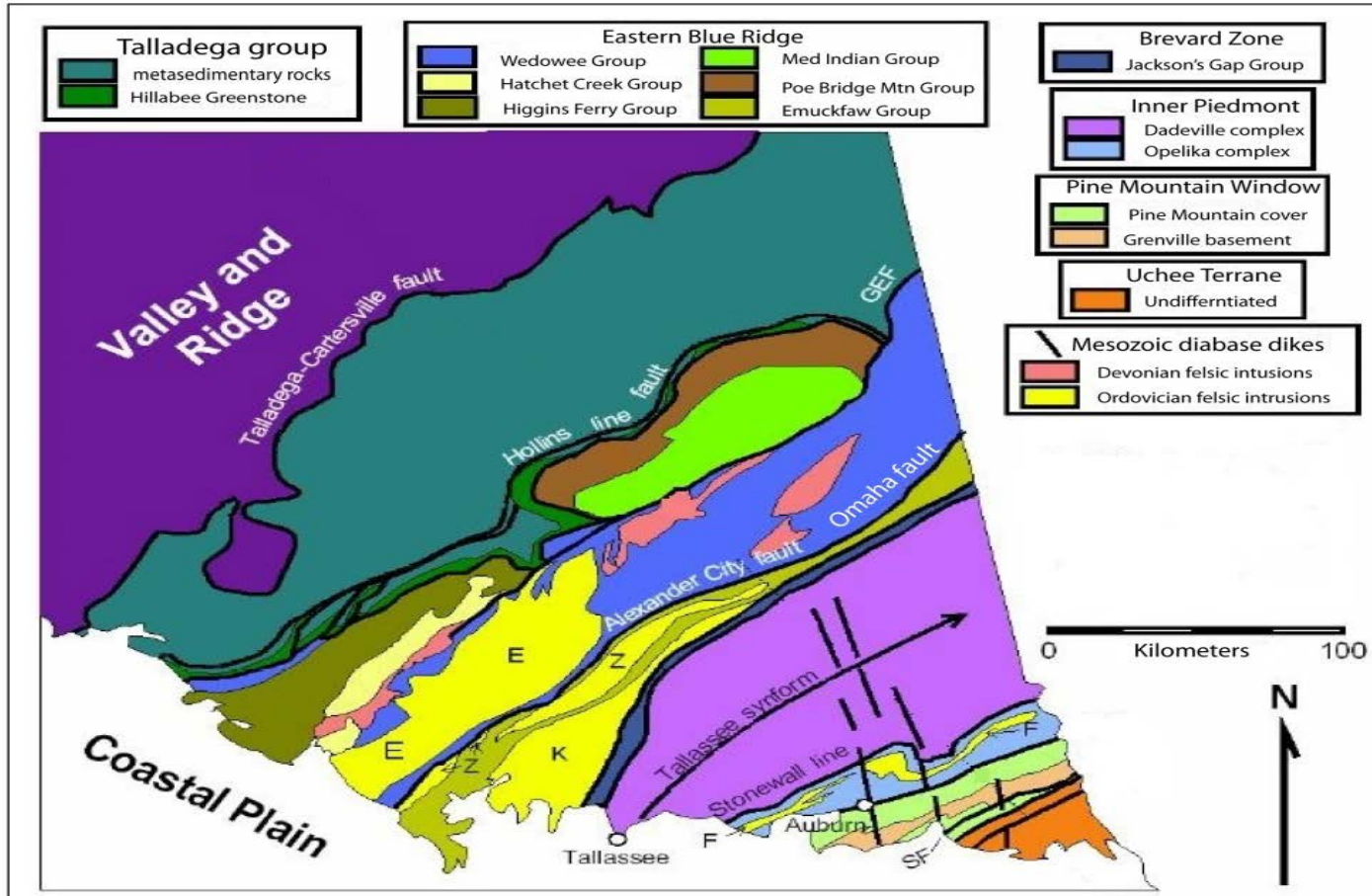


Figure 47: Geologic map showing the various lithotectonic units in the Alabama Piedmont province (modified after Osborne, 1988; Hatcher et al., 1990; Steltenpohl, 2005).

7.2 Comparison of Provenance of Upper Pottsville with the Lower Pottsville in Cahaba Basin

The composition of the Pottsville Formation in the Cahaba basin varies with stratigraphic position. Peavy (2008) worked mostly on the quartzarenite measures and the mudstone measures of the Pottsville Formation in the Cahaba basin. The composition of sandstones in the lower Pottsville differs from that of the sand-sized matrix in the upper conglomerate measures. The sandstones of the quartzarenite measures and mudstone measures are mature and contain higher percentages of monocrystalline quartz. The sands in the matrix of conglomerates in the upper Pottsville are less mature and contain higher percentages of lithics grains and polycrystalline quartz. These differences are reflected in the ternary plots of the sands from the lower and upper Pottsville Formations (Fig. 48). Qt-F-L and Qm-F-Lt plots suggest recycled orogenic and transitional recycled provenances for sandstones of the lower Pottsville. Gomes (2012) worked on sequence stratigraphy and petrofacies of the Pottsville Formation in the Cahaba basin and noted an increase in feldspar and lithic fragments in the upper part of the Pottsville Formation and suggested a recycled orogenic source terrane to the east (Appalachian).

Petrological studies of the Straven Conglomerate of the Pottsville Formation in the Cahaba basin indicate that the source area consisted of chert, carbonates, and sandstones with some volcanic, granitic, and metamorphic rocks. In the Straven Conglomerate, ~78% of the clasts consist of chert and sandstone (Osborne, 1988). The remaining clasts are composed of quartzite, volcanics, and schist. The dominance of the sedimentary clasts in the Straven Conglomerate suggests that the source area consisted primarily of sedimentary rocks. The compositions of sandstones from the Straven Conglomerate are plotted along

with those from the lower Pottsville in figure 47. The Qm-F-Lt ternary plot shows that the percentages of lithic grains are higher in the Straven Conglomerate than the lower Pottsville. Osborne (1988) interpreted that sediments of the Straven Conglomerate are presumably derived from the inner part of the Appalachian Piedmont.

Demirpolat (1989) studied selected sandstones and conglomerates in the southern part of the Cahaba basin and suggested that sediments were transported from the southeast, which was probably the up-slope direction at the time of deposition. Heavy mineral analyses and electron microprobe analyses of selected heavy minerals (e.g., garnet, rutile) from the lower Pottsville suggest that sediments were derived from medium- to high-grade metamorphic source terranes (Peavy, 2008).

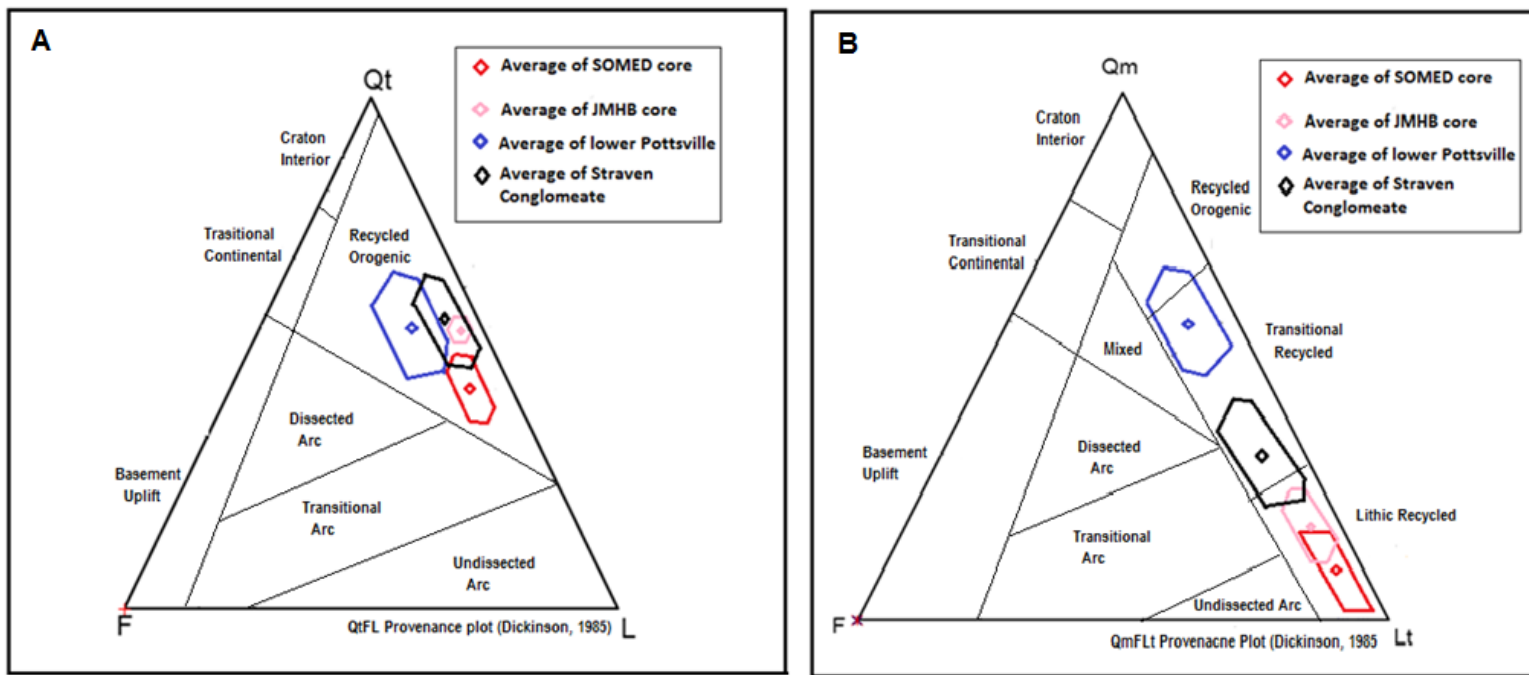


Figure 48: Compositional comparison of sands from the Pottsville Formation from the present work and previous studies, (A). Shows QtFL ternary plot. (B). Shows QmFLt ternary plot. Blue polygon shows the composition of sandstone from the lower Pottsville (quartzarenite and mudstone measures; from Peavy, 2008), black polygon shows the composition of sandstone from the Straven Conglomerate (from Osborne, 1988), and pink and red polygons show the composition of sands from the conglomerate measures in SOMED core and JMHB core, respectively (this study). The result of the present work in comparison with previous studies show that the lithic content increases up section.

7.3 Discussions of the Provenance of Upper Pottsville Conglomerate

Conglomerate clasts in the upper Pottsville Formation consist mainly of sedimentary (chert, sandstone, and mudstone), metasedimentary (phyllite, schist, and quartzite), igneous and metaigneous lithic fragments. The relative abundance of different lithic fragment types varies with stratigraphic position. Sedimentary lithic fragments, including chert decreases and metamorphic lithic fragments increases upsection (Fig. 49).

Similarities of clasts composition in Pottsville conglomerates in Cahaba basin to Paleozoic lithologies in the Appalachian fold and thrust belt and to rocks in the Alabama-Georgia Piedmont suggest that the sediments were mostly derived from the Appalachians to the south-southeast. Mega channels (e.g., Ganges-Brahmaputra scale) may have contributed fine sediments from the central and northern Appalachians to the Cahaba basin (Archer and Greb, 1995; Uddin and Lundberg, 1998; 2004). However, the presence of large sedimentary lithic fragments, including chert and mudstone, in the conglomerates indicate they were derived from a nearby source. Chert is the dominant clast type present in the conglomerates (average ~45%). One of the potential sources of the chert could be the chert-bearing Copper Ridge Dolomite in the lower unit of the Knox Group (Raymond et al., 1988). Alternatively, chert may have been derived from the Mississippian Fort Payne Chert. Derivation of chert from Ouachita is unlikely given the long distance of transport that would require.

Modal analyses of sand matrix in conglomerates suggest that sediments in upper Pottsville Formation mostly derived from a recycled and collisional orogenic provenance.

Qt-F-L and Qm-F-Lt plots for the sand suggest a recycled orogenic and lithic recycled provenance, respectively.

Metamorphic clasts, including phyllite, schist and quartzite, are similar to metasedimentary rocks present in the Piedmont of Alabama and Georgia. The textures in some of the metamorphic clasts indicate medium- to upper medium-grade metamorphic source terranes. Notably, heavy mineral assemblages in sandstones of the upper Pottsville conglomerate measures also suggest medium- to upper medium-grade metamorphic source terranes.

The presence of ultra-stable minerals and low abundance of heavy minerals reflect intense chemical weathering and recycling during deposition of these sediments. This suggests an equatorial weathering regime, which is consistent with the inferred location of the basin during the Pottsville time. Electron microprobe analyses of garnet from the upper Pottsville conglomerate measures indicates the prevalence of almandine type, which indicates amphibolite facies metamorphic source for the upper Pottsville. Rocks in the Ouachitas reached zeolite to lower greenschist facies metamorphism (Goldsten and Reno, 1952; Flawn et al., 1961) and, therefore, could not be the source of medium- to upper medium-grade metamorphic clasts and minerals present in the upper Pottsville of the Cahaba basin. Metamorphic rocks in the Piedmont province of Alabama and Georgia range from low-grade greenschist facies in the northwest to amphibolite facies in southeast. Amphibolite facies in the southeast Piedmont are locally associated with high-grade migmatite facies (Raymond et al., 1988). Thus, the Piedmont could have been the source of garnet, rutile and other medium- to upper medium-grade metamorphic minerals present in the upper Pottsville conglomerates. The Northern Piedmont experienced a prograde

Barrovian-style dynamothermal metamorphic event. By assuming a pelitic source rocks and garnet was in equilibrium with biotite and formed under Barrovian or Buchan/Abukuma conditions, the estimated temperature from the Fe/Fe+Mg ratios in garnet are in the range of 520-750°C. The plot of garnets in Sp-Alm-Py ternary diagram also suggest an amphibolite facies provenance.

The $^{40}\text{Ar}/^{39}\text{Ar}$ analyses of the andesite clasts in this study indicate a plagioclase crystallization age of ~323 Ma and provides evidence for andesitic volcanism in the source terrane during peak Alleghenian orogenesis. The minimum age of the metatonalite sample provides a maximum depositional age of 300 Ma for the Pottsville Formation in Cahaba basin, which also is confirmed by biostratigraphic evidence provided by the miospore *Schultzospora rara* (Eble, 1994). Notably, a $^{40}\text{Ar}/^{39}\text{Ar}$ age of plagioclase crystals from an ash bed (at ~3300 feet depth) from the central Black Warrior basin (BWb) in Mississippi provides a plateau age of 308.58 ± 0.92 Ma (Uddin et al., 2010), which constraints the depositional age of the Pottsville Formation in the BWb. The result reported for the ash layer from the upper section of the Black Warrior Basin in Mississippi and the maximum age of the metatonalite clast of the present study indicate the deposition of the Pottsville sequences in Alabama continued till at least the latest Pennsylvanian.

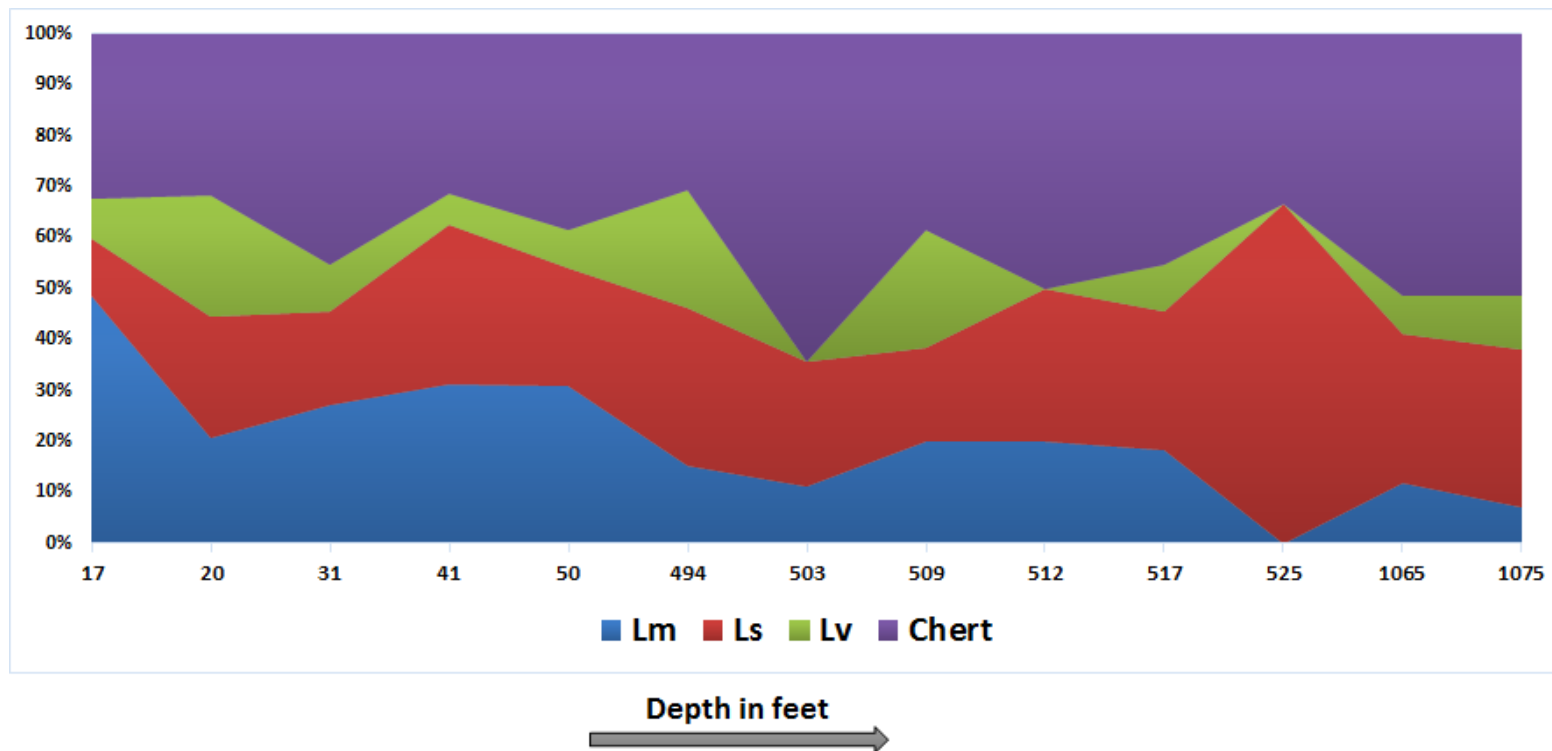


Figure 49: Profile plot of changes in percentage of clast types with stratigraphic position in the upper Pottsville conglomerate measures. Percentages of metamorphic lithics (Lm) increase and percentages of sedimentary lithics (Ls) and chert decrease upsection. Percentages of volcanic clasts (Lv) show no clear pattern throughout the section.

7.4 Conclusions

Conglomerates contain the actual fragments of the rocks contained in source terranes and, thus, provide unequivocal information on provenance. Based on study of conglomerate clasts from the upper Pottsville conglomerate measures, the following conclusions can be drawn about the provenance of these lower Pennsylvanian siliciclastic sediments:

- Conglomerate clasts from the upper Pottsville conglomerate measures mainly consist of chert, sedimentary, metamorphic, and lesser amount of volcanic lithic fragments.
- Clast size, shape and composition confirm that the conglomerates in the upper part of the Cahaba basin were derived from proximal sources in the Valley and Ridge and Piedmont province of the southern Appalachians. However, megachannels (e.g., Ganges-Brahmaputra scale) potentially could have contributed finer sediments from the central and northern Appalachians (e.g., Moore, 2012).
- The QtFL, QmPK, QmFLt and QpLvLs ternary plots of sandstone matrix composition suggest a collisional orogen to recycled orogenic provenance.
- Heavy mineral assemblages from sandstone of the upper Pottsville conglomerate measures suggest a medium- to upper medium-grade metamorphic source terrane in the Piedmont.
- The dominance of almandine garnets suggest that an amphibolite facies metamorphic source rocks supplied sediment to the Cahaba basin.

- Detritus of the Cahaba basin records andesitic volcanism at 323 Ma (Upper Mississippian) suggesting a causal relationship between crustal thickening of the Laurentian margin and andesitic volcanism during the Alleghenian orogeny.
- The minimum age of ~295 Ma (Upper Pennsylvanian) for the metatonalite clast can be interpreted to present a minimum constraint age to the timing of metamorphism of the protoliths and a maximum permissible stratigraphic age for the conglomerate.
- Future work on the sedimentary petrography and geochronology of clasts from the Cahaba basin will help to test the observations of this study and lead to a more comprehensive stratigraphic and tectonic understanding of the basin.

REFERENCES

- Adams, C.J., and Kelley, S., 1998, Provenance of Permian-Triassic and Ordovician metagraywacke terranes in New Zealand: Evidence from Ar-40/Ar-39 dating of detrital micas: Geological Society of America Bulletin, v. 110, p. 422–432.
- Archer, A.W., and Greb, S.F., 1995, An amazon-scale drainage system in the early Pennsylvanian of central North America: The Journal of Geology, v. 103, p. 611–627.
- Armstrong, J.T., 1988, Quantitative analysis of silicate and oxide materials: comparison of Monte Carlo, ZAF and Φ (ρ_z) procedures, D.E. Newbury (Ed.), Microbeam Analysis: San Francisco Press, p. 239-246.
- Bassett, K.N., 2000, Isotopic provenance analysis and terrane tectonics: a warning about sediment transport distances. In: Skilbeck, C., Hubble, T.C. (Eds.), understanding planet earth: Searching for a sustainable Future. Abstracts of the 15th Australian Geological Convention. University of Technology, Sydney, NSW, Australia, 24 p.
- Basu, A., 1985, Influence of climate and relief on compositions of sands released at source areas, provenance of arenites: Springer Netherlands, p. 1-18.
- Basu, A., Young, S.W., Suttner, L.J., James, W.C., and Mack, G.H., 1975, Re-evaluation of the use of undulatory extinction and polycrystallinity in detrital quartz for provenance interpretation: Journal of Sedimentary Research, v. 45, p. 873-882.
- Beck, R.A., Vondra, C.F., Filkins, J.E., and Olander, J.D., 1988, Syntectonic sedimentation and Laramide basement thrusting, Cordilleran foreland; timing of deformation, in Schmidt, C.J., and Perry, W.J., Jr., eds., Interaction of the Rocky Mountain Foreland and the Cordilleran Thrust Belt: Geological Society of America Memoir, v. 171, p. 465–487.
- Benson, D.J., and Mink, R.M., 1983, Depositional history and petroleum potential of the middle and upper Ordovician of the Alabama Appalachians: Gulf Coast Association of Geological Societies Transactions, v. 33, p. 13-21.
- Bentley, R.D., and Neathery, T.L., 1970, Geology of the Brevard fault zone and related rocks of the inner Piedmont of Alabama: Alabama Geological Society Field Trip Guidebook, p. 1-80.
- Bradley, D.C., 1989, Taconic plate kinematics as revealed by foredeep stratigraphy, Appalachian orogen: Tectonics, v. 8, p. 1037-1049.
- Bream, B.R., 2003, Tectonic Implications of Geochronology and Geochemistry of Para and Orthogneisses from the Southern Appalachian Crystalline Core, [Ph.D. dissertation]: University of Tennessee, Knoxville, Tennessee, 296 p.

- Butts, C., 1927, Bessemer-Vandiver folio: U.S. Geological Survey Geologic Atlas, v. 221, 22 p.
- Butts, C., 1940, Description of the Montevallo and Columbiana Quadrangles, Alabama: Geological Survey Geologic Atlas, v. 226, 20 p.
- Carrigan, C.W., Bream, B.R., Miller, C.F., and Hatcher, R.D., Jr., 2001, Ion microprobe analyses of zircon rims from the eastern Blue Ridge and Inner Piedmont, NC-SC-GA: Implications for the timing of Paleozoic metamorphism in the southern Appalachians: Geological Society of America, Abstracts with Programs, v. 33, p. A-7.
- Cawood, P.A., Nemchin, A.A., Leverenz, A., Saeed, A., and Ballance, P.F., 1999, U/Pb dating of detrital zircons: Implications for the provenance record of Gondwana margin terranes: Geological Society of America Bulletin, v. 111, p. 1107–1119.
- Chesnut, D.R., Jr., 1991, Paleontological Survey of the Pennsylvanian rocks of the eastern Kentucky coal field: Kentucky Geological Survey, Series 11, v. 36, 71 p.
- Cooper, B.N., 1964, Relation of stratigraphy to structure in the southern Appalachians, in Lowry, W. D., ed., Tectonics of the southern Appalachians: Virginia Polytechnic Institute Memoir 1, P. 81-114.
- Dávila, F.M., Martina, F., and Astini, R.A., 2004, Cartografía y cinemática de una rampa lateral en el distrito minero Río Blanco, faja plegada y corrida del borde oriental del Famatina ($28^{\circ}43'S$), La Rioja: Revista de la Asociación Geológica Argentina, Serie D, Publicación Especial, v. 7, p. 101–106.
- Dávila, F.M., and Astini, R.A., 2007, Cenozoic provenance history of synorogenic conglomerates in western Argentina (Famatina belt): Implications for Central Andean foreland development: Geological Society of America Bulletin, v. 119, p. 609–622.
- DeCelles, P.G., 1994, Late Cretaceous–Paleocene synorogenic sedimentation and kinematic history of the Sevier thrust belt, northeast Utah and southwest Wyoming: Geological Society of America Bulletin, v. 106, p. 32–56.
- DeCelles, P.G., and Cavazza, W., 1999, A comparison of fluvial megafans in the Cordilleran (Upper Cretaceous) and modern Himalayan foreland basin systems: Geological Society of America Bulletin, v. 111, p. 1315–1334.
- DeCelles, P.G., Pile, H.T., and Coogan, J.C., 1993, Kinematic history of the Meade thrust based on provenance of the Bechler conglomerate at Red Mountain, Idaho, Sevier thrust belt: Tectonics, v. 12, p. 1436–1450.
- DeCelles, P.G., 1988, Lithological provenance modelling applied to the Late Cretaceous synorogenic Echo Canyon conglomerate, Utah: A case of multiple source areas: Geology, v. 16, p. 1039–1043.

- DeCelles, P.G., Tolson, R.B., Graham, S.A., Smith, G.A., Ingersoll, R.V., White, J., Schmidt, C.J., Rice, R., Moxon, I., Lemke, L., Handschy, J.W., Follo, M.F., Edwards, D.P., Cavazza, W., Caldwell, M., and Bargar, E., 1987, Laramide thrust-generated alluvial-fan sedimentation, Sphinx conglomerate, southwestern Montana: American Association Petroleum Geologists Bulletin, v. 71, p. 135–155.
- Demirpolat, S., 1989, Environment of deposition of selected sandstones and conglomerates in southern part of Cahaba Basin, Alabama [Ph.D. Thesis]: Florida State University, Tallahassee, Florida, 121 p.
- Demko, T.M., and Gastaldo, R.A., 1996, Eustatic and autocyclic influences on deposition of the lower Pennsylvanian Mary Lee coal zone, Warrior Basin, Alabama: International Journal of Coal Geology, v. 31, p. 3–19.
- Dickinson, W.R., 1985, Interpreting provenance relations from detrital modes of sandstones, in Zuffa, G.G., ed., Reading Provenance of Arenites: Dordrecht, The Netherlands, Riedel, p. 333–361.
- Dickinson, W.R., 1970, Interpreting detrital modes of greywacke and arkose: Journal of Sedimentary Petrology, v. 40, p. 695–707.
- Dickinson, W.R., and Suczek, C., 1979, Plate tectonics and sandstone compositions: American Association of Petroleum Geologists Bulletin, v. 63, p. 2164–2182.
- Dorsey, R.J., 1988, Provenance evolution and unroofing history of a modern arc-continent collision: Evidence from petrography of Plio-Pleistocene sandstones, eastern Taiwan: Journal of Sedimentary Petrology, v. 58, p. 208–218.
- Drahovzal, J.A., and Neathery, T.L., (Eds.). 1971, The Middle and Upper Ordovician of the Alabama Appalachians: Alabama Geological Society, v. 9, 104 p.
- Drake, A.A. Jr., Sinha, A.K., Laird, J., and Guy, R.E., 1989, The taconic orogen: The Appalachian-Ouachita orogen in the United States: Geological Society of America, Geology of North America, v. 2, p. 101–177.
- Eble, C.F., 1994, Palynostratigraphy of selected Middle Pennsylvanian coal beds in the Appalachian Basin, in Rice, C.L., ed., Elements of Pennsylvanian stratigraphy, central Appalachian Basin: Geological Society of America Special Paper, v. 294, p. 55–68.
- Eichelberger, J. C., 1975, Origin of andesite and dacite: evidence of mixing at Glass Mountain in California and at other circum-Pacific volcanoes: Geological Society of America Bulletin, v. 86, p. 1381–1391.
- Engel, A.E., 1952, Quartz crystal deposits of western Arkansas: United States Geological Survey Bulletin, v. 973-E, p. 173–260.

- Faill, R.T., 1985, The Acadian orogeny and the Catskill delta, in Woodrow, D.L., and Sevon, W.D., editors, The catskill delta: Geological Society of America Special Paper, v. 201, p. 15-37.
- Faill, R.T., 1997, A geologic history of the north-central Appalachians: Part 1. Orogenesis from the Mesoproterozoic through the Taconic orogeny: American Journal of Science, v. 297, p. 551–569.
- Fenneman, N.M., 1938, Physiography of Eastern United States. McGraw-Hill, New York, 714 p.
- Ferguson, R., Hoey, T., Wathen, S., and Werritty, A., 1996, Field evidence for rapid downstream fining of river gravels through selective transport: Geology, v. 24, p. 179–182.
- Flawn, P.T., Goldstein, A., Jr., King, P.B., and Weaver, C.E., 1961, The Ouachita System: University of Texas Bureau of Economic Geology Publication, v. 6120, 401 p.
- Gibson, R.G., and Speer, J.A., 1986, Contact aureoles as constraints on regional P-T trajectories: an example from the Northern Alabama Piedmont, USA: Journal of Metamorphic Geology, v. 4, p. 285-308.
- Gillespie W.H., and Rheams, L.J., 1985, Plant megafossils from the Carboniferous of Alabama, USA: Compte rendu Dixième Congrès International de Stratigraphie et de Géologie du Carbonifère, Madrid, v. 2, p. 191–202.
- Goldstein, A., Jr., 1959, Cherts and novaculites of Ouchita Facies: In Ireland, H. A., Editor, Silica in sediments: Soc. Econ. Paleontologists Mineralogists Special Publication, v. 7, p. 135-149.
- Goldstein, A., and Reno, D.H., 1952, Petrography and metamorphism of sediments of Ouachita facies: American Association of Petroleum Geologists Bulletin, v. 36, p. 2275–2290.
- Graham, S.A., Dickinson, W.R., and Ingersoll, R.V., 1975, Himalayan-Bengal Model for Flysch Dispersal in the Appalachian-Ouachita System: Geological Society of America Bulletin, v. 86, p. 273–286.
- Graham, S.A., Ingersoll, R.V., and Dickinson, W.R., 1976, Common provenance for lithic grains in Carboniferous sandstones from Ouachita Mountains and Black Warrior Basin: Journal of Sedimentary Petrology, v. 46, p. 620-632.
- Graham, S.A., Tolson, R.B., DeCelles, P.G., Ingersoll, R.V., Bargar, E., Caldwell, M., Cavazza, W., Edwards, D.P., Follo, M.F., Handschy, J.W., Lemke, L., Moxon, I., Rice, R., Smith, G.A., and White, J., 1986, Provenance modelling as a technique for analysing source terrane evolution and controls on foreland sedimentation, in Allen,

- P.A., and Homewood, P., eds., *Foreland Basins: International Association of Sedimentologists Special Publication*, v. 8, p. 425–436.
- Greb, S.F., Pashin, J.C., Martino, R.L., and Eble, C.F., 2008, Appalachian sedimentary cycles during the Pennsylvanian: Changing influences of sea level, climate, and tectonics: Geological Society of America Special Papers, v. 441, p. 235-248.
- Gomes, W.S., 2012, A Sequence Stratigraphic Synthesis of the Lower Pennsylvanian Pottsville Formation Encountered in two drill cores in the Cahaba synclinorium, Alabama, [M.S. Thesis]: Auburn University, Auburn, Alabama, 126 p.
- Guthrie, G.M., and Dean, L., 1989, Geology of the New Site 7.5-Minute Quadrangle. Tallapoosa and Clay Counties, Alabama: Geological Survey of Alabama Quadrangle Series Map no. 9, 41 p.
- Guthrie, G.M., and Lesher, C.M., 1989, Geologic setting of lode gold deposits in the Northern Piedmont and Brevard zone, Alabama. Gold deposits of Alabama: Alabama Geological Survey Bulletin, v. 136, p. 11-27.
- Hatcher, R. D., 2005, Southern and Central Appalachians: London, Elsevier, p. 72–81.
- Haque, Z., Uddin, A., Hames, W. E., and Pashin, J. C., 2014, Detrital history of the conglomerate measures of the Pottsville Formation in the Cahaba synclinorium, southern Appalachians, Alabama: Geological Society of America, Abstracts with Programs, v. 46, p. 771.
- Haque, Z., Uddin, A., Hames, W. E., and Pashin, J. C., 2015, Coarse clast petrography and geochronology of the upper Pottsville conglomerate measures, Cahaba synclinorium, southern Appalachian thrust belt, Alabama: Geological Society of America, Abstracts with Programs, v. 47, p. 587.
- Hatcher, R.D., Thomas, W.A., Geiser, P.A., Snoker, A.W., Mosher, S., Wiltschko, D.V., 1989. Alleghenian orogen: The Appalachian-Ouachita Orogen in the United States: The Geological Society of America, The Geology of North America, v. F-2, p. 233-318.
- Hatcher, R.D., 2002, Alleghanian (Appalachian) orogeny, a product of zipper tectonics: Rotational transpressive continent-continent collision and closing of ancient oceans along irregular margins: Geological Society of America Special Paper, v. 364, p. 199-208.
- Hatcher, R., Bream, B., and Merschat, A., 2007, Tectonic map of the southern and central Appalachians: A tale of three orogens and a complete Wilson cycle: The Geological Society of America Memoir, v. 200, p. 1-38.

Hatcher R.D. Jr., Osberg, P.H., Robinson, P., and Thomas, W.A., 1990, Tectonic map of the US Appalachians: Geological Society of America, *The Geology of North America*, v. F-2, Plate, 1.

Haughton, P.D.W., Todd, S.P., and Morton, A.C., 1991, Development in sedimentary provenance studies, in Morton, A.C., Todd, S.P., and Haughton, P.D.W., (Eds)., *Developments in Sedimentary Provenance Studies*: Geological Society of London special publication, v. 57, p. 1–11.

Henry, D.J., and Dutrow, B.L., 1990, Tourmaline as a low grade clastic metasedimentary rock: an example of the petrogenetic potential of tourmaline: *Contributions to Mineralogy and Petrology*, v. 112, p. 203-218.

Henry, D.J., and Guidotti, C.V., 1985, Tourmaline as a petrogenetic indicator mineral: an example from the staurolite grade metapelites of NW Maine: *American Mineralogists*, v. 70, p. 1-15.

Hess, H.H., 1966, Notes on operation of Frantz isodynamic magnetic separator, Princeton University: User manual guide, p. 1-6.

Hobday, D.K., 1974, Beach-and barrier-island facies in the upper Carboniferous of northern Alabama: *Geological Society of America Special Papers*, v. 148, p. 209–224.

Hewitt, J.L., 1984, Geologic overview, coal, and coalbed methane resources of the Warrior Basin–Alabama and Mississippi: *American Association of Petroleum Geologists special publication*, v. 17, p. 73-104.

Horsey, C.A., 1981, Depositional environments of the Pennsylvanian Pottsville Formation in the Black Warrior basin of Alabama: *Journal of Sedimentary Research*, v. 51, p. 799-806.

Horton, J.W., Jr., Drake, A.A., and Rankin, D.W., 1989, Tectonostratigraphic terranes and their boundaries in the central and southern Appalachians: *Geological Society of America Special Paper* 230, p. 213-245.

Ingersoll, R.V., and Suczek, C.A., 1979, Petrology and provenance of Neogene sand from Nicobar and Bengal Fans, DSDP sites 211 and 218: *Journal of Sedimentary Petrology*, v. 54, p. 1217-1228.

Ireland, T.R., 1992, Crustal evolution of New Zealand: evidence from age distributions of detrital zircons in Western Province paragneisses and Torlesse greywacke: *Geochimica et Cosmochimica Acta*, v. 56, p. 911– 920.

- Ireland, T.R., Floettmann, T., Fanning, C.M., Gibson, G.M., Preiss, W.V., 1998, Development of the early Paleozoic Pacific margin of Gondwana from detrital-zircon ages across the Delamerian Orogen: *Geology*, v. 26, p. 243– 246.
- Kidd, J.T., 1975, Pre-Mississippian Subsurface Stratigraphy of the Warrior Basin in Alabama: *Gulf Coast Association of Geological Societies Transactions*, v. 25, p. 20-39.
- Kodama, Y., 1994, Downstream changes in the lithology and grain size of fluvial gravels, the Watarase River, Japan: Evidence of the role of abrasion in downstream fining: *Journal of Sedimentary Research*, v. 64, p. 68– 75.
- Li, R., Lib, S., Jin, F., Wan, Y., Zhang, S., 2004, Provenance of Carboniferous sedimentary rocks in the northern margin of Dabie Mountains, central China and the tectonic significance: constraints from trace elements, mineral chemistry and SHRIMP dating of zircons: *Sedimentary Geology*, v. 166, p. 245–264.
- Liu, Y., and Gastaldo, R.A., 1992, Characteristics and provenance of log-transported gravels in a Carboniferous channel deposit: *Journal of Sedimentary Petrology*, v. 62, p. 1072-1083.
- Lutgens, K.F., Tarbuck, J.E., and Tasa, G.D., 2015, Earth Science (14th edition), Pearson Education, Inc, 719 p.
- Mack, G.H., Thomas, W.A., and Horsey, C.A., 1983, Composition of Carboniferous sandstone and tectonic framework of southern Appalachian-Ouachita Orogen: *Journal of Sedimentary Petrology*, v. 53, p. 931-946.
- Mange, M.A., and Maurer, H.F.W., 1992, Heavy Minerals in Color: Chapman and Hall, London, 147 p.
- McBride, E.F., 1985, Diagenetic processes that affect provenance determinations in sandstone: *NATO ASI Series. Series C: Mathematical and Physical Sciences*, v. 148, p. 95-113.
- McClellan, E.A., and Miller, C.F., 2000, Ordovician age confirmed for the Hillabee Greenstone, Talladega belt, southernmost Appalachians: *Geological Society of America Abstract with Programs*, v. 32, p. 117.
- McConnell, K.I., Abrams, C.E., and German, J.M., 1986, Gold deposits in the Northern Piedmont of Georgia and Alabama and their relationship to lithostratigraphic units. Volcanogenic sulfide and precious metal mineralization in the southern Appalachians: *University of Tennessee, Department of Geological Sciences, Studies in Geology*, v. 16, p. 164-181.

- McDougall, I., and Harrison, T.M., 1999, Geochronology and Thermochronology by the $^{40}\text{Ar}/^{39}\text{Ar}$ Method: Oxford University Press, Oxford, 269 p.
- McQueen, H.J., and Jonas, J.J., 1975, Recovery and recrystallization during high temperature deformation: Treatise on materials science and technology, v. 6, p. 393-493.
- Merrihue, C., and Turner, G., 1966, Potassium-argon dating by activation with fast neutrons: Journal of Geophysical Research., v. 71, p. 2852-2857.
- Merschat, J.A., 2009, Assembling the Blue Ridge and Inner Piedmont: Insights into the nature and timing of terrane accretion in the southern Appalachian orogen from geologic mapping, stratigraphy, kinematic analysis, petrology, geochemistry, and modern geochronology, [Ph.D. Thesis]: University of Tennessee, Knoxville, Tennessee, 472 p.
- Miller, B.V., Fetter, A.H., and Steward, K.G., 2006, Plutonism in three orogenic pulses, Eastern Blue Ridge Province, southern Appalachians: Geological Society of America Bulletin, v. 118, p. 171-184.
- Moore, F.M., 2012, $^{40}\text{Ar}/^{39}\text{Ar}$ Dating of detrital muscovite and sediment compositional analysis of the Pottsville Formation in the Black Warrior basin in Alabama: Implications for tectonics and sedimentation, [MS Thesis]: Auburn University Auburn, AL, 142 p.
- Morton, A.C., 1985, Heavy minerals in provenance studies: in G.G. Zuffa (editor), Provenance of Arenites, D. Reidel Publishing, Boston, p. 249-277.
- Morton, A.C., 1986, Influences of provenance and diagenesis on detrital garnet suites in the Paleocene Forties sandstones, central North Sea: Journal of Sedimentary Petrology, v. 57, p. 1027-1032.
- Morton, A.C., and Hallsworth, C.R., 1999, Processes controlling the composition of heavy mineral assemblages in sandstones: Sedimentary Geology, v. 124, p. 3-30.
- Morton, A.C., and Taylor, P.N., 1991, Geochemical and isotopic constraints on the nature and age of basement rocks from Rockall Bank, NE Atlantic: Journal of Geological Society of London, v. 148, p. 631-634.
- Muangnoicharoen, N., 1975, The geology and structure of a portion of the northern Piedmont, east-central Alabama, [M.S. thesis]: University of Alabama, Tuscaloosa, Alabama, 74 p.
- Nanayama, F., 1997, An electron microprobe study of the Amazon Fan: Proceedings the Ocean Drilling Program, Scientific Results, v. 155, p. 147-168.

Neathery, T.L., 1975, Rock units in the high-rank belt of the northern Alabama Piedmont, in Neathery, T.L., and Tull, J.F., eds., Geologic Profiles of the Northern Alabama Piedmont: Alabama Geological Society, 13th Annual Field Trip Guidebook, p. 9–42.

Neathery, T.L., Bentley, R.D., Higgins, M.W., and Zietz, I., 1976, Preliminary interpretation of aeromagnetic and aeroradioactivity maps of the Alabama Piedmont: *Geology*, v. 4, p. 375–381.

Neathery, T.L., and Copeland, C.W., 1983, New information on the basement and Lower Paleozoic stratigraphy of north Alabama: Geological Society of America, Southeastern Section in Abstracts with Programs, p. 98.

Neathery, T.L., and Reynolds, J.W., 1975, Geology of the Lineville East, Ofelia, Wadley North, and Mellow Valley Quadrangles, Alabama: Geological Survey of Alabama Bulletin, v. 109, 120 p.

Neathery, T.L., and Thomas, W.A., 1983, Geodynamics transect of the Appalachian orogen in Alabama, Profiles of orogenic belts: American Geophysical Union series, v. 10, p. 301–307.

Osberg, P.H., Tull, J.F., Robinson, P., Hon, R., Butler, J.R., 1989, The Acadian orogen, in Hatcher, R.D., Jr., Thomas, W.A., Viele, G.W., (editors), The Appalachian–Ouachita orogen in the United States,: Geological Society of America, The geology of North America, v. F-2, p. 179–232.

Osborne, E.T., 1988, Provenance and depositional environment of the Straven conglomerate member, Pottsville Formation (Pennsylvanian), Cahaba Synclinorium, Central Alabama, [M.S. Thesis]: University of Alabama, Tuscaloosa, Alabama, 116 p.

Osborne, E.T., 1991, Depositional environment and provenance of the Straven conglomerate member, Pottsville Formation in Thomas, W.A., and Osborne, W.E., eds., Mississippian-Pennsylvanian tectonic history of the Cahaba synclinorium: Alabama Geological Society Guidebook, 28th Annual Field Trip, p. 73–93.

Osborne, W.E., and Guthrie, G.M., 1986, Polyphase deformation of lateral ramps in Appalachian foreland fold and thrust belt and Talladega slate belt in Alabama: American Association of Petroleum Geologists Bulletin, v. 70, p. 628–629.

Pashin, J., 2004, Cyclothsems of the Black Warrior Basin, Alabama, USA.: Eustatic snapshots of foreland basin tectonism, in Pashin, J. C. and Gastaldo, R. A., editors, Sequence stratigraphy, paleoclimate, and tectonics of coal-bearing strata: American Association of Petroleum Geologists, Studies in Geology, v. 51, p. 199–218.

Pashin, J., and Carroll, R.E., 1999, Geology of the Cahaba Coalfield: A Guidebook for the 36th Annual Field Trip of the Alabama Geological Society, 93 p.

Pashin, J., Carroll, R.E., Barnett, R.L., and Beg, M.A., 1995, Geology and coal resources of the Cahaba coal field: Alabama Geological Survey Bulletin, v. 163, 49 p.

Pashin, J.C., Carroll, R.E., McIntyre, M.R., and Grace, R., 2010, Geology of unconventional gas plays in the southern Appalachian thrust belt: Alabama Geological Survey Guidebook for field trip 7, American Association of Petroleum Geologists annual conference and exposition, 86 p.

Peavy, T., 2008, Provenance of lower Pennsylvanian Pottsville Formation, Cahaba synclinorium, Alabama, [M.S. Thesis]: Auburn University, Auburn, AL, 106 p.

Pettijohn, F.J., Potter, P.E., and Siever, R., 1987, Sand and Sandstone: New York, Springer-Verlag, 553 p.

Pell, S.D., Williams, I.S., and Chivas, A.R., 1997, The use of protolith zircon-age fingerprints in determining the protosource areas for some Australian dune sand sediment: *Sedimentary Geology*, v. 109, p. 233–260.

Pickard, A.L., Adams, C.J., Barley, M.E., 2000, Provenance of New Zealand Late Permian to Cretaceous depocentres at the Australian margin of Gondwanaland: Evidence from detrital zircon SHRIMP dating: *Australian Journal of Earth Sciences*, v. 47, p. 987– 1007.

Poole, F.G., Perry, W. J., Madrid, R. J., and Amaya-Martinez, R., 2005, Tectonic synthesis of the Ouachita-Marathon-Sonora orogenic margin of southern Laurentia: Stratigraphic and structural implications for timing and deformational events and plate-tectonic model: *Geological Society of America Special Paper*, v. 393, p. 543-596.

Raymond, D.E., Osborne, W.E., Copeland, C.W., and Neathery, T.L., 1988, Alabama stratigraphy: Alabama Geological Survey Circular, v. 140, 97 p.

Reading, H.G., and Levell, B.K., 1996, Controls on the sedimentary rock record, in Reading, H.G., ed., *Sedimentary environments: Processes, Facies and Stratigraphy*: Blackwell Science, Oxford, p. 5-36.

Rheams, L.J., and Benson, D.J., 1982, Depositional setting of the Pottsville Formation in the Black Warrior Basin: Alabama Geological Society, Field Trip Guidebook, v. 19, 94 p.

Richards, I.J., Connelly, J.B., Gregory, R.T., and Gray, D.R., 2002, The importance of diffusion, affection, and host-rock lithology on vein formation: A stable isotope study from the Paleozoic Ouachita orogenic belt, Arkansas and Oklahoma: *Geological Society of America Bulletin*, v. 114, p. 1343-1355.

- Robinson, A.J.R., and Prave, R.A., 1995, Cratonal contributions to a “classic” molasse: The Carboniferous Pottsville Formation of eastern Pennsylvania revisited: *Geology*, v. 23, p. 369-372.
- Rowley, D.B., and Kidd, W.S.F., 1981, Stratigraphic relationships and detrital composition of the Middle Ordovician flysch of western New England: Implications for the tectonic evolution of the Taconic orogeny: *Journal of Geology*, v. 89, p. 199–218.
- Russell, G. S., 1978, U-Pb, Rb-Sr, and K-Ar isotopic studies: Bearing on the tectonic development of the southernmost Appalachian orogen, Alabama, [Ph.D. thesis]: Florida State University, Florida, Tallahassee, 179 p.
- Sapp, C.D., and Emplaincourt, J., 1975, Physiographic regions of Alabama: Geological Survey of Alabama, map 168.
- Schlee, J., 1963, Early Pennsylvanian currents in the southern Appalachian Mountains: *Geological Society of America Bulletin*, v. 74, p. 1439-1452.
- Secor, D.T.Jr., Snock, A.W., and Dallmeyer, R.D., 1986, Character of the Alleghenian orogeny in the southern Appalachians: Part III. Regional tectonic relations: *Geological Society of America Bulletin*, v. 97, p. 1345-1353.
- Sircombe, K.N., 1999, Tracing provenance through the isotope ages of littoral and sedimentary detrital zircons, Eastern Australia: *Sedimentary Geology*, v. 124, p. 47–67.
- Smith, E.W., 1979, Pennsylvanian stratigraphy of Alabama, The Mississippian and Pennsylvanian (Carboniferous) systems in the United States--Alabama and Mississippi: US Geological Survey Professional Paper, p. 23-36.
- Spear, F.S., and Cheney, J.T., 1989, A petrogenetic grid for pelitic schists in the system $\text{SiO}_2\text{-Al}_2\text{O}_3\text{-FeO}\text{-MgO}\text{-K}_2\text{O}\text{-H}_2\text{O}$, A petrogenetic grid for pelitic schists in the system $\text{SiO}_2\text{-Al}_2\text{O}_3\text{-FeO}\text{-MgO}\text{-K}_2\text{O}\text{-H}_2\text{O}$: Contributions to Mineralogy and Petrology, v. 101, p. 149-164.
- Squire, J., 1890, Report on the Cahaba coal field: Alabama Geological Survey Special Report 2, 189 p.
- Steltenpohl, M.G., 2005, An introduction to the terranes of the southernmost Appalachians of Alabama and Georgia, in Steltenpohl, M.G., Southernmost Appalachian terranes, Alabama and Georgia: Field trip Guidebook for the Geological Society of America Southeastern Section Annual Meeting, p. 1-18.
- Steltempohl, M.G., and Moore, W.B., 1988, Metamorphism in the Alabama Piedmont: Geological Survey of Alabama Circular 138, 27 p.

- Stipp, M., Holger S., Renée H., and Stefan M.S., 2002, The eastern Tonale fault zone: a 'natural laboratory' for crystal plastic deformation of quartz over a temperature range from 250 to 700 C: *Journal of Structural Geology*, v. 24, p. 1861-1884.
- Thomas, W.A., 1982, Stratigraphy and structure of the Appalachian fold and thrust belt in Alabama in: Thomas, W.A., and Neathery, T.L., (Eds.), *Appalachian Thrust Belt in Alabama: Tectonics and Sedimentation*, 95th Annual Meeting Geological Society of America Guidebook for Field Trip, 13, p. 55–78.
- Thomas, W.A., 1989, The Black Warrior basin. In: L.L. Sloss (Editor), *Sedimentary Cover North American Craton: Geological Society of America, The Geology of North America*, A, 185 p.
- Thomas, W.A., 1976, Evolution of Appalachian-Ouachita salients and recesses from reentrants and promontories in the continental margin: *American Journal of Science*, v. 277, p. 1233-78.
- Thomas, W.A., 2005, Tectonic inheritance at continental margin: *GSA Today*, v. 16, p. 4-11. Thomas, W.A., Chowns, T.M., Daniels, D.L., Neathery, T.L., Glover, L., III, Gleason, R.J., 1989b. Pre-Mesozoic paleogeologic map of Appalachian-Ouachita orogen beneath Atlantic and Gulf Coastal Plains. In: Hatcher Jr., R.D., Thomas, W.A., Viele, G.W., (Eds.), *The Appalachian-Ouachita orogen in the United States: Geological Society of America, The Geology of North America*, F-2, Plate 6.
- Thomas, W.A., and Bayona, G., 2005, The Appalachian thrust belt in Alabama and Georgia: thrust-belt structure, basement structure, and palinspastic reconstruction: *Alabama Geological Survey Monograph*, v. 16, 48 p.
- Thomas, W.A., and Mack, G. H., 1982, Paleogeographic relationship of a Mississippian barrier-island and shelf-bar system (Hartselle Sandstone) in Alabama to the Appalachian-Ouachita orogenic belt: *Geological Society of America Bulletin*, v. 93, p. 6-19.
- Thomas, W. A., and Neathery, T. L., 1980, Tectonic framework of the Appalachian orogen in Alabama, in Frey, R. W., ed., *Excursions in southeastern Geology*: Fallss Church, Virginia, American Geological Institute, p. 465-526.
- Trepmann, C. A., and Stöckhert, B., 2003, Quartz microstructures developed during non-steady state plastic flow at rapidly decaying stress and strain rate: *Journal of Structural Geology*, v. 25, p. 2035-2051.
- Tull, J.F., 1978, Structural development of the Alabama Piedmont northwest of the Brevard zone: *American Journal of Science*, v. 278, p. 442-460.

- Uddin, A., Hames, W. E., Peavy, T., and Pashin, J. C., 2010, Stratigraphic and detrital source constraints for lower paleozoic Pottsville Formation of Alabama and Mississippi: Geological Society of America, Abstract with Programs, v. 42, p. 196.
- Uddin, A., Kumar, P., Sarma, J.N., and Akhter, S.H., 2007, Heavy-mineral constraints on provenance of Cenozoic sediments from the foreland basins of Assam, India and Bangladesh: Erosional history of the eastern Himalayas and the Indo-Burman ranges, in Mange, M.A., and Wright, D.T., eds., Heavy minerals in use, Developments in Sedimentology, Elsevier, Amsterdam, v. 58, p. 823-847.
- Uddin, A., and Lundberg, N., 2004, Miocene sedimentation and subsidence during continent-continent collision, Bengal Basin, Bangladesh: *Sedimentary Geology*, v. 164, p. 131-146.
- Uddin, A., and Lundberg, N., 1998, Cenozoic history of the Himalayan-Bengal system: Sand composition in the Bengal basin, Bangladesh: *Geological Society of America Bulletin*, v. 110, p. 497-511.
- Wampler, J.M., Neathery, T.L., and Bentley, R.D., 1970, Age relations in the Alabama Piedmont, in Bentley, R.D., and Neathery, T.L., eds., *Geology of the Brevard Fault Zone and related rocks of the Inner Piedmont of Alabama: Alabama Geological Society 8th annual Field Trip, Guidebook*, p. 81-90.
- Wandres, A.M., Bradshaw, J.D., Weaver, S., Maas, R., Ireland, T., and Eby, N., 2004, Provenance of the sedimentary Rakaia sub-terrane, Torlesse Terrane, South Island, New Zealand: the use of igneous clast compositions to define the source: *Sedimentary Geology*, v. 168, p. 193–226.
- Weltje, G.J., 2006, Ternary sandstone composition and provenance: an evaluation of the “Dickinson model”: *Geological Society of London, Special Publications*, 264, p. 79–99.
- Zack, T., von Eynatten, H., and Kronz, A., 2004, Rutile geochemistry and its potential use in quantitative provenance studies: *Sedimentary Geology*, v. 171, p. 37–58.
- Zahid, K.M., 2005, Provenance history of Paleogene and Paleogene-Neogene transitional sediments from Bengal Basin, Bangladesh, [M.S. Thesis]: Auburn University, Auburn, Alabama, 142 p.
- Zhang, H.F., Menzies, M.A., and Mattey, D., 2003, Mixed mantle provenance: diverse garnet compositions in polymict peridotites, Kaapvaal craton, South Africa: *Earth Planet Science Letters*, v. 216, p. 329–346.

APPENDICES

Appendix A. Electron microprobe standards used in this study.

Electron microprobe standards		
Element	Standard	Source
Cr	Chromite#5	C M Taylor Corp
Mg	Pyrope#39	C M Taylor Corp
Fe	Magnetite#9	Harvard Mineral Museum
Mn	Spessartine#4b	C M Taylor Corp
Al	Syn.spinel	C M Taylor Corp
Si	ALmandine	Harvard Mineral Museum

Appendix B. Calculation of garnet end members composition from the electron microprobe analysis data.

	Garnet Standar d	ZH- 1_Grt_ 2	ZH- 1_Grt_ 4	ZHS- 16_s2_grt_ 2	ZHS- 16_s2_grt	ZHS- 29_s2_grt	ZHS- 29_s2_grt_ 2	ZHS- 29_s2_grt_ 3	ZH- 22_s_1_G rt	ZH- 22_s_2_G rt	ZH- 22_s_2_Grt _1	ZHS- 7_Grt	ZH- 10_Grt_ 1	ZH- 1_Grt_ 3
SiO ₂	39.07	37.20	36.26	36.23	36.89	36.74	36.41	36.76	36.91	36.43	36.12	36.86	36.79	35.69
TiO ₂	0.09	-0.07	0.07	0.04	0.02	0.14	0.07	0.02	0.03	0.10	0.05	0.07	0.07	0.02
Al ₂ O ₃	22.02	21.73	21.73	21.42	21.15	21.51	20.79	21.05	20.69	20.54	21.66	20.73	21.10	21.68
FeO	23.53	33.92	37.33	33.99	30.41	33.79	32.61	30.90	34.30	32.81	32.62	33.18	35.61	35.87
MnO	0.62	0.55	0.11	0.35	5.69	0.24	0.53	1.63	0.21	2.43	0.16	2.15	1.01	0.37
MgO	11.50	3.91	2.45	2.18	2.19	1.67	2.39	4.33	4.00	1.09	3.27	2.95	1.85	3.48
CaO	4.12	2.93	2.29	4.40	4.15	6.04	4.60	3.08	2.51	5.36	5.05	3.07	3.72	0.97
Na ₂ O	0.01	0.01	0.04	0.04	0.01	-0.01	0.01	0.05	0.07	0.05	0.06	0.05	0.03	0.06
Total	100.95	100.18	100.27	98.64	100.50	100.10	97.39	97.83	98.71	98.80	98.99	99.06	100.16	98.13
Si	2.951	2.97	2.93	2.96	2.97	2.96	2.99	2.98	2.99	2.99	2.92	2.99	2.98	2.93
Ti	0.005	0.00	0.00	0.00	0.00	0.01	0.00	0.00	0.00	0.01	0.00	0.00	0.00	0.00
Al	1.96	2.04	2.07	2.06	2.01	2.04	2.02	2.01	1.98	1.99	2.06	1.98	2.01	2.10
Total	1.965	2.04	2.07	2.06	2.01	2.05	2.02	2.02	1.98	1.99	2.07	1.99	2.02	2.10
Fe	1.486	2.26	2.52	2.32	2.05	2.27	2.24	2.10	2.33	2.25	2.21	2.25	2.41	2.46
Mn	0.04	0.04	0.01	0.02	0.39	0.02	0.04	0.11	0.01	0.17	0.01	0.15	0.07	0.03
Mg	1.295	0.46	0.29	0.26	0.26	0.20	0.29	0.52	0.48	0.13	0.39	0.36	0.22	0.43
Ca	0.333	0.25	0.20	0.38	0.36	0.52	0.41	0.27	0.22	0.47	0.44	0.27	0.32	0.09
Na	0.002	0.00	0.01	0.01	0.00	0.00	0.00	0.00	0.01	0.01	0.01	0.01	0.00	0.01
Total	3.156	3.02	3.03	3.00	3.06	3.01	2.98	3.01	3.05	3.03	3.06	3.03	3.03	3.01
End.memb s														
Alm	47.08	75.03	83.45	77.50	67.01	75.53	75.34	69.86	76.48	74.44	72.37	74.49	79.70	82.10
Sp	1.27	1.22	0.24	0.81	12.70	0.55	1.24	3.74	0.46	5.57	0.35	4.89	2.28	0.85
Pyr	41.03	15.42	9.75	8.85	8.59	6.63	9.82	17.47	15.89	4.40	12.92	11.80	7.36	14.20
Gr	10.55	8.31	6.56	12.84	11.71	17.29	13.60	8.93	7.17	15.59	14.36	8.82	10.66	2.85
Total	99.94	100	100	100	100	100	100	100	100	100	100	100	100	100

Appendix C: Raw data for $^{40}\text{Ar}/^{39}\text{Ar}$ geochronology. au27.5c.and.11 & au27.5c.and.12 is for the two aliquots of andesite and au27.5a.plg.10 is for the metatonalite age date.

Sensitivity (Moles/volt):	1.62E-14	2E-16
Agee Assigned to Fish Canyon		
Sandine :	28020000	112080
Measured 40/36 of Air:	288.0	1.5
(36/37)Ca:	0.0003005	0.0000044
(39/37)Ca:	0.0008200	0.0000820
(40/39)K:	0	4E-04
(38/39)K:	0.01	0.01
% of Sample in Split	0.58	
Date of Irradiation:	2/4/2015	
Date of Analysis:	6/19/2015	

Measurement data are provided in volts, with the standard deviation, unless indicated otherwise.
Data have been corrected for mass discrimination, blank, and interfering nuclear reactions.

	$^{40}\text{Ar}(*+\text{Atm})$	^{39}ArK	$^{38}\text{ArCl}+\text{Atm}$	$^{37}\text{ArCa}$	$^{36}\text{ArAtm}$	M ^{40}Ar	Rad%	R	Age	%sd
Sample ID	^{40}Ar	^{39}Ar	^{38}Ar	^{37}Ar	^{36}Ar					
au27.5c.and.11b.txt	0.03865 \pm 0.000466	0.00076 \pm 0.000083	0.00004 \pm 0.000024	0.00032 \pm 0.000180	0.000097 \pm 0.000019	2.97E-16	25.5%	12.9976	418.38 \pm 329.47	78.75%
au27.5c.and.11c.txt	1.73129 \pm 0.001668	0.06933 \pm 0.000464	0.00209 \pm 0.000042	0.00130 \pm 0.000244	0.003783 \pm 0.000026	1.33E-14	35.4%	8.8491	295.08 \pm 7.64	2.59%
au27.5c.and.11d.txt	1.98122 \pm 0.001664	0.15638 \pm 0.000259	0.00304 \pm 0.000046	0.00208 \pm 0.000115	0.002564 \pm 0.000022	1.52E-14	61.8%	7.8252	263.31 \pm 1.62	0.62%
au27.5c.and.11e.txt	1.97353 \pm 0.001554	0.20386 \pm 0.000373	0.00362 \pm 0.000045	0.00370 \pm 0.000279	0.001751 \pm 0.000034	1.52E-14	73.8%	7.1441	241.85 \pm 1.80	0.75%
au27.5c.and.11f.txt	2.21372 \pm 0.001046	0.25302 \pm 0.000741	0.00446 \pm 0.000042	0.00363 \pm 0.000305	0.001129 \pm 0.000021	1.70E-14	84.9%	7.4319	250.95 \pm 1.20	0.48%
au27.5c.and.11g.txt	4.00874 \pm 0.003526	0.42396 \pm 0.000743	0.00761 \pm 0.000070	0.00513 \pm 0.000121	0.001657 \pm 0.000018	3.08E-14	87.8%	8.3014	278.15 \pm 0.76	0.27%
au27.5c.and.11h.txt	6.45553 \pm 0.006045	0.65816 \pm 0.001226	0.01044 \pm 0.000075	0.00645 \pm 0.000282	0.001468 \pm 0.000017	4.96E-14	93.3%	9.1504	304.32 \pm 0.73	0.24%
au27.5c.and.11i.txt	9.16110 \pm 0.008540	0.90059 \pm 0.001404	0.01301 \pm 0.000117	0.00697 \pm 0.000235	0.001167 \pm 0.000018	7.04E-14	96.2%	9.7900	323.79 \pm 0.64	0.20%
au27.5c.and.11j.txt	10.89630 \pm 0.007498	1.07094 \pm 0.001344	0.01391 \pm 0.000114	0.00872 \pm 0.000146	0.000497 \pm 0.000022	8.37E-14	98.7%	10.0382	331.29 \pm 0.52	0.16%
au27.5c.and.11k.txt	10.70542 \pm 0.003731	1.04890 \pm 0.001574	0.01311 \pm 0.000111	0.00786 \pm 0.000172	0.000293 \pm 0.000028	8.22E-14	99.2%	10.1246	333.89 \pm 0.58	0.17%
au27.5c.and.11l.txt	7.73866 \pm 0.008123	0.76404 \pm 0.001251	0.00934 \pm 0.000069	0.00473 \pm 0.000303	0.000137 \pm 0.000029	5.94E-14	99.5%	10.0763	332.44 \pm 0.75	0.23%
au27.5c.and.11m.txt	7.83809 \pm 0.008968	0.77907 \pm 0.001291	0.00962 \pm 0.000076	0.00373 \pm 0.000459	0.000148 \pm 0.000027	6.02E-14	99.4%	10.0052	330.30 \pm 0.75	0.23%
au27.5c.and.11n.txt	8.11488 \pm 0.008735	0.81762 \pm 0.001114	0.01042 \pm 0.000067	0.00576 \pm 0.000341	0.000246 \pm 0.000024	6.23E-14	99.1%	9.8367	325.21 \pm 0.64	0.20%

au27.5c.and.11o.txt	9.12430	± 0.011437	0.92735	± 0.001474	0.01242	± 0.000131	0.00590	± 0.000303	0.000297	± 0.000024	7.01E-14	99.0%	9.7451	322.43	± 0.70	0.22%
au27.5c.and.11p.txt	4.98560	± 0.003468	0.50780	± 0.000786	0.00649	± 0.000068	0.00330	± 0.000283	0.000116	± 0.000024	3.83E-14	99.3%	9.7512	322.62	± 0.72	0.22%
au27.5c.and.11q.txt	6.01354	± 0.005224	0.61513	± 0.000897	0.00793	± 0.000080	0.00450	± 0.000215	0.000159	± 0.000023	4.62E-14	99.2%	9.7001	321.07	± 0.66	0.21%
au27.5c.and.11r.txt	6.27023	± 0.007228	0.64482	± 0.000889	0.00838	± 0.000091	0.00459	± 0.000237	0.000176	± 0.000013	4.82E-14	99.2%	9.6439	319.37	± 0.61	0.19%
au27.5c.and.11s.txt	5.47471	± 0.006116	0.55971	± 0.001146	0.00726	± 0.000046	0.00391	± 0.000228	0.000164	± 0.000029	4.21E-14	99.1%	9.6955	320.93	± 0.91	0.28%
au27.5c.and.11t.txt	4.40154	± 0.004906	0.44669	± 0.000907	0.00583	± 0.000033	0.00348	± 0.000268	0.000194	± 0.000014	3.38E-14	98.7%	9.7258	321.85	± 0.81	0.25%
au27.5c.and.11u.txt	3.58659	± 0.002505	0.36483	± 0.000835	0.00475	± 0.000041	0.00267	± 0.000295	0.000155	± 0.000016	2.75E-14	98.7%	9.7057	321.24	± 0.89	0.28%
au27.5c.and.11v.txt	3.58673	± 0.002491	0.36514	± 0.000834	0.00484	± 0.000046	0.00284	± 0.000295	0.000157	± 0.000016	2.75E-14	98.7%	9.6964	320.96	± 0.89	2.77E-03
au27.5c.and.11w.txt	4.95595	± 0.003493	0.50228	± 0.000846	0.00676	± 0.000047	0.00436	± 0.000392	0.000304	± 0.000013	3.81E-14	98.2%	9.6889	320.73	± 0.65	2.02E-03
au27.5c.and.11x.txt	4.66332	± 0.003639	0.47578	± 0.000641	0.00639	± 0.000056	0.00462	± 0.000242	0.000265	± 0.000014	3.58E-14	98.3%	9.6377	319.18	± 0.58	1.83E-03
au27.5c.and.11y.txt	4.08907	± 0.003184	0.41662	± 0.001091	0.00556	± 0.000048	0.00418	± 0.000186	0.000235	± 0.000014	3.14E-14	98.3%	9.6492	319.52	± 0.95	2.96E-03
au27.5c.and.11z.txt	3.70830	± 0.002495	0.37772	± 0.000693	0.00516	± 0.000054	0.00456	± 0.000323	0.000235	± 0.000021	2.85E-14	98.1%	9.6352	319.10	± 0.84	2.64E-03
au27.5c.and.11aa.txt	4.32145	± 0.003167	0.43852	± 0.001198	0.00625	± 0.000069	0.00681	± 0.000233	0.000371	± 0.000015	3.32E-14	97.5%	9.6060	318.21	± 0.98	3.09E-03
au27.5c.and.11ab.txt	5.42008	± 0.004962	0.54597	± 0.000725	0.00747	± 0.000052	0.01038	± 0.000291	0.000552	± 0.000016	4.16E-14	97.0%	9.6303	318.95	± 0.60	1.88E-03
au27.5c.and.11ac.txt	5.41422	± 0.005062	0.54224	± 0.000807	0.00756	± 0.000064	0.01200	± 0.000366	0.000625	± 0.000017	4.16E-14	96.6%	9.6467	319.45	± 0.66	2.06E-03
au27.5c.and.11ad.txt	5.18356	± 0.005029	0.51666	± 0.000970	0.00728	± 0.000062	0.01263	± 0.000443	0.000708	± 0.000018	3.98E-14	96.0%	9.6302	318.95	± 0.78	2.44E-03
au27.5c.and.11ae.txt	4.98349	± 0.003312	0.49394	± 0.000952	0.00701	± 0.000071	0.01270	± 0.000322	0.000696	± 0.000016	3.83E-14	95.9%	9.6751	320.31	± 0.75	2.35E-03
au27.5c.and.11af.txt	6.83873	± 0.003283	0.67385	± 0.000624	0.01027	± 0.000080	0.02152	± 0.000329	0.001019	± 0.000018	5.25E-14	95.6%	9.7049	321.22	± 0.44	1.37E-03
au27.5c.and.11ag.txt	6.91170	± 0.007411	0.67772	± 0.000900	0.01049	± 0.000064	0.02506	± 0.000399	0.001109	± 0.000019	5.31E-14	95.3%	9.7185	321.63	± 0.64	1.99E-03
au27.5c.and.11ah.txt	4.38694	± 0.003922	0.42836	± 0.000773	0.00635	± 0.000078	0.01162	± 0.000419	0.000780	± 0.000016	3.37E-14	94.7%	9.7060	321.25	± 0.78	2.43E-03
au27.5c.and.11ai.txt	3.02588	± 0.002930	0.29462	± 0.000726	0.00423	± 0.000049	0.00695	± 0.000404	0.000534	± 0.000015	2.32E-14	94.8%	9.7371	322.19	± 1.03	3.19E-03
au27.5c.and.11aj.txt	2.81967	± 0.002282	0.27475	± 0.000620	0.00393	± 0.000040	0.00634	± 0.000276	0.000507	± 0.000017	2.17E-14	94.7%	9.7197	321.66	± 1.02	3.18E-03
au27.5d.and.11aj.txt	3.85346	± 0.002365	0.37396	± 0.000661	0.00572	± 0.000059	0.01119	± 0.000304	0.000694	± 0.000014	2.96E-14	94.7%	9.7590	322.85	± 0.74	0.23%
au27.5c.and.11ak.txt	6.56109	± 0.002804	0.63398	± 0.000585	0.00956	± 0.000046	0.01778	± 0.000504	0.001185	± 0.000017	5.04E-14	94.7%	9.7995	324.08	± 0.44	0.13%
au27.5c.and.11al.720AM.txt	3.45303	± 0.002888	0.33663	± 0.000645	0.00519	± 0.000187	0.01008	± 0.001192	0.000440	± 0.000046	2.65E-14	96.2%	9.8740	326.34	± 1.50	0.46%
au27.5c.and.11al.txt	3.45355	± 0.001728	0.33700	± 0.000570	0.00518	± 0.000056	0.01011	± 0.000293	0.000444	± 0.000012	2.65E-14	96.2%	9.8614	325.95	± 0.69	0.21%
au27.5c.and.11am.txt	1.15649	± 0.001229	0.11118	± 0.000355	0.00169	± 0.000033	0.00332	± 0.000309	0.000223	± 0.000014	8.88E-15	94.3%	9.8137	324.51	± 1.66	0.51%
au27.5c.and.11an.txt	5.03045	± 0.002507	0.48673	± 0.000618	0.00827	± 0.000054	0.02268	± 0.000265	0.000757	± 0.000014	3.86E-14	95.6%	9.8801	326.52	± 0.55	0.17%

au27.5d.and.12b.txt	0.55780	± 0.000729	0.02926	± 0.000228	0.00087	± 0.000025	0.00064	± 0.000280	0.001184	± 0.000015	4.28E-15	37.3%	7.1116	240.82	± 8.01	3.32%
au27.5d.and.12c.txt	1.14550	± 0.000888	0.07435	± 0.000343	0.00172	± 0.000034	0.00120	± 0.000173	0.001769	± 0.000019	8.80E-15	54.4%	8.3783	280.54	± 3.70	1.32%
au27.5d.and.12d.txt	1.68884	± 0.001574	0.12946	± 0.000495	0.00258	± 0.000036	0.00225	± 0.000206	0.001841	± 0.000021	1.30E-14	67.8%	8.8453	294.96	± 2.42	0.82%
au27.5d.and.12e.txt	2.27141	± 0.001368	0.19138	± 0.000536	0.00365	± 0.000101	0.00313	± 0.000281	0.001781	± 0.000021	1.74E-14	76.8%	9.1201	303.40	± 1.60	0.53%

au27.5d.and.12e.txt	2.27046	± 0.001369	0.19125	± 0.000538	0.00363	± 0.000101	0.00342	± 0.000281	0.001799	± 0.000021	1.74E-14	76.6%	9.0931	302.57	± 1.60	0.53%
au27.5d.and.12f.txt	1.42134	± 0.001159	0.14171	± 0.000355	0.00216	± 0.000033	0.00208	± 0.000153	0.000413	± 0.000027	1.09E-14	91.4%	9.1711	304.96	± 2.08	0.68%
au27.5d.and.12g.txt	2.79075	± 0.001826	0.25303	± 0.000591	0.00410	± 0.000033	0.00430	± 0.000271	0.001676	± 0.000035	2.14E-14	82.3%	9.0739	301.98	± 1.64	0.54%
au27.5d.and.12h.txt	2.49917	± 0.001258	0.24800	± 0.000720	0.00383	± 0.000064	0.00344	± 0.000236	0.000798	± 0.000018	1.92E-14	90.6%	9.1279	303.63	± 1.21	0.40%
au27.5d.and.12i.txt	3.77128	± 0.003164	0.36049	± 0.000754	0.00573	± 0.000075	0.00504	± 0.000269	0.001486	± 0.000016	2.90E-14	88.4%	9.2451	307.22	± 0.90	0.29%
au27.5d.and.12j.txt	5.06780	± 0.004371	0.49253	± 0.000843	0.00756	± 0.000072	0.00757	± 0.000249	0.001484	± 0.000020	3.89E-14	91.3%	9.4006	311.96	± 0.76	0.24%
au27.5d.and.12j.txt	5.06732	± 0.004372	0.49256	± 0.000842	0.00754	± 0.000074	0.00722	± 0.000249	0.001452	± 0.000019	3.89E-14	91.5%	9.4183	312.51	± 0.76	0.24%
au27.5d.and.12k.txt	6.56943	± 0.003318	0.64825	± 0.001209	0.00941	± 0.000036	0.00816	± 0.000264	0.001298	± 0.000019	5.05E-14	94.2%	9.5438	316.32	± 0.71	0.22%
au27.5d.and.12l.txt	6.54223	± 0.005158	0.64500	± 0.001145	0.00907	± 0.000068	0.00789	± 0.000175	0.000873	± 0.000014	5.03E-14	96.1%	9.7441	322.40	± 0.69	0.21%
au27.5d.and.12m.txt	8.43549	± 0.008449	0.82689	± 0.001422	0.01127	± 0.000077	0.00886	± 0.000190	0.000977	± 0.000013	6.48E-14	96.6%	9.8534	325.71	± 0.69	0.21%
au27.5d.and.12n.txt	10.23492	± 0.011754	0.99912	± 0.000921	0.01321	± 0.000095	0.01054	± 0.000265	0.000842	± 0.000042	7.86E-14	97.6%	9.9960	330.02	± 0.65	0.20%
au27.5d.and.12o.txt	12.86717	± 0.007908	1.24782	± 0.002009	0.01655	± 0.000111	0.01415	± 0.000374	0.001039	± 0.000037	9.88E-14	97.6%	10.0668	332.15	± 0.65	0.20%
au27.5d.and.12o.txt	12.86717	± 0.007908	1.24782	± 0.002009	0.01655	± 0.000111	0.01415	± 0.000374	0.001039	± 0.000037	9.88E-14	97.6%	10.0668	332.15	± 0.65	0.20%
au27.5d.and.12p.txt	10.14215	± 0.005007	0.98794	± 0.001391	0.01322	± 0.000127	0.00982	± 0.000302	0.000648	± 0.000019	7.79E-14	98.1%	10.0730	332.34	± 0.54	1.62E-03
au27.5d.and.12q.txt	10.89487	± 0.009890	1.05787	± 0.001206	0.01396	± 0.000089	0.01273	± 0.000247	0.000894	± 0.000042	8.37E-14	97.6%	10.0503	331.66	± 0.63	0.19%
au27.5d.and.12r.txt	10.50950	± 0.007023	1.02626	± 0.001269	0.01351	± 0.000074	0.01301	± 0.000274	0.000858	± 0.000017	8.07E-14	97.6%	9.9947	329.98	± 0.50	0.15%
au27.5d.and.12s.txt	9.42043	± 0.005634	0.91747	± 0.001162	0.01227	± 0.000071	0.00991	± 0.000237	0.000820	± 0.000024	7.24E-14	97.4%	10.0046	330.28	± 0.54	0.16%
au27.5d.and.12t.txt	7.98386	± 0.004312	0.77893	± 0.001841	0.01068	± 0.000080	0.00827	± 0.000178	0.000749	± 0.000022	6.13E-14	97.2%	9.9666	329.13	± 0.87	0.26%
au27.5d.and.12t.txt	7.98386	± 0.004312	0.77893	± 0.001841	0.01068	± 0.000080	0.00827	± 0.000178	0.000749	± 0.000022	6.13E-14	97.2%	9.9666	329.13	± 0.87	0.26%
au27.5d.and.12u.txt	8.20875	± 0.004941	0.79164	± 0.001324	0.01070	± 0.000056	0.00842	± 0.000580	0.001058	± 0.000038	6.31E-14	96.2%	9.9752	329.39	± 0.77	0.23%
au27.5d.and.12v.txt	7.09353	± 0.009159	0.68754	± 0.001172	0.00939	± 0.000092	0.00755	± 0.000214	0.000874	± 0.000037	5.45E-14	96.4%	9.9426	328.41	± 0.90	0.27%
au27.5d.and.12w.txt	6.44643	± 0.006031	0.62275	± 0.001527	0.00838	± 0.000067	0.00830	± 0.000211	0.000931	± 0.000035	4.95E-14	95.7%	9.9109	327.45	± 1.05	0.32%
au27.5d.and.12x.txt	5.90865	± 0.005175	0.56464	± 0.000988	0.00771	± 0.000072	0.00864	± 0.000279	0.000966	± 0.000015	4.54E-14	95.2%	9.9603	328.94	± 0.74	0.22%
au27.5d.and.12y.txt	5.58563	± 0.004250	0.53045	± 0.000754	0.00723	± 0.000055	0.00850	± 0.000390	0.001109	± 0.000014	4.29E-14	94.1%	9.9136	327.53	± 0.62	0.19%
au27.5d.and.12y.txt	5.58563	± 0.004250	0.53045	± 0.000754	0.00723	± 0.000055	0.00850	± 0.000390	0.001109	± 0.000014	4.29E-14	94.1%	9.9136	327.53	± 0.62	0.19%
au27.5d.and.12z.txt	7.92158	± 0.005080	0.74553	± 0.000887	0.01066	± 0.000091	0.01703	± 0.000140	0.001776	± 0.000040	6.08E-14	93.4%	9.9236	327.83	± 0.71	0.22%
au27.5d.and.12aa.txt	7.18788	± 0.009238	0.68354	± 0.001682	0.00994	± 0.000089	0.01802	± 0.000483	0.001537	± 0.000022	5.52E-14	93.7%	9.8538	325.72	± 1.02	0.31%
au27.5d.and.12ab.txt	6.63520	± 0.005673	0.62949	± 0.001157	0.00933	± 0.000089	0.01685	± 0.000419	0.001469	± 0.000019	5.10E-14	93.5%	9.8536	325.72	± 0.77	0.23%
au27.5d.and.12ac.txt	6.72900	± 0.006408	0.63238	± 0.001104	0.00948	± 0.000070	0.02016	± 0.000377	0.001687	± 0.000020	5.17E-14	92.6%	9.8555	325.77	± 0.76	0.23%
au27.5d.and.12ad.txt	7.04219	± 0.003995	0.66021	± 0.000858	0.01063	± 0.000134	0.02646	± 0.000298	0.001827	± 0.000023	5.41E-14	92.3%	9.8528	325.69	± 0.61	0.19%
au27.5d.and.12ad.txt	7.04219	± 0.003995	0.66021	± 0.000858	0.01063	± 0.000134	0.02646	± 0.000298	0.001827	± 0.000023	5.41E-14	92.3%	9.8528	325.69	± 0.61	0.19%
au27.5d.and.12ae.txt	9.76862	± 0.005178	0.91250	± 0.001539	0.01493	± 0.000096	0.04607	± 0.000319	0.002658	± 0.000026	7.50E-14	92.0%	9.8494	325.59	± 0.69	0.21%
au27.5d.and.12af.txt	9.59089	± 0.010847	0.89662	± 0.001766	0.01443	± 0.000200	0.03698	± 0.000396	0.002613	± 0.000021	7.37E-14	91.9%	9.8395	325.29	± 0.84	0.26%
au27.5d.and.12ag.txt	10.12079	± 0.013416	0.94160	± 0.001865	0.01522	± 0.000113	0.04511	± 0.000422	0.002842	± 0.000040	7.77E-14	91.7%	9.8614	325.95	± 0.94	0.29%

au27.5d.and.12ah.txt	8.44632	± 0.010319	0.78288	± 0.001200	0.01268	± 0.000116	0.04637	± 0.000391	0.002446	± 0.000031	6.49E-14	91.4%	9.8712	326.25	± 0.80	0.25%
au27.5d.and.12ai.txt	8.12320	± 0.010587	0.75246	± 0.001352	0.01245	± 0.000095	0.04158	± 0.000410	0.002406	± 0.000021	6.24E-14	91.2%	9.8559	325.79	± 0.84	0.26%
au27.5d.and.12aj.txt	9.86420	± 0.005782	0.90653	± 0.001577	0.01550	± 0.000067	0.05445	± 0.000488	0.003197	± 0.000025	7.58E-14	90.4%	9.8451	325.46	± 0.71	0.22%
au27.5d.and.12ak.txt	4.12702	± 0.003242	0.38453	± 0.000439	0.00596	± 0.000058	0.01371	± 0.000250	0.001188	± 0.000025	3.17E-14	91.5%	9.8232	324.80	± 0.81	0.25%
au27.5d.and.12ak.txt	4.12594	± 0.003251	0.38432	± 0.000443	0.00594	± 0.000059	0.01362	± 0.000250	0.001186	± 0.000024	3.17E-14	91.5%	9.8271	324.92	± 0.78	0.24% 2.86E-
au27.5d.and.12al.txt	6.85902	± 0.006071	0.63071	± 0.001115	0.01062	± 0.000058	0.03119	± 0.000301	0.002205	± 0.000039	5.27E-14	90.5%	9.8466	325.51	± 0.93	03 3.21E-
au27.5d.and.12am.txt	3.94637	± 0.003023	0.36239	± 0.000700	0.00660	± 0.000052	0.02270	± 0.000453	0.001316	± 0.000027	3.03E-14	90.1%	9.8229	324.79	± 1.04	03

au27.5a.plg.10a.txt	0.15775	± 0.000444	0.00846	± 0.000084	0.00047	± 0.000032	0.00059	± 0.000217	0.000214	± 0.000013	1.21E-15	59.9%	11.1707	365.12	± 16.53	4.53%
au27.5a.plg.10b.txt	1.28151	± 0.002552	0.06008	± 0.000264	0.00262	± 0.000034	0.00281	± 0.000169	0.001002	± 0.000022	9.84E-15	76.9%	16.4075	513.78	± 4.78	0.93%
au27.5a.plg.10c.txt	1.62971	± 0.000953	0.09704	± 0.000267	0.00255	± 0.000046	0.00459	± 0.000251	0.000835	± 0.000016	1.25E-14	84.9%	14.2570	454.21	± 2.14	0.47%
au27.5a.plg.10d.txt	1.65797	± 0.001523	0.12033	± 0.000511	0.00252	± 0.000033	0.00798	± 0.000200	0.000825	± 0.000018	1.27E-14	85.3%	11.7596	382.46	± 2.43	0.64%
au27.5a.plg.10e.txt	1.33215	± 0.001394	0.11584	± 0.000359	0.00211	± 0.000043	0.01159	± 0.000243	0.000552	± 0.000016	1.02E-14	87.7%	10.1006	333.17	± 1.81	0.54%
au27.5a.plg.10f.txt	0.89495	± 0.001310	0.08637	± 0.000295	0.00146	± 0.000034	0.01276	± 0.000274	0.000359	± 0.000013	6.87E-15	88.1%	9.1469	304.22	± 1.93	0.64%
au27.5a.plg.10g.txt	0.84899	± 0.001583	0.08554	± 0.000278	0.00139	± 0.000034	0.01094	± 0.000253	0.000314	± 0.000016	6.52E-15	89.1%	8.8517	295.16	± 2.21	7.50E-03
au27.5a.plg.10h.txt	1.53705	± 0.001138	0.15452	± 0.000306	0.00237	± 0.000047	0.02327	± 0.000422	0.000490	± 0.000013	1.18E-14	90.6%	9.0245	300.47	± 1.08	0.36%
au27.5a.plg.10i.txt	1.40117	± 0.001190	0.13982	± 0.000363	0.00200	± 0.000025	0.02301	± 0.000344	0.000283	± 0.000015	1.08E-14	94.0%	9.4394	313.15	± 1.38	4.40E-03
au27.5a.plg.10j.txt	1.20702	± 0.001087	0.11777	± 0.000275	0.00174	± 0.000033	0.02223	± 0.000582	0.000250	± 0.000013	9.27E-15	93.9%	9.6394	319.23	± 1.36	4.26E-03
au27.5a.plg.10k.txt	0.89736	± 0.001022	0.08668	± 0.000314	0.00137	± 0.000029	0.01938	± 0.000336	0.000240	± 0.000013	6.89E-15	92.1%	9.5560	316.69	± 1.94	6.13E-03
au27.5a.plg.10l.txt	1.12989	± 0.001082	0.10598	± 0.000385	0.00173	± 0.000019	0.02593	± 0.000191	0.000358	± 0.000016	8.68E-15	90.6%	9.6864	320.65	± 2.02	6.29E-03
au27.5a.plg.10m.txt	1.29104	± 0.001099	0.11352	± 0.000359	0.00224	± 0.000040	0.04386	± 0.000487	0.000690	± 0.000018	9.92E-15	84.2%	9.6129	318.42	± 2.02	6.35E-03
au27.5a.plg.10n.txt	1.23619	± 0.000665	0.10079	± 0.000293	0.00224	± 0.000031	0.04657	± 0.000537	0.000894	± 0.000016	9.50E-15	78.6%	9.6900	320.76	± 2.00	6.23E-03
au27.5a.plg.10o.txt	1.08998	± 0.000723	0.08242	± 0.000297	0.00205	± 0.000046	0.04842	± 0.000551	0.000956	± 0.000017	8.37E-15	74.1%	9.8547	325.75	± 2.63	8.06E-03
au27.5a.plg.10p.txt	1.02047	± 0.000497	0.07516	± 0.000279	0.00195	± 0.000024	0.04253	± 0.000383	0.000928	± 0.000016	7.84E-15	73.1%	9.9820	329.60	± 2.74	8.32E-03
au27.5a.plg.10q.txt	0.97965	± 0.001266	0.06766	± 0.000277	0.00196	± 0.000026	0.04449	± 0.000380	0.001012	± 0.000016	7.52E-15	69.5%	10.1247	333.90	± 3.11	9.31E-03
au27.5a.plg.10r.txt	0.94941	± 0.001235	0.06367	± 0.000174	0.00193	± 0.000029	0.03683	± 0.000856	0.000933	± 0.000013	7.29E-15	71.0%	10.6364	349.24	± 2.49	7.14E-03
au27.5a.plg.10s.txt	0.73416	± 0.001467	0.05095	± 0.000124	0.00148	± 0.000030	0.02611	± 0.000477	0.000754	± 0.000022	5.64E-15	69.6%	10.0850	332.70	± 4.48	1.35E-02
au27.5a.plg.10t.txt	0.61235	± 0.000807	0.04011	± 0.000173	0.00116	± 0.000026	0.02341	± 0.000318	0.000655	± 0.000017	4.70E-15	68.4%	10.4967	345.06	± 4.75	1.38E-02